Role of Peptidyl-prolyl cis-trans isomerase NIMA-interacting 1 (PIN-1) in pulmonary hypertension

Inaugural Dissertation submitted
to the Faculty of Medicine
in partial fulfillment of the requirements
for the degree of Doctor of Human
Biology in the Faculty of Medicine
of the Justus Liebig University of
Giessen

Presented
by

NABHAM RAI

from Delhi, India

Gießen, 2021

From the Department of Medicine,
Justus-Liebig-University Gießen

Supervisor: **Prof. Dr. Ralph Schermuly**

Supervisor: **PD. Dr. Troidl**

Date of the disputation:
05.10.2021

Dedicated to
all my family
members.

TABLE OF CONTENTS

LIST OF FIGURES

LIST OF TABLES

LIST OF ABBREVIATION

5-hydroxytryptamine	Serotonin
Akt	RAC-alpha serine/threonine-protein kinase
ALK	Activin like-kinase
AML	Acute myeloid leukemia
AR	Androgen receptor
AA	Antimycin A
Ang II	Angiotensin II
APP	Amyloid precursor protein
APS	Ammonium persulfate
BAEC	Bovine aortic endothelial cells
Bax	BCL2-associated X protein
Bcl-2	B-cell CL/lymphoma 2
BIRC5	Baculoviral IAP Repeat Containing 5
BrdU	5-bromo-2deoxyuridine
BMP	Bone Morphogenetic Protein family
BMPR2	Bone morphogenetic protein receptor type 2
Brd4	Bromodomain-containing protein 4
BSA	Bovine serum albumin
C/EBPα	CCAAT enhancer binding protein alpha
Cav-1	Caveolin-1
Cdc25	Cell division cycle 25
CFs	Cardiac fibroblasts
CBP/p300	CREB-binding protein/p300
CI	Cardiac index
CO	Cardiac output

CyP	Cyclophilins
DAMP	Damage-associated molecular patterns
DCA	Dichloroacetate
DMSO	Dimethyl sulfoxide
E2F	E2 transcription factor
ECL	Enhanced chemiluminescence
EDTA	Ethylenediaminetetraacetic acid
EGF	Epidermal Growth Factor
EGFR	Epidermal growth factor receptors
EndMT	Endothelial–mesenchymal transition
EVG	Elastica-van Gieson
eNOS	Endothelial nitric oxide synthase
EMT	Epithelial-mesenchymal transition
ERK	Extracellular signal-regulated kinase
ECM	Extra-cellular matrix
FGF-2	Fibroblast growth factor 2
FMT	Fluorescence Molecular Tomography
FOXO1	Forkhead box protein O1
FKBP	FK506-binding proteins
GADD45A	Growth arrest and DNA damage-inducible 45 alpha
Glut	Glucose transporter
HPRT	Hypoxanthine-guanine phosphoribosyl transferase
HMGB1	High mobility group box protein 1
Her2/Neu	Human epidermal growth factor receptor 2
HIPK2	Homeodomain-interacting protein kinase 2
hbFGF	Human basic fibroblast growth factor

HIF-1	Hypoxia-inducible factor-1
ID1	Inhibitor of differentiation 1
IGF	Insulin-like Growth Factor
IPAH	Idiopathic pulmonary hypertension
IL	Interleukins
KCl	Potassium chloride
KH2PO4	Monopotassium phosphate
LMD	Laser-assisted microdissection
Leu	Leucine
Met	Methionine
MAPK	Mitogen-activated protein kinase
MCP1	Monocyte chemoattractant protein–1
MCT	Monocrotaline
MDM2	Mouse double minute 2
MIP2	Macrophage inflammatory protein 2
MMP-2	Metalloprotease 2
mPAP	Mean pulmonary arterial pressure
MWT	Medial wall thickness
Na3VO4	Sodium Orthovanadate
NIMA	Never in Mitosis gene A
Nrf2	Nuclear factor E2-related factor-2
NO	Nitric oxide
Notch1	Neurogenic locus notch homolog protein 1
NF-κB	Nuclear factor kappa B
OCT-4	Octamer-binding transcription factor 4
p53	Tumor protein p53

PAH	Pulmonary Arterial Hypertension
PAEC	Pulmonary artery endothelial cell
PARP	Poly-ADP ribose polymerase
PASMC	Pulmonary arterial smooth muscle cell
PAWP	Pulmonary artery wedge pressure
PCNA	Proliferating cell nuclear antigen
PCR	Polymerase chain reaction
PCWP	Pulmonary capillary wedge pressure
PDGF-BB	Platelet-derived growth factor-BB
PFA	Paraformaldehyde
Phe	Phenylalanine
PH	Pulmonary hypertension
Pin1	Peptidyl-prolyl isomerase 1
PPARγ	Peroxisome proliferator-activated receptor
PLK1	Polo-like kinase 1
PVR	Pulmonary vascular resistance
PDH	Pyruvate dehydrogenase
PDK	Pyruvate dehydrogenase kinase
qPCR	Quantitative real-time polymerase chain reaction
Rb	Retinoblastoma protein
RV	Right ventricle
RVID	Right ventricle internal diameter
RVSP	Right ventricular systolic pressure
SDS-PAGE	SDS-polyacrylamide gel electrophoresis
SMAD	Small mothers against decapentaplegic
SmBM	Smooth Muscle Basal Medium

α-SMA	α-smooth muscle actin
Sp1	Specificity protein 1
SuHx	Sugen5416/hypoxia
sPAP	Systolic pulmonary artery pressure
TAPSE	Tricuspid annular plane systolic excursion
TBST	Tris-buffer saline with tween-20
TCA	Tricarboxylic acid
TFs	Transcription factors
TGF-1β	Tranforming growth factor 1β
Tie2	Endothelium-specific tyrosine kinase-2
TIMP-1	Metalloprotease-1
TNF-α	Tumor necrosis factor alpha
TUNEL	Terminal deoxynucleotidyl transferase dUTP nick end labeling
VEGF	Vascular endothelial growth factor
VSMC	Vascular smooth muscle cells
VWF	Von Willebrand factor
WU	Wood units

INTRODUCTION

1.1 Definition and classification of Pulmonary Hypertension

Pulmonary hypertension (PH) is a progressive disease of the pulmonary vasculature characterized by an increased pulmonary vascular resistance (PVR) leading to right ventricular failure and death [1]. Clinically, PH is defined by an increase in mean pulmonary arterial pressure (mPAP) over 25 mmHg. Pulmonary Arterial Hypertension (PAH) refers to the subgroup of PH patients defined by a pulmonary artery wedge pressure (PAWP) ≤15 mmHg and a PVR >3 Wood units (WU) characterized hemodynamically, in the absence of other causes of precapillary PH such as PH due to lung disease, CTEPH or other rare diseases [2]. The median survival rate of patients after the diagnosis is only 2.8 years. PH in all its forms is estimated to effect 100 million people worldwide [3].

Clinical classification of PH serves to classify and group patients according to the clinical symptoms associated with PH, similar pathophysiology, clinical presentation, haemodynamic measurement and therapeutic management.

Clinical classification of (PH)

Group 1: Pulmonary Arterial Hypertension (PAH)
1.1 Idiopathic PAH
1.2 Heritable PAH
1.3 Drug- and toxin-induced PAH
1.4 PAH associated with:
1.4.1 Connective tissue disease
1.4.2 HIV infection
1.4.3 Portal hypertension
1.4.4 Congenital heart disease
1.4.5 Schistosomiasis
1.5 PAH long-term responders to calcium channel blockers
1.6 PAH with overt features of venous/capillaries (PVOD/PCH) involvement

1.7 Persistent PH of the newborn syndrome

Group 2: PH due to left heart disease

2.1 PH due to heart failure with preserved LVEF

2.2 PH due to heart failure with reduced LVEF

2.3 Valvular heart disease

2.4 Congenital/acquired cardiovascular conditions leading to post-capillary PH

Group 3: PH due to lung diseases and/or hypoxia

3.1 Obstructive lung disease

3.2 Restrictive lung disease

3.3 Other lung disease with mixed restrictive/obstructive pattern

3.4 Hypoxia without lung disease

3.5 Developmental lung disorders

Group 4: PH due to pulmonary artery obstructions

4.1 Chronic thromboembolic PH

4.2 Other pulmonary artery obstructions

Group 5: PH with unclear and/or multifactorial mechanisms

5.1 Haematological disorders

5.2 Systemic and metabolic disorders

5.3 Others

5.4 Complex congenital heart disease

Table 1: Updated classification of PH (6th WSPH, 2019) [2].

The Task Force of 6th World Symposia on PH (WSPH) 2019 suggested to streamline the core of the clinical classification of PH (table 1) which has been developed in additional tables. Updated classification of group 1 includes “PAH long-term responders to calcium channel blockers” and “PAH with overt features of venous/capillaries (PVOD/PCH) involvement” due to similar clinical representation to PH. Group 3 includes other parenchymal lung diseases and group 5 (PH with unclear and/or multifactorial mechanisms) was streamlined and simplified [2].

Functional classification of PH

Class I

Patients with PH without resulting limitation of physical activity. Ordinary physical activity does not cause undue dyspnoea or fatigue, chest pain or near syncope

Class II

Patients with PH resulting in slight limitation of physical activity but comfortable at rest. Ordinary physical activity causes undue dyspnoea or fatigue, chest pain or near syncope.

Class III

Patients with PH resulting in marked limitation of physical activity but comfortable at rest. Less than ordinary activity causes undue dyspnoea or fatigue, chest pain or near syncope.

Class IV

Patients with PH with inability to carry out any physical activity without symptoms. Patients manifest signs of right heart failure. Dyspnoea and/or fatigue may even be present at rest. Discomfort is increased by any physical activity.

Table 2: Current World Health Organisation / New York Heart Association Classification of functional status in patients with pulmonary hypertension. The severity of PAH in patients can be classified using the WHO functional class system. Patients with the mildest form of disease in early-stage PAH are placed in class I and patients with the most severe are placed in class IV. The WHO functional class system is helpful in aiding decision making for PAH therapy and serves as an accurate predictor of patient mortality [4].

1.2 Pathology of PH

The pathology of PH is complex and multifactorial. Vasoconstriction and remodeling of small to midsized (less than 500μm) [5] pulmonary vessels and arterioles results in the thickening of the intima, media, and adventitia contributing to an increased pulmonary vascular resistance (PVR) [6]. Regardless of the cause, an elevated PVR has a devastating effect on the right ventricle due to the increased workload leading to right heart failure and ultimately death [7]. The elevated PVR in patients with PH is primarily due to vessel lumen narrowing and eventual occlusion, intimal fibrosis, and the development of concentric and plexiform lesions [8].

1.2.1 Pulmonary vasculature

Normal pulmonary circulation provides a high compliance, low resistance, and low-pressure vascular bed [9]. Pulmonary vasculature consists of arteries, capillary bed and veins connected to each in series. The arterial wall layers consists of tunica interna (intima), tunica media (media) and tunica externa (adventitia) [10]. Intima is made up of endothelial cells, media comprises of smooth muscle cells and tunica adventitia consists fibroblast cells [11]. Vessel remodeling is pivotal in vascular diseases, and is a major target for therapeutic interventions. Structural changes in vascular remodeling include cell growth, cell death, and cell migration, as well as degradation and reorganization of the extracellular matrix scaffold in the vessel wall [12].

Pulmonary arterial smooth muscle cells (PASMCs) are involved in both vasoconstriction and vascular remodeling. This makes PASMCs an exciting target for research towards the understanding the underlying molecular mechanisms that contribute to PH. While PASMCs of the proximal pulmonary arteries have a heterogeneous phenotype, the cells of the distal pulmonary arteries, which are more involved in PH development, have a more uniform phenotype. These PASMCs have a well differentiated phenotype that expresses many factors indicative of a contractile capacity and a low proliferative potential. These cells are key in modulating vascular tone that allows for control of pulmonary artery pressure and changes in flow rate seen during periods of activity [13]. In a healthy pulmonary artery, there are three regions when viewed cross-sectionally. The inner layer is the intima comprised of pulmonary artery endothelial cells (PAECs). Next is the medial layer of PASMCs and finally the adventitial layer which signals the transition to other lung structures. The adventitial

layer is comprised of other cell types including fibroblasts. In a PH artery, the intima may be infiltrated by SMCs; medial SMCs will proliferate and increase in size, while the adventitial layer will experience an increase in fibroblasts and macrophage infiltration [14]. These changes contribute to the main pathological signs of PH such as medial hypertrophy leading to reduced lumen in previously muscular arteries and an increased abundance of muscular arteries due to muscularization of peripheral arteries and potentially plexiform lesions [15].

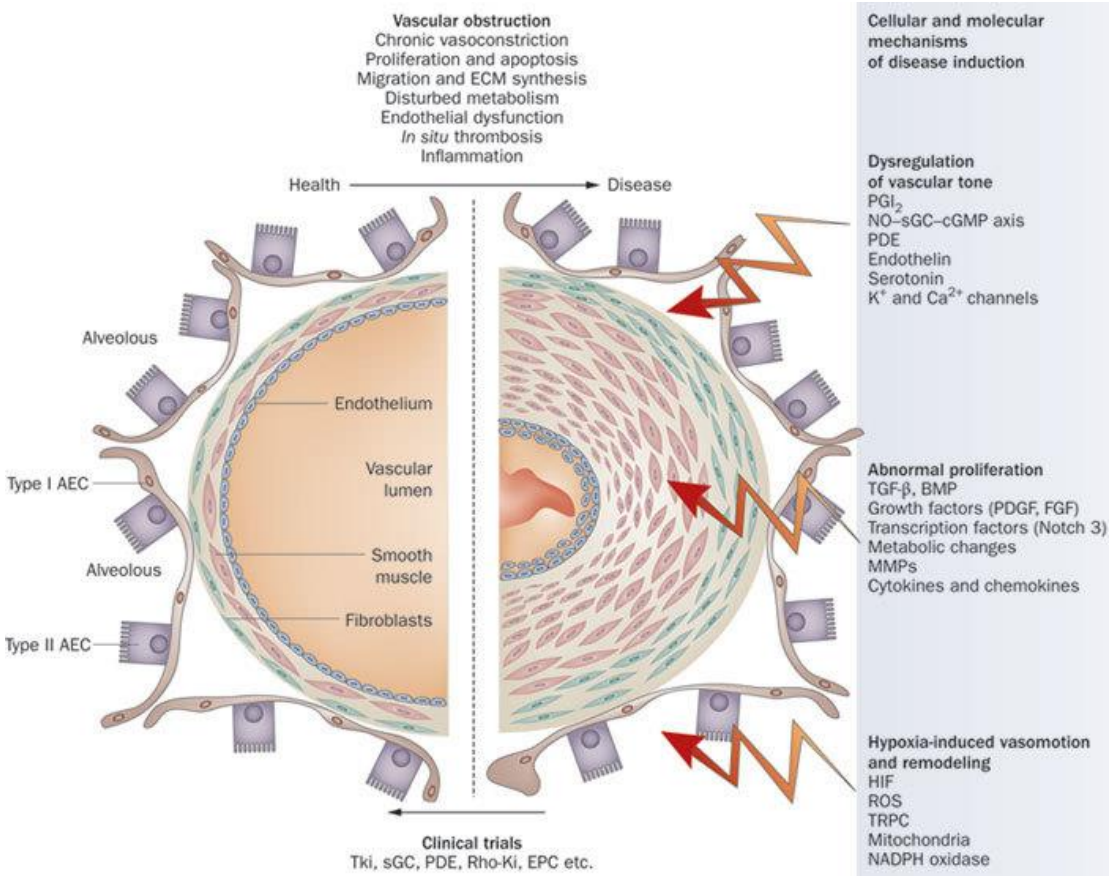

Figure 1. **Vascular remodeling in PAH.** PAH is distinguished by extreme pulmonary vasoconstriction and pathological vascular remodeling processes that typically involve intima, media, and adventitia layers [1].

1.3 Remodeling of the vascular wall

1.3.1 Intimal changes in pulmonary hypertension

Various degrees of intimal thickening occur in the pulmonary arteries, leading to occlusive vessels and plexiform lesions in severe cases [8]. In the pathogenesis of PAH, PAEC alterations precede pulmonary artery muscularization and remodeling [16]. Proliferation of PASMCs can be induced by PAECs. For example, increased

endothelium-specific tyrosine kinase-2 (Tie2) receptor expression releases serotonin in patients with IPAH, resulting in PASMC hyperproliferation [17]. It is suspected that distal pulmonary artery loss (vascular pruning) is caused by PAEC apoptosis [18]. A subpopulation of PAECs survives this cell death, becomes apoptosis-resistant and hyperproliferative and contributes to vessel destruction and formation of neointima [19]. This mechanism includes the migration and proliferation of cells of uncertain origin, which express α-smooth muscle actin (SMA) and are considered to be a subpopulation of PASMCs [20]. This subpopulation may also originate from stem cells [21], fibrocytes [22] or transformed PAECs [23]. Due to the clonal expansion of apoptosis resistant PAECs, migration and proliferation of PASMCs and aggregation of circulating cells such as macrophages and endothelial progenitor cells, plexiform lesions are formed in the obliterated lumen in severe PAH [24].

Angiogenesis involves the regeneration of damaged vessels and once disrupted, contributes to the progression of PAH [25]. Coordinated mechanisms orchestrated by dysfunctional PAECs result in the exploitation of angiogenesis leading to extracellular matrix remodeling and SMC, fibroblast and pericyte recruitment [23]. Plexiform lesions are formed by a process of disordered angiogenesis. Growth factors such as fibroblast growth factor (FGF)-2, Angiotensin II (Ang II) [26], and platelet-derived growth factor-BB (PDGF-BB) [27] are released by PAECs to induce the proliferation of PASMCs. Monoclonal endothelial cells which characterize plexiform lesions express angiogenesis-related proteins like vascular endothelial growth factor (VEGF) and have decreased expression of the pro-apoptotic member of the B-cell CL/lymphoma 2 (Bcl-2) gene family, BCL2-associated X protein (Bax) [28, 29]. The loss of expression of caveolin-1 (Cav-1) and increased expression of ET-1 and Baculoviral IAP Repeat Containing 5 (BIRC5) are some of the elements responsible for hyperproliferation and anti-apoptotic characteristics acquired by PAECs and PASMCs [19, 30]. The presence of macrophages and lymphocytes in these lesions and increased production of interleukins (IL), namely IL-1, IL-6, IL-8 and IL-12 by PAECs strongly suggest a role of inflammation in PH [31].

1.3.2 Media alterations in pulmonary hypertension

A typical pathological feature of PH involves muscularization of pulmonary arteries and occurs in mild/moderate and severe PAH. Distal arteries sized between 70-500 μm

diameter and pre-capillary vessels below 70μm diameter are pre-dominantly involved in this process [14]. A combination of hypertrophy, hyperplasia, survival, and differentiation of cells results in an increase of the tunica media in pulmonary arteries in PAH [32]. In hypoxia pericytes are the potential precursor cells causing hypertrophy and metaplasia whereas in neonatal bovine pulmonary arteries, a cluster of cells negative for smooth muscle cell markers are interspersed, exhibiting varying cellular heterogeneity in the pulmonary arteries [14].

Bone morphogenetic protein receptor type 2 (BMPR2) mutations and deficiency of BMPR2 signaling have been demonstrated to contribute to disturbed SMC proliferation and EC abnormalities [33, 34]. Serotonin (5-hydroxytryptamine) is internalized by PASMCs, facilitating vasoconstriction, cell growth, and enhancement of hypoxia-induced remodeling and PH [35]. PDGF-BB is shown to induce a proliferative and migratory phenotype of PASMCs. Expression of PDGF ligands and the corresponding receptors (PDGFR-α, PDGFR-β) is shown to be elevated in pulmonary arteries of IPAH patients. Administration of imatinib, a PDGFR antagonist, reversed the vascular remodeling in a hypoxia model of PH [36].

Increased expression of extracellular proteins such Tenascin has been associated with intimal and medial layer remodeling in pulmonary arteries [37]. According to studies in cultured human SMCs, the expression of other extracellular matrix proteins such as the metalloprotease-1 (TIMP-1) and of the metalloprotease (MMP)-2 tissue inhibitor is increased, but only MMP-2 expression is observed to be increased in the pulmonary arteries *in vivo* in IPAH lungs [38].

Peroxisome proliferator-activated receptor (PPAR)γ, apart from being involved in the regulation of lipid and glucose metabolism, also exerts anti-proliferative effects in pulmonary arteries. Induced by BMPR2, PPARγ inhibits the PDGF induced proliferation of PASMCs, and mutations in BMPR2 gene lead to suppression of this inhibitory effect in IPAH patients [39]. Recently Forkhead box protein O1 (FOXO1) was shown to be downregulated in PAH. FOXO1 is a transcription factor which negatively regulates the pro-proliferative and anti-apoptotic PASMC phenotype by regulation of proliferative genes like Cyclin D1, p27, and apoptotic genes such as BCL6 and growth arrest and DNA damage-inducible 45 alpha (GADD45A). FoxO1 is also involved in

positive regulation of BMPR2 expression and downstream signaling in PH [40].

1.3.3 Adventitial changes in pulmonary hypertension

Adventitial fibroblasts are potent modulators of vascular wall function in pulmonary as well as systemic circulation. Adventitia functions as an extra-cellular matrix (ECM) scaffold containing a nutrient supply pipeline, as well as resident cells including fibroblasts, progenitor cells and immune cell counterparts [41]. Evidence of adventitial remodeling is found in hypoxia-induced pulmonary hypertension [42]. Resident fibroblasts are activated and undergo a series of functional alterations in response to environmental pressures such as hypoxia or vascular distension [43]. The proliferation of pulmonary arterial fibroblasts and secretion of chemical chemokines has been shown to promote the recruitment of inflammatory cells due to environmental stress. Numerous studies have reported high expression of inflammatory mediators, for instance monocyte chemoattractant protein–1 (MCP1), macrophage inflammatory protein 2 (MIP2), IL-1β, and IL-6 in pulmonary arterial fibroblasts, resulting in an increase of macrophages and neutrophils in the hypoxic animals [44, 45].

In humans, increased numbers of neutrophils and macrophages, as well as augmented expression of tumor necrosis factor (TNF)-α, IL-1β, IL-6, and IL-8 have been also reported [46]. The modulation of vascular cell growth, migration and differentiation is specifically controlled by these cytokines. IL-6, for instance, induces PASMC proliferation via elevation of FGF-2 and when overexpressed in mice caused an exaggerated pulmonary hypertensive response to hypoxia [47], IL-1β stimulates both ET-1 and PDGF production and hence, may act as a link between endothelial dysfunction, increased matrix synthesis and inflammation [48]. Pulmonary arterial fibroblasts can also differentiate into myofibroblasts upon environmental stress, leading to increased production of extracellular matrix proteins such as collagen and further can migrate to the medial or intimal layer, supporting neointima formation [49].

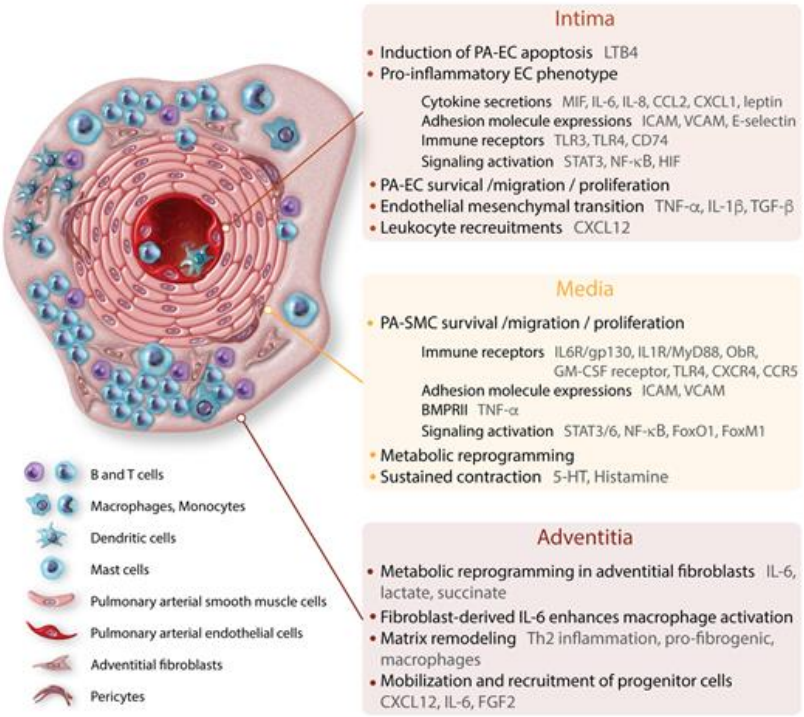

Figure 2. Remodeled artery in PAH. Remodeling of three vascular compartments of pulmonary artery in PAH [50].

1.4 Vascular wall damage and inflammation

One of the early and acknowledged mechanisms involved in PAH initiation and progression is injury of pulmonary vascular cells. Early reports suggest that inhibition of the primary endothelial prosurvival signaling molecule, VEGF, in combination with hypoxia, induces apoptosis of pulmonary endothelial cells (ECs), leading to severe angioproliferative PAH [51]. The Sugen-hypoxia model, where blockade of VEGF in combination with hypoxia causes plexiform lesions due to highly proliferative pulmonary vascular cells, has become a gold standard of experimental PAH that resembles the features observed in humans. The proposed mechanism links proliferation of vascular cells to the initial apoptosis of PAECs leading to a transition and selection of surviving cells which are pro-proliferative and anti-apoptotic in nature [19].

As paradoxical as it seems, this mechanism requires growth factor inhibition to stimulate the occurrence of hyperproliferative cells. The main impetus, however, in the stimulation of the proliferative potential of the surviving cells is the induction of vascular cell damage and not growth inhibition itself. Evidence suggests that naive cells could acquire apoptotic resistance once exposed to conditioned media from apoptotic cells

[19]. Activation of apoptotic pathways induced by UV irradiation [52], shear stress [53], drugs [54] and mitochondrial dysfunction [55] could induce PAH. Although the role of initial vascular wall damage in PAH is acknowledged, the mechanisms in pulmonary vascular cells involved in altering the apoptotic into the proliferative pathways are still largely unknown. Apoptosis is generally an effective regulator of tissue integrity and homeostasis that replaces damaged or no longer functional cells. It is a silent form of damage to cells with no detectable activation of the immune system. This silence, however, is not complete; phagocytic clearance of apoptotic cells involves the production of chemoattractants that are critical for the phagocytes to identify and engulf the dying cell [56]. This signaling, together with the later discovered ability of apoptotic cells to monitor their local environment by releasing pro-apoptotic, anti-apoptotic, and mitogenic pathway regulators, can explain the ultimate role of continuing vascular apoptosis in the subsequent proliferation of neighboring cells [57].

Death-resistance is conferred to the apoptotic cells via apoptotic mechanisms. VEGF plays a major role in the survival of apoptotic cells in PAH. Apoptotic pulmonary microvascular endothelial cells secrete VEGF and induce resistance to apoptosis and increased survival not only in endothelial cells but also in vascular smooth muscle cells (VSMCs). Secreted from dying ECs, VEGF induces apoptosis resistance in surviving ECs and VSMCs [53]. Angiopoietin-1, an important factor for endothelial cell survival, is produced not only by apoptotic cells but also by monocytes communicating with apoptotic cells [58]. Inflammatory cells are also a source of IL-6, a pleiotropic cytokine that serves to block apoptosis in different vascular cells exposed to the toxic environment [59]. In contrast, apoptotic ECs promote the survival of macrophages in a sphingosine-1-phosphate dependent manner, thus ensuring the rapid phagocytosis of dying cells [60]. This double-sided defense is a functional network of different cell types, stabilizing the vascular wall cohesively against injury.

The combination of pro- and antiapoptotic stimuli does not fully explain the process of making the survival-versus-apoptosis decision for each affected cell. The present view appears to regard a cell population as a mixture of cells that are more susceptible or less resistant to apoptotic stimuli. This view indicates that under conditions of sustained self-perturbed apoptosis, circumstances favor the selection of apoptosis-resistant cells, leading to the death of susceptible cells and the activation of apoptosis tolerance in the survivors [61]. In addition, this balance changes towards survival, growth and

eventual vascular remodeling through the secretion of apoptotic cell prosurvival factors. Thus, transforming growth factor 1β (TGF-1β) released from the apoptotic ECs promotes intimal hyperplasia [62], SMC proliferation and migration [53], endothelial–mesenchymal transition (EndMT) with EC-derived SMC accumulation, and ECM deposition [63]. Conditioned media collected from ECs exposed to hypoxia, a condition known to promote EC apoptosis [64], stimulated proliferation of SMCs through the prostaglandin-mediated mechanism and the growth of fibroblasts via secretion on basic fibroblast growth factor [65]. It was also reported that fibroblasts exposed to apoptotic media undergo myofibroblast differentiation in a connective tissue growth factor responsive manner via Caspase-3 [66]. Endothelial injury impairs the secretion of NO, a main paracrine vasodilator with anti-mitogenic properties, and then stimulates the secretion of endothelin-1 [67], a potent vasoconstrictor and mitogen. Apoptosis is also associated with the increased production of ROS, which can initiate and control different aspects of apoptosis-induced proliferation [68].

PAH exhibits severe inflammatory changes in the pulmonary vascular wall regardless of the anti-inflammatory nature of apoptosis [69]. Interestingly, the activation of the innate and adaptive immune responses in PAH is directly associated with pulmonary vascular damage. However, it has to be acknowledged that apoptosis is not the only outcome once the cell is damaged. Necroptosis or necrosis is also one of result of the severe cell damage in PAH. Surprisingly, the role of these forms of cell death to PAH pathogenesis is almost unexplored. Many damage-associated molecular patterns (DAMPs) activate inflammatory channels and are secreted by necrotic cells. High mobility group box protein 1 (HMGB1) is released into extracellular space during the initial stages of monocrotaline (MCT)-induced PAH and contributes to the production of PAH [70, 71]. Apoptotic cells do not release HMGB1 even after secondary necrosis due to hypoacetylation of one or more of the chromatin components that occurs during apoptosis and holds HMGB1 firmly bound to chromatin [72]. Therefore, because the release of HMGB1 distinguishes necrotic cells from apoptotic cells, it could be predicted that MCT or VEGF receptor antagonist (SU5416) with hypoxia would be associated with necrotic cell death. This necrosis activates TLR4/IL1β/E-Selectin axis to induce inflammatory signals in the pulmonary arteries, activating ECs and further

increasing inflammatory cell recruitment [70].

1.5 Metabolic Reprogramming

Pulmonary vascular cells which show cancer-like characteristics require metabolic alterations for the amplified demand of dividing cells. Vascular cell types are diverse and can adapt in a manner specific to each cell type. Mutations in BMPR2 has been shown to be linked with the upregulation of glycolysis and pentose phosphate pathways in human pulmonary microvascular endothelial cells with PAH [34]. A significant rise in glucose and its intermediary products has also been observed. In contrast, these cells also have displayed a decline in carnitine homeostasis, fatty acid oxidation pathways, and tricarboxylic acid (TCA) cycle metabolites. Thus, on one hand, the cytosolic glycolysis was upregulated in ECs and on the other, there was a downregulation in mitochondrial-based metabolic pathways. It has also been shown that in the model of increased pulmonary blood flow due to cardiac defects, carnitine homeostasis, which is responsible for transporting fatty acids to the mitochondria, is decreased by inhibition of the carnitine acetylation/deacetylation mechanism [73].

The modified transport of fatty acids could therefore contribute significantly to the reduction of fatty acid oxidation and the subsequent reduction of TCA activity, as well as oxidative phosphorylation. On the contrary, SMCs from PAH patients instead exhibited decreased glucose metabolism and increased fatty acid biosynthesis [74]. Isolated from MCT animals, PASMCs displayed decreased oxidative phosphorylation and increased glycolysis rates [75]. This disparity may be attributed to several reasons, such as stability of the metabolic phenotype in relation to isolation methods, cell formation, effects of the cell culture media, etc. However, whether or not endothelial and SMC lineages have identical metabolic changes in PAH still remains unanswered. Antimycin A (AA) inhibition of mitochondrial respiration has also been reported to shift ECs towards glycolysis more effectively than in SMCs [76]. Hypoxia-inducible factor-1 (HIF-1) and RAC-alpha serine/threonine-protein kinase (Akt) play a regulatory function in the metabolic transition in PAH. HIF-1 upregulates expression of glycolysis genes such as Phosphofructokinase, hexokinase-2, Glucose transporter (Glut) 1 & 3, and growth factors that in turn can induce Akt [77]. Akt activation can result in induction of cell proliferation, apoptosis resistance and a feedback loop with further activation of glycolysis by the induction of HIF signaling [78]. Activation of Akt also leads to

mammalian target of rapamycin (mTOR) phosphorylation, which is known to play a role in the regulation of lung vascular remodeling and right heart hypertrophy [79]. Furthermore, increased oxidative stress contributes to HIF-1 and Akt activation, activating a feedforward loop. In addition, HIF-1α upregulates the expression of pyruvate dehydrogenase kinase (PDK), which inhibits the activity of pyruvate dehydrogenase (PDH) [80]. PDH has been shown to be involved to the disease pathology, while its inactivation limits pyruvate influx into the TCA cycle [81]. PDH insufficiency can lead to a glycolytic transition by restricting the formation of oxidative phosphorylation substrates in the mitochondrial matrix. The PDK inhibitor dichloroacetate (DCA), by inducing the activation of PDH and enhancing mitochondrial respiration, improved RV function and reversed RV remodeling [82]. DCA provided to idiopathic PAH patients decreased mean pulmonary artery pressure and pulmonary vascular resistance and increased functional capability, reinforcing the essential role of PDH involvement in PAH pathogenesis, while displaying a variety of individual responses [83].

2.1 Peptidyl prolyl isomerases

Peptidyl prolyl isomerases consist of three families: cyclophilins (CyPs), FK506-binding proteins (FKBPs) and parvulins. Several members of these protein families have been identified as targets for the development of immunosuppressive drugs including CyPs and FKBPs, which have been identified as targets of cyclosporin and rapamycin respectively. Similar to parvulins, both the CyPs and the FKBPs are able to catalyze peptidyl-prolyl isomerization; however, their sequences and structures show no noticeable similarities. Each of the three enzyme families has a different recognition motif for residues preceding a proline [84]. The parvulin family, so named because of the small size of the proteins, has two protein sub-classes: the non-Pin1 parvulins and the Pin1-like parvulins. The non-Pin1 sub-class does not depend on phosphorylation of residue preceding a Pro. Pin1 catalyzes the isomerization of cis–trans peptidyl-prolyl bonds only of phosphorylated targets (i.e. phosphorylated serine or threonine ahead of the proline target) and since there is frequent occurrence of phosphorylation in cell signaling, Pin1 has been shown to play a key role in cell cycle initiation, gene expression, signal transduction pathways, and cell proliferation [85].

FKBP12 is a small 12 kDa protein which binds to the glycine- and serine-rich motif (GS) region of the TGF-β or activin like-kinase (ALK)-5 type 1 receptor. Binding to FKBP12 makes ALK- 5 more stable by protecting phosphorylation sites. The FKBP PPI-ase activity domain plays a crucial role in this interaction. It has been shown that FK506 inhibits this interaction by blocking the binding site on FKBP12 [86] (7518616). Rabinovitch *et al.* showed FK506, also known as tacrolimus, released FKBP12 from type I activin receptor-like kinase 1 (ALK1), ALK2, and ALK3 and could activate downstream small mothers against decapentaplegic 1/5 (SMAD1/5) and mitogen-activated protein kinase (MAPK) signaling and inhibitor of differentiation 1 (*ID1*) gene regulation. Tacrolimus reversed dysfunctional BMPR2 signaling in IPAH ECs, and low-dose FK506 reversed PAH in monocrotaline and SU5416-hypoxia rats, and thus could be useful in the treatment of PAH [87]. Cyclophilin A forms a complex with caveolin, heat shock protein 56 and cholesterol [88]. Secreted cyclophilin activates endothelial cells and promotes a chemotactic response [89]. VSMCs release Cyclophilin in response to reactive oxygen species (ROS) and play a role in augmenting oxidative stress in tissues. Cyclophilin stimulates extracellular signal-regulated kinase (ERK) 1/2 phosphorylation, enhances DNA synthesis and increases the proliferation of VSMC

[90]. Secreted cyclophilin also increases the expression of adhesion molecules on endothelial cells, acts as a leucocyte chemoattractant and blocks nitric oxide (NO)-induced apoptosis of VSMC [91]. Endothelial cell secreted cyclophilin A could increase EC apoptosis, inflammation, and oxidative stress and causes PAH and its inhibition could be a novel PAH therapy [92].

2.1.1 Peptidyl-prolyl isomerase 1 (Pin1)

Pin1 is a peptidyl-prolyl isomerase that binds to phosphorylated substrates preceding a Pro residue and controls their isomeric conformation to catalyze the interconversion between cis/trans isomers of a peptide bond [93]. Depending on the sequence, the cis isomer population could be between roughly 5 and 40 percent. Pin1 was originally recognized as a cell cycle protein believed to interact with the Never in Mitosis gene A (NIMA) encoded protein, a key protein involved in mitosis control [94]. Pin1 is essential for catalyzing isomer-specific enzymes and is known to be important in promoting protein binding that only recognizes one of the isomers. In the laboratory of Gunter Fischer, the first parvulin was detected and isolated from Escherichia coli. Human Pin1 being a crucial protein contains a yeast homologous sequence considered to be a critical protein for yeast development [95]. The function of Pin 1 was first described in mitotic control, but it is now recognized that Pin1 catalyzes protein isomerization in apoptosis, progression of the cell cycle, apoptosis and proliferation, DNA repair, stress responses, as well as transcription [96-98].

2.1.2 Structural features of Pin1

Pin1 is a small 18 kDa protein that has no nuclear localization or export signals; however, a novel putative nuclear localization sequence was identified by Lufei et al [99]. Pin1's N-terminal extension includes a WW domain sequence and the C-terminal PPI-ases enzymatic domain. It has two different structural domains. The domains are divided between residues 1-39 of the WW domain and residues 50-163 of the isomerase domain by a versatile linker of 10 residues. Phospho-Ser/Thr-ProBoth domains are recognized by both domains. Both proline-led binding and isomerization are well-known and extensively studied pathways. Pin1 has three anti-parallel β-sheets in the WW domain that contain a hydrophobic region on the surface in its secondary

structure. The PPI-ase domain consists of 4 α-helices and 3 β-parallel sheets. The PPI-ase domain has 2 major regions: a proline binding pocket and a binding region of phosphate. These recognized structural areas are situated on opposite sides of the active site of the Cys residue protein. His-59, His-157 and Ser-154 are all active site amino acids. These residues are structured into a pocket-like configuration by a substrate peptide bond. The prolines are a hydrophobic groove with retained residues of leucine (Leu), methionine (Met) and phenylalanine (Phe). The phosphate binding loop contains positive residues that can bind to a phosphate moiety that is negatively charged. The key amino acids controlling this binding are Lys-63, Arg-68 and Arg-69 [100].

The WW domain of Pin1 is known to bind to substrates with a higher affinity than the PPI-ase domain. This domain enhances substrate specificity when a binding motif is located on a peptide. The WW domain of Pin1 has been shown to have a ten-fold higher binding as compared to the PPI-ase protein domain. Thus the WW domain is considered to be responsible for targeting and identification of substrates, while the PPI-ase domain alone is typically unable to bind recognized substrates but plays the role of catalyzing imide bond isomerization [101]. Some of the Pin1 proteins have single binding site, while others have several. The downstream binding site may be bound to the WW domain, and the upstream site may be bound and/or isomerized by the PPI-ase domain. One such example of several binding sites exists in Tau protein, a protein located in neural tissues, and another is CDC25C, a mitotic initiator protein [93]. Pin1's catalytic mechanism consists of covalent coupling, where Pin1 binds with a ligand and adopts an intermediate tetrahedral conformation. For isomerization, the phosphorylated residue on the substrate fits into the binding pocket, and the peptide bond is rotated. Pin1 interacts with its substrates in a non-covalent manner, and the enzymatic action of Pin1 is mediated by variables such as charge [102].

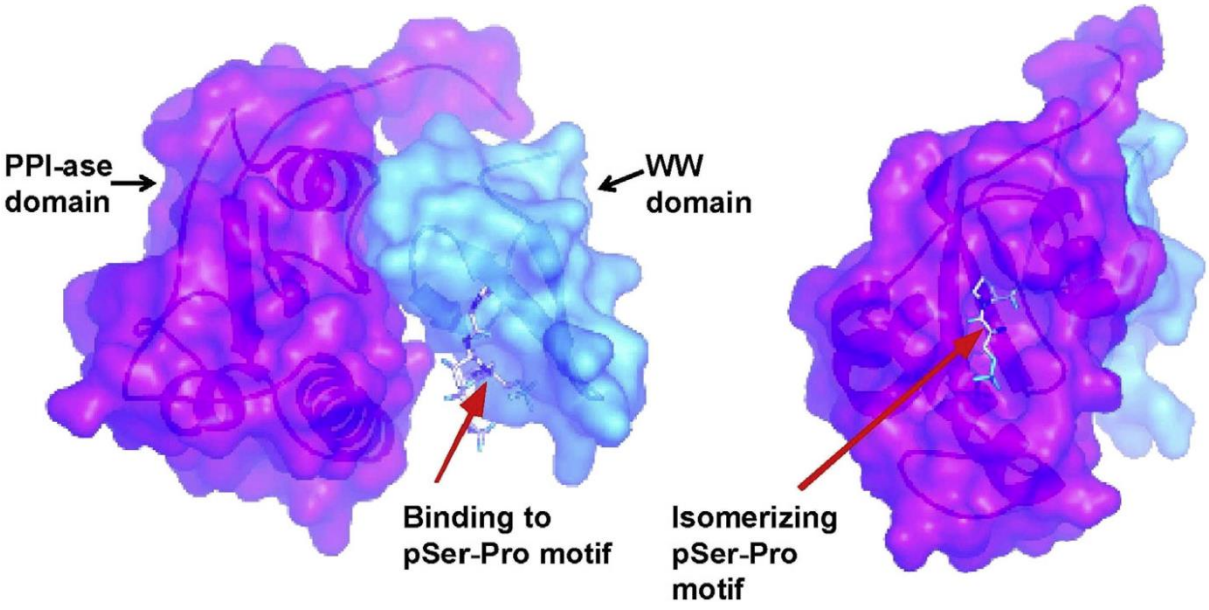

Figure 3. Structure of Pin1. Pin1 with its two-domain structure. The WW domain precisely binds to a proline followed by the phosphorylated serine/threonine residue, and the PPI-ase domain rotates the protein around the proline connection [103].

2.1.3 Cellular function of Pin1

The activity of Pin1 can be regulated post-translationally, through phosphorylation by protein kinases, sumolytion, and oxidation. The reduction and oxidation of Pin1 has been studied in relation to its role in Alzheimer's disease [104]. Ser residues 16 and 65 can both be phosphorylated to decrease substrate binding or to increase protein stability by reducing the occurrence of further modifications on the site [105] . Pin1 is localized *in vitro* to the nucleus and the cytoplasm, with the former being its predominant location [106]. Pin1 is the only peptidyl-prolyl cis/trans isomerase known to date that acts as a phosphorylation-directed enzyme. For several substrate proteins involved in signaling pathways mediating cancers and neurodegenerative diseases, Pin1 controls the conformational changes of the substrates involved in the pathogenesis [98, 107-109].

Pin1 interacts with Cyclin D1, a protein that forms a complex with cyclin-dependent kinases and functions as a regulatory subunit in the G1 to S phase transition of the cell cycle [110]. Once bound, Cyclin D1 transcription is increased as Pin1 can promote upstream signaling factors. These signaling factors include Jun N-terminal kinases, which generate phosphorylated c-Jun to stimulate further transcription of Cyclin D1.

Cyclin D1 is also unable to exit the nucleus and is therefore unable to be targeted to the proteasome for degradation [111]. Pin1 disables the re-generation of β-catenin and targets it to the nucleus where it can promote the transcription of other genes. The p65/RelA binding site located on nuclear factor kappa light chain enhancer of activated B cells (NF-κB) undergoes isomerization by Pin1, and the conformational change detaches NF-κB from an inhibitor, enabling nuclear targeting. Once in the nucleus, NFκB aids in promoting cell cycle progression. The transcription of E2 transcription factor (E2F) is positively controlled by Pin1 and this mechanism is used in cancerous tumors by the proteins human epidermal growth factor receptor 2 (Her2/Neu) and Ras to stimulate continuous cell growth in mammary epithelial cells [112].

Proliferating cell nuclear antigen (PCNA) is a protein involved in DNA replication however, other essential cellular processes, including chromatin remodeling, DNA repair, and cell cycle regulation, have been associated with PCNA [113]. PCNA is known to regulate remodeling in pulmonary arteries by controlling the proliferative status of various cells [114], and in breast cancer, over-expression of Pin1 led to an increase in PCNA affecting the tumor growth *in-vivo* [115]. In the wire-injury model, down-regulation of Pin1 via lentivirus mediated shRNA suppressed proliferation and caused senescence in VSMCs [116]. The activation of proliferative signals, as well as inhibition of apoptosis leading to survival of cells have been reported in several vascular proliferative diseases, including PH [117]. Braun *et al*. showed Pin1 depletion promotes apoptosis, since inhibition of Pin1 led to increased amount of cleaved poly-ADP ribose polymerase (PARP), an apoptotic substrate of Caspase-3 [118]. For this purpose, the inhibition or down regulation of Pin1 could effectively target cancers evading multiple pathways.

In addition to the above-mentioned example, previous studies have also identified a variety of other cellular proteins that interact with Pin1 including Akt [119], B-cell lymphoma 2 (Bcl-2) [120], Cell division cycle 25 (Cdc25) [121], tumor protein p53 (p53) [122] and Tau [123]. Amongst Pin1 substrates are numerous proteins, such as retinoblastoma protein (Rb) [124], neurogenic locus notch homolog protein 1 (Notch1) [125], and homeodomain-interacting protein kinase 2 (HIPK2) [126]. In association with various signaling pathways, cell cycle progression, gene transcription, tumor development, oxidative stress and apoptosis are markedly affected by Pin1 [106]; thus,

regulation driven by Pin1 provides a new platform for assembly of multiple protein networks.

2.1.4 Pin1 in transcriptional regulation

Pin1 influences multiple biological mechanisms and is implicated in human diseases such as cancer and neurological disorders. Pin1 regulates many transcription factors and alters the stability, subcellular localization, protein-protein or protein-DNA/RNA interactions of these proteins associated with transcription. The modulation by Pin1 at the transcription level affects several cell proliferation-related genes, as well as apoptosis and immune response [127].

Pin1 directly binds to and stabilizes HIF-1α in a phosphorylation dependent manner and controls its transcriptional activity [128]. Pin1 induces and maintains pluripotency by interacting with phosphorylated octamer-binding transcription factor 4 (OCT-4), transactivating its functions and stability [129]. Pin1 mediated isomerization of specificity protein 1 (Sp1) are important for promoting progression of the cell cycle during mitosis [130]. Androgen receptor (AR) is involved in cancer initiation, progression and metastasis and by modulating AR function, Pin1 actively participates in prostate cancer pathogenesis [131].

Increased Snail transcriptional activity and protein expression are involved during breast cancer development, and knockdown of Pin1 led to decreased Snail activity, implicating Pin1 in the epithelial-mesenchymal transition (EMT). The tumor suppressor function of CCAAT enhancer binding protein α (C/EBPα) is known to play an important role in granulopoiesis, and patients with acute myeloid leukemia (AML) have mutations in the C/EBPα gene. Inhibition of Pin1 leads to upregulation of C/EBPα levels and might provide a potential therapy in patients with C/EBPα mutations [132].

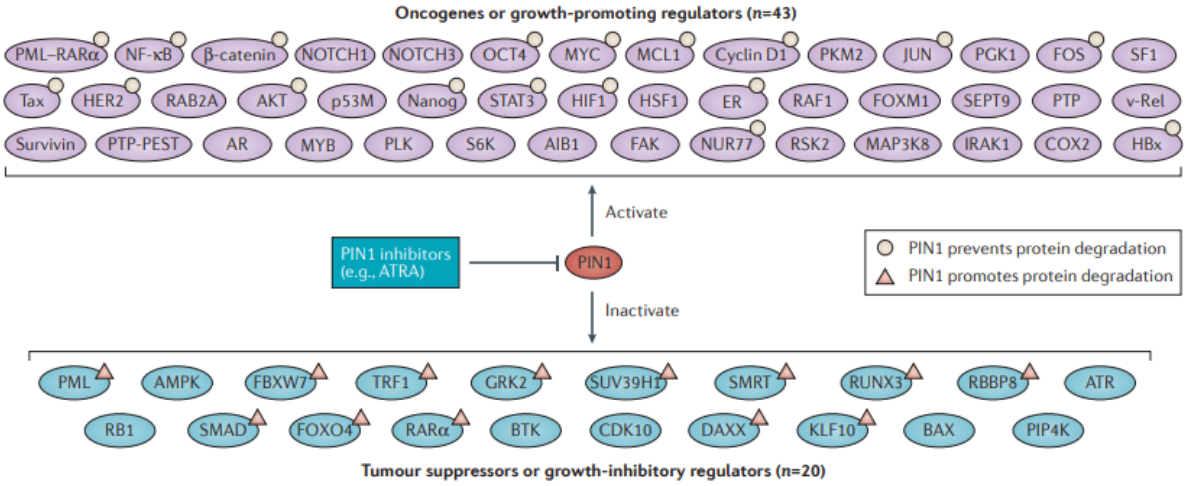

Figure 4. Pin1 activates various oncogenes and inactivates numerous tumor suppressors. Isomerization catalyzed by Pin1 controls the activity and function of various transcription factors [133].

2.1.5 Role of Pin1 in neurodegenerative diseases and cancer

In neurogenerative disorders, multiple lines of evidence have identified Pin1 as a major player in disease pathology [134]. Pin1 phosphorylates tau, which is known to be involved in Alzheimer's disease. Neurofibrillary tangles can develop in neurons when Tau becomes hyper-phosphorylated through a lack of Pin1 and PP2A function. Such tangles are common occurrences in the neurodegeneration process [135]. In many neurogenerative diseases, amyloid precursor protein (APP) forms plaques, and Pin1 interacts with the binding motif these proteins and helps to regulate the amount of amyloid beta peptides generated. The accumulation of amyloid beta peptides in the brain is increased by the cis amyloid beta peptides, and Pin1 is responsible for the cis to trans conversion of these peptides [136]. The absence of Pin1 (downregulated in Alzheimer disease) leads the pathogenic form to take over.

The cancer symptoms of Pin1 are in contrast to those of Alzheimer's as Pin1 is down-regulated in Alzheimer's and its degradation contributes to cell death, while in cancer the protein is up-regulated and is postulated to stimulate tumor development. Pin1 has a role in many forms of cancer including breast, liver, colon, and lung cancer [111, 137-139]. Upon further characterization, overexpression of Pin1 has been implicated as a symptom of poor prognosis and a higher risk of recurrence in prostate cancer [140]. Pin1 is induced at the mRNA and protein levels in cancerous tumors. Pin1 has been extensively studied in tumors caused by the dysregulation of the protein pathways

Her2/Neu or Ras. Overexpression of Pin1 promotes the oncogenic effects of Neu and Ras, whereas Pin1-deficient mice do not display such effects. Neu and Ras affect the E2F augmented Cyclin D1 levels and a feedback loops leads to increased expression of Pin1 [141]. Pin1 inactivates as well as activates several tumor suppressors in cancer. In addition, Pin1 triggers growth arrest and apoptosis following oncogenic or genotoxic stress signals by the inhibiting tumor suppressing activities of p53 family members, such as p53 itself and p73 [106]. Pin1 has therefore been recognized as a potential therapeutic target because of its diverse implications in disease.

2.1.6 Role of Pin1 in cardiovascular disease

In recent years, Pin1 has gained a lot of attention in the field of cardiovascular disease. Pin1 plays an important role as a 'molecular orchestrator' in the heart by fine-tuning the signal amplitude and duration of various cardiovascular signaling pathways [142]. Pin1 is involved in neointima formation and in promoting pro-proliferative pathways. Pin1 deletion in VSMCs resulted in cell cycle arrest leading to apoptosis via the β-catenin/cyclin D1/CDK4 cascade [143]. Pin1 via signal transducer and activator of transcription 3 (STAT3) induced cell cycle arrest and affected apoptosis in VSMCs in type 2 diabetic mice [144]. Pin1 regulates cardiac hypertrophy by controlling the intensity and duration of hypertrophic signaling networks. Pin1 interacts with Akt, Raf-1 and MEK directly wherein Pin1 depletion leads to attenuation of Akt and MEK hypertrophic signaling. Overexpression of Pin1 caused MEK activation impairment through Raf-1 interaction [145]. Pin1 plays a role in neointima formation as it is expressed in the intimal as well as medial layers of the injured arteries, and via downregulation of nuclear factor E2-related factor-2 (Nrf2), stimulated uncontrolled proliferation of VSMCs [146].

Nitric oxide (NO) is a vasodilator, having a vasoprotective reaction, which is crucial for normal physiological functions of blood vessels [147]. It is important in blood pressure control, in the formation of atherosclerotic lesions and in PH [148]. Endothelial nitric oxide synthase (eNOS) produces nitric oxide in endothelial cells, and its activity is regulated by post-transcriptional modifications as a result of protein–protein interactions and reversible phosphorylation [149]. Chiasson et al. showed that Pin1 promotes Ser116-dephosphorylation of eNOS and thus enhances eNOS activity and NO production. In endothelial cells, Pin1 deletion by short interference RNA or

inhibition with juglone enhanced the phosphorylation of Ser116 on eNOS and inhibited vascular endothelial growth factor-induced Ser116 dephosphorylation [150]. In contrast, Paneni et al. demonstrated that Pin1 modulates pSer116 of eNOS and promotes its interaction with caveolin-1 (repressor), leading to blunted eNOS activity and reduced NO release [151]. Thus, Pin1 acts as a double-edged sword in the regulation of nitric oxide signaling in pulmonary vessels.

2.2 Aims of the study

Pulmonary arterial hypertension is a chronic condition caused by obliterative pulmonary vasculopathy, which primarily affects the small arteries of the lungs. Abnormal proliferation and resistance to apoptosis of vascular cells causes vessel wall thickening and dysregulation of vascular tone, leading to vasoconstriction of pulmonary vessels. At present, no pharmacotherapeutic approaches provide a cure for PAH. Currently PAH approved drugs are vasodilators, calcium-channel blockers, blood-thinners and diuretics. While these therapeutic interventions alleviate the pulmonary vasoconstrictive element of the disease and offer symptomatic relief as well as improvement in prognosis, no clear evidence is available to support the direct anti-proliferative and pro-apoptotic action of these vasodilators on pulmonary vascular cells. Thus, new pharmacotherapies for PAH should target the pulmonary vasculature, and a number of drug candidates are currently under review for vascular remodeling.

The multiple roles played by PPI-ases in folding newly synthesized proteins, immune system function and cell cycle control elevates the importance of this enzyme family. The unique ability of Pin1 to bind with phosphorylated trans forms of Ser/Thr-containing proteins that either enhances degradation and/or stabilizes the protein and makes it an effective molecular switch of multiple downstream cellular functions. Due to the role of Pin1 in cell transformation and uncontrolled cell growth in oncology, it is speculated to function as a regulator of SMCs proliferation. Thus, Pin1 represents a novel target and potential new strategy for the prevention of cardiovascular diseases, including pulmonary arterial hypertension. The overall focus of the work presented in this thesis is on elucidating the role Pin1 in PH. Specifically, we aimed to:

- Examine the expression of Pin1 in experimental and clinical PAH
- Investigate the effect of Pin1 inhibition on proliferation of human PASMCs and PAECs
- Investigate the effect of Pin1 inhibition on survival of human PASMCs and PAECs
- Investigate Pin1 and its interacting transcriptional regulators
- Investigate the effect of Pin1 inhibitor Juglone in mouse model of chronic-hypoxia
- Investigate the effect of Pin1 inhibitor Juglone in rat model of SU5416/hypoxia

MATERIALS AND METHODS

3.1 Materials

3.1.1 Chemicals, kits and reagents

Product	Company
Acetic acid	Sigma-Aldrich, USA
Acrylamide	Roth, Germany
Ammonium persulfate (APS)	Sigma-Aldrich, USA
Bone Morphogenic Proteins	PeproTech, USA
Bovine serum albumin (2 mg/ml)	Bio-Rad, USA
Bovine serum albumin (20 mg/ml)	Sigma-Aldrich, USA
Bovine serum albumin powder	Serva, Germany
Cell Proliferation ELISA, BrdU (colorimetric)	Roche, USA
Cresyl Violet perchlorate	Sigma-Aldrich, USA
DAB substrate kit	Vector, Germany
DharmaFECT1	GE Dharmacon
DC™ Protein Assay	Bio-Rad, USA
Dimethyl sulfoxide (DMSO)	Sigma-Aldrich, USA
Disodium phosphate (Na2HPO4)	Roth, Germany
Eosin Y	Sigma-Aldrich, USA

Enhanced chemiluminescence (ECL) kit	Amersham, USA
Epidermal Growth Factor	PeproTech, USA
Ethanol 70%	SAV LP, Germany
Ethanol 96%	Otto Fischhar, Germany
Ethanol 99.9%	Berkel AHK, Germany
Ethylenediaminetetraacetic acid (EDTA)	Sigma-Aldrich, USA
Glycerol	Sigma-Aldrich, USA
Glycine	Roth, Germany
Heparin	Ratiopharm, Germany
Human PIN1 ELISA kit	LSBio
Hydrogen peroxide 30%	Vector, Germany
In-situ Cell death detection kit	Roche, Switzerland
Interleukin-6	Peprotech, USA
Isopropanol	Sigma-Aldrich, USA
iScript cDNA synthesis kit	Bio-Rad, USA
Isoflurane	Baxter, UK
iTaq SYBR Green Supermix	Bio-Rad, USA
Juglone	Santa Cruz, USA

Ketamine	Bela Pharm, Germany
Monopotassium phosphate (KH2PO4)	Roth, Germany
Non-fat milk powder	Roth, Germany
Normal horse serum	Vector, Germany
Paraformaldehyde (PFA) 3.7%	Sigma-Aldrich, USA
Paraplast® Plus paraffin embedding medium	Sigma-Aldrich, USA
Prolong™ gold antifade reagent	Thermo-fischer, USA
PDGF-BB	R&D Systems, USA
Potassium chloride (KCl)	Sigma-Aldrich, USA
Precision Plus Protein Dual Standards	Bio-Rad, USA
RIPA buffer	Santa Cruz, USA
RNeasy Plus Mini Kit	Qiagen, Germany
Saline (NaCl 0.9%)	B. Braun, Germany
SDS Solution, 20% w/v	AppliChem, Germany
SDS polyacrylamide gel	Thermo-Scientific, USA
SIRCOL collagen assay	Biocolor Ltd., UK
Sodium Orthovanadate (Na3VO4)	Sigma-Aldrich, USA
SU5416	Tocris, UK

Tissue-Tek® O.C. T™ Compound	Sakura, Japan
TF Activation Profiling Plate Array II	Signosis, USA
Tris Base	Roth, Germany
Tris-HCl	Roth, Germany
Triton-X100	Sigma-Aldrich, USA
Tumor Necrosis Factor-alpha	Peprotech, USA
Tween®20	Sigma-Aldrich, USA
Xylol (isomere) >98%	Roche, Germany
β-Mercaptoethanol	Sigma-Aldrich, USA

3.1.2 Cell culture medium

Product	**Company**
Cascade Biologicals Medium 200	Gibco, USA
DPBS	PAN, Germany
Endothelial Cell GM MV 2	PromoCell, Germany
Fetal bovine serum	Roth, Germany
Opti-MEM I	Gibco, USA
Smooth Muscle Basal Medium (SmBM)	Lonza, Germany

Smooth Muscle Growth Medium-2 (SmGM-2)	Lonza, Germany
Rat Fibroblasts Basal Medium	Cell Applications Inc., USA

3.1.3 Antibodies

3.1.3.1 Primary antibodies

Antibody (catalog no.)	**Company**
Caspase-3 (#9662)	CST, USA
C/EBP-α (sc-365318)	Santa Cruz, USA
Cleaved-PARP (#9541)	CST, USA
Cyclin D1 (sc-8396)	Santa Cruz, USA
HIF-1α (ab2185)	Abcam, UK
PARP (#9532)	CST, USA
Pan-actin (#4968)	CST, USA
PCNA (sc-7907)	Santa Cruz, USA
p-STAT3 (#9145)	CST, USA
Pin1 (sc-46660)	Santa Cruz, USA
STAT3 (#4904)	CST, USA

3.1.3.2 Secondary antibodies

Horseradish peroxidase (HRP)–conjugated secondary antibody:

1. Sheep anti-rabbit IgG (1:10000), GE Healthcare, USA
2. Donkey anti-mouse IgG (1:5000), GE Healthcare, USA

3.1.4 Primers

Gene	**Species**	**Sequence**
HPRT	Homo sapiens	Fw 5'-TGACACTGGCAAAACAATGCA-3'
HPRT	Homo sapiens	Rev 5'-GGTCCTTTTCACCAGCAAGCT-3'
HPRT	Mus musculus	Fw 5´-CAGTCCCAGCGTCGTGATTA-3´
HPRT	Mus musculus	Rev 5´-TGGCCTCCCATCTCCTTCAT-3´
HPRT	Rattus norwegicus	Fw 5'-ACAGGCCAGACTTTGTTGGAT-3'
HPRT	Rattus norwegicus	Rev 5'-GGCCACAGGACTAGAACGT-3'
Pin1	Homo sapiens	Fw 5'-GCAGCTCAGGCCGAGTGTA-3'
Pin1	Homo sapiens	Rev 3'-TGCGGAGGATGATGTGGATG-5'
Pin1	Mus musculus	Fw 5'-CACCCTACGCACCTTCCATT-3'

Pin1	Mus musculus	Rev 3'-GTTGAGGGGGCCTCTGTTAC-5'
Pin1	Rattus norwegicus	Fw 5'-AGCTCAGGCCGTGTCTACTA-3'
Pin1	Rattus norwegicus	Rev 3'-TGCTTTTCGCAACGGAACAG-5'

3.1.5 Equipment

Equipment	**Company**
Aspiration system, Integra Vaccusafe	Integra Biosciences, Germany
Amersham™ Imager 600	GE Healthcare, UK
Balance XS205	Mettler Toledo, USA
Balance PCB 200-2 Precision	Kern, Germany
BioDoc Analyzer	Biometra, USA
Catheter SPR-671	Millar Instruments, USA
Cell culture incubator	Heraeus, Germany
Centrifuge Rotina 420R	Hettich, Germany
Centrifuge Mikro 200R	Hettich, Germany
Centrifuge 5417R	Eppendorf, Germany
Electrophoresis Cell Xcell Surelock	Thermo fisher, USA
Fluorescence microscope BZ-9000	Keyence, Japan
Freezer (+4°C, -20 °C, -80 °C)	Bosch, Germany

Hypoxia Chambers	Bio Spherix, USA
Hypoxic gas (10% O2) ventilation	Praxair, Germany
Incubator Hera Cell 150	Thermo Scientific, USA
Incubator hood, TH15	Edmund Bühler, Germany
Infinite® 200 microplate reader	Tecan, Switzerland
Inolab PH meter	WTW, Germany
Laser-assisted micro dissector	PALM Microlaser Technologies, Germany
Light microscope DM IL	Leica, Germany
LightCycler® 480 Instrument	Roche, Germany
Microtome RM2165	Leica, Germany
Mounting bath HI1210	Leica, Germany
Mounting heating plate HI1220	Leica, Germany
Multifuge centrifuge Mx3000P	Heraeus, Germany
NanoDrop spectrophotometer	Thermo fisher, USA
qPCR	Stratagene, USA
Pipetboy and pipettes	Eppendorf, USA
Precellys®24 homogenizer	BertinTech., France
Rice cooker	Gastrobach, Germany
Shaker WT-16	Biometra, Germany
ThermoMixer F1.5	Eppendorf, Germany

Thermocycler T3000	Thermo fisher, USA
VEVO 1100 Imager	Visualsonics, Toronto, Canada
Vortex machine	VWR, Germany
Water bath, SWB series	Stuart Equipment, UK
Western blot transfer	Bio-Rad, USA
Western blot, Powerpac basic	Bio-Rad, USA

3.1.6 Materials

Name	**Company**
6-well, 24-well, 96-well microplate	Corning, USA
96er PCR-plate	Steinbrenner, Germany
Cell culture dishes, plates	Sarstedt, Germany
Chemiluminescence Amersham Hyperfilm	GE Healthcare, UK
Cover glass	Langenbrinck, Germany
Falcon tubes	BD Biosciences, USA
Film cassettes	Kodak, USA
Filter tips (10, 100, 1000µl)	Nerbe plus, Germany
Gel blotting paper	Whatman, USA
Needles 26-20G (0.45-0.9mm)	Microlance™ 3 BD, Ireland

Nitrocellulose membrane	Bio-Rad, USA
Parafilm, PM-996	Bemis, USA
Scalpels	Feather, Japan
Syringes 1, 2, 5, 10, 25 ml	B. Braun, Germany
Tips (10, 100, 1000 µl)	Eppendorf, USA

3.1.7 Softwares

Adobe Illustrator CS6	Adobe, USA
Adobe Photoshop CS6	Adobe, USA
Fluorescence BZ-II Viewer and Analyzer	Keyence, Japan
Graph Pad Prism® v6.05	GraphPad statistics, USA
i-Control	Tecan, Austria
LightCycler® 480 Software	Roche, Germany
Magellan v.6.3	Tecan, Austria
MxPro™ QPCR Software	MS® Agilent Technologies, USA

3.2 Methods

3.2.1 Human pulmonary artery smooth muscle cells (PASMC)

Human primary PASMCs from control donors (n = 4) Lonza (CC-2581, Switzerland) or from patients with IPAH (n = 9) (obtained both from Lonza and UGLMC Giessen Biobank of the Justus-Liebig University Giessen (Giessen, Germany)). Human primary PASMCs were used between 5-8 passages. They were cultured in Smooth Muscle Cell (SMC) Growth Medium-2 (SmGM-2) with the supplement mix containing 5% fetal bovine serum, human fibroblast growth factor (2 ng/ml), human epidermal growth factor (0.5 ng/ml), and insulin (5 µg/ml) (Lonza, Germany).

3.2.1.1 Seeding and culture

The cryopreserved cells were thawed either in the hand or in the water-bath for 1 min and seeded in in 100 mm dishes and placed in the incubator at 37°C and 5% CO2. They were incubated at 37°C and 5% CO2 until the cells reached confluency. For further culture, the cells were trypsinized with 5% trypsin, and cell pellets were re-suspended in the fresh SmGM-2 growth medium. Cell count was determined using a hemocytometer under the light microscope. Cells seeding density were 3,500 cells/cm^2.

3.2.1.2 Cryopreservation

Upon confluency, cells were washed and trypsinized by adding warm 5% trypsin. Complete growth medium (SmGM-2) was added to stop the trypsin activity. The cells were collected in a falcon tube and centrifuged at 1,000 *rpm* and 22°C for 10 mins. The pellet was then resuspended in a cooled freezing cryopreservation medium (SmGM-2: DMSO: FBS, 8:1:1), kept in a cell-freezing container for 24 hours at -80°C, and was later transferred to liquid nitrogen and stored for future use.

3.2.1.3 siRNA transfections

120,000 PASMCs per well were seeded in a 6-well plate. The cells were serum starved with SmBM for 24 hours and then next day transfected with 30 nM of Pin1 (or control siRNA) lipoplexed with DharmaFECT1 (GE Dharmacon, USA) in Opti-MEM I medium (Gibco, USA). Medium with siRNA complex was replaced with complete growth

medium after 6 h (SmGM-2), and the knockdown efficiency was examined 24h after transfection via western blot.

3.2.1.4 Transcription Factor Activation Profile Array

siRNA tranfections with Pin1 siRNA or scrambled-siRNA in PAMSCs were performed as described above. Nuclear protein was extracted with the nuclear extraction kit (Thermo-Scientific, USA). The nuclear extracts were incubated at room temperature with biotin-labeled probe mix and TF buffer for 30 minutes. The isolation column was equilibrated with 200 µl of pre-chilled Filter Binding buffer. To separate the TF-probe complexes from free DNA probes, the above reaction mixture was centrifuged at 6000 rpm for 1 min and collected in a collection tube. The reaction mixture was transferred directly onto the filter of isolation column, avoiding the bubbles, and was incubated on ice for 30 mins. The isolation column then was washed with pre-chilled filter wash buffer and incubated on ice for 3 mins. The isolation column was centrifuged at 6000 rpm for 1 min in a microcentrifuge at 4°C. Flow-through was discarded. The column was again washed with pre-chilled wash buffer on ice. The isolation column was centrifuged at 6000 rpm for 1 min and flow-through was discarded. The washing steps were repeated additionally for a total of 4 washes. To elute the bound probes, elution buffer was added at the center of the column and incubated at room temperature for 5 mins. The column was centrifuged at 10,000 rpm for 2 mins at room temperature. The eluted probe was transferred to a PCR tube and denatured at 98°C for 5 mins. Immediately the denatured probes were transferred to prechilled ddH20 and were placed on ice. To hybridize, the eluted probes were mixed with pre-warmed hybridization buffer in a reservoir. 100µl of the mixture was added onto the 96-well hybridization plate using multi-channel pipette. The 96-well plate was then placed in an incubator at 42°C overnight. To detect the bound probe, the 96-well plate was inverted and the contents were expelled forcibly. The plate was washed with pre-warmed hybridization wash buffer and incubated for 5 mins at a shaker. The contents were again forcibly removed on a paper towel and washing steps were repeated two more times. 200 µl of blocking buffer was added to each well and plate was incubated for 5 mins at room temperature. The plate was inverted and contents were removed. Diluted streptavidin-HRP conjugate was added to the wells and incubated at room temperature for 45 mins. The contents of the plate were then removed and the plate

was washed with detection wash buffer and incubated 5 mins each on a gentle shaker. The washing step was repeated two more times. Freshly prepared substrate solution was added to the plate and incubated for 1 min at room temperature outside, followed by 4 mins incubation in the luminometer (TECAN, Switzerland). The luminescence (RLU) was recorded within 5-20 mins.

3.2.2 Human pulmonary artery endothelial cells (PAEC)

Human pulmonary artery endothelial cells (PAECs) from healthy individuals were purchased directly from Lonza (Basel, Switzerland). Human primary PAECs were used between 3-6 passages. They were cultured in Endothelial Cell GM MV 2 (PromoCell, Germany) with a supplement mix including 5 % Fetal Calf Serum (FCS), 5 ng/ml recombinant human epidermal growth factor (hEGF), 10 ng/ml recombinant human basic fibroblast growth factor (hbFGF), 20 ng/ml Insulin-like Growth Factor (IGF), 0.5 ng/ml ml recombinant human vascular endothelial growth factor 165 (VEGF), 1 µg/ml ascorbic acid (AA) and 0.2 µg/ml Hydrocortisone.

3.2.3 Proliferation assay

Pulmonary artery smooth muscle cells and endothelial cells were seeded at 4000 cells per well in a 96-well plate. The cells were serum starved for 24 h and stimulated with, in case of PAMSCs, human recombinant PDGF-BB (30 ng/ml; R&D Systems, USA) and with 10 % FBS (fetal bovine serum) for endothelial cells, in the presence or absence of juglone (1, 5, 10 µM; Santa Cruz USA) for 24 h. For knockdown analysis, PASMCs were transfected with Pin1 siRNA or control siRNA and were serum starved for 24 h. The cells were stimulated with human recombinant PDGF-BB after starvation and proceeded with proliferation assay. The proliferation of cells was assayed with a kit from Roche (Basel, Switzerland) that monitors the incorporation of 5-bromo-2deoxyuridine (BrdU) into newly synthesized DNA. The incorporated BrdU was detected using anti-BrdU–peroxidase conjugate in accordance with the manufacturer's instructions. After the reactions were stopped, absorbance was measured at 450 nm using a Tecan M200 (Tecan, Switzerland) infinite multi-mode microplate reader.

3.2.4 Apoptosis assay

Pulmonary artery smooth muscle cells and endothelial cells were seeded at 18000 cells per well and 24000 cells per well, respectively, on a cover glass pre-coated with gelatin in a 24-well plate. The cells were treated with varying concentrations of juglone (1, 5, 10 µM) for 20 h. The detection of apoptosis in cells was examined by Terminal deoxynucleotidyl transferase dUTP nick end labeling (TUNEL) analysis. Apoptosis results in cleavage of genomic DNA producing nick-ends, which can be labelled and detected under a fluorescence microscope. *In-situ* cell death detection kit-TMR (Roche, Switzerland) was employed to monitor apoptosis. The cells were air-dried, followed by fixation with 4% paraformaldehyde. The cells were washed with PBS (1X) and were then further permeabilized with triton-X100 (0.1%) and labelled with labelling solution. For TUNEL analysis in lung tissues, the tissue was deparaffinized by two washes in xylene. The tissue was then rehydrated in an alcohol series (99.6%, 96%, 70% ethanol) for five minutes each. Slides were boiled in citrate buffer for 10 mins and then cooled at room temperature for 20 mins. After washing the slides in PBS, lungs were labelled with labelling solution for 1 h. Slides were washed in PBS and kept in primary antibody overnight. Next day, slides were washed with PBS and stained with secondary antibody and DAPI respectively. A BZ-9000 fluorescence microscope (Keyence, Japan) was used to detect the fluorescence from labelled cells.

3.2.5 Western blotting

3.2.5.1 Protein Isolation

The total protein was extracted using RIPA buffer containing proteinase/phosphatase inhibitor cocktail. For protein isolation from lung tissue, 30 mg of lung tissue was homogenized in 300 µl of RIPA containing proteinase/phosphatase inhibitor cocktail and PMSF. Cells were washed with PBS and 100 µl of RIPA was added to the PASMCs from one six-well plate. Cells were scraped with a cell-scraper and cell lysate was incubated in RIPA for 30mins on ice. Cell lysate was collected in a tube and centrifuged at 12,000 *rpm* for 15 minutes at 4°C. Lysates were further used for protein measurements or stored at - 80°C.

3.2.5.2 Concentration measurements

According to the manufacturer's protocol for the microplate assay procedure, protein concentration was measured using a Bio-Rad DC protein assay. The reaction between Protein and copper interacts in an alkaline medium (Reagent A) and leads to the reduction of Folin (Reagent B) reagent resulting in blue color formation. The bovine serum albumin (BSA) concentration in the range 0.25-2 mg/ml, was used as the standard for cell lysate protein and 1.25-20 mg/ml was used as the standard for tissue lysate protein. The protein samples were incubated in the Reagent A and B for 15 mins at room temperature. Once the blue color was developed, absorbance at 750 nm was measured with the help of Tecan microplate reader. The final protein concentration was measured with accompanying Magellan™ software using the linear regression method.

3.2.5.2 SDS-polyacrylamide gel electrophoresis (SDS-PAGE)

Normalized protein samples were mixed with SDS gel loading buffer at a ratio of 4:1 (v/v) along with reducing agent (1:10) and denatured at 95°C for five minutes. NuPAGE™ 4-12% Bis-Tris (Thermo Fischer, USA) polyacrylamide gels were used to run the protein samples. Protein samples and dual protein markers were loaded into the lanes of SDS-PAGE gel and NuPAGE™ MOPS SDS running buffer (20X, Thermo Fischer, USA) was used. All the samples were run at 120V for 2-3 hours to separate.

The proteins that were separated with the SDS-PAGE were transferred to a nitrocellulose membrane at 100V for one hour using a blotting apparatus and running buffer with Tris-HCL, Glycine and SDS with final concentrations of 25mM, 192mM and 0.1% (w/v) respectively. The membranes were blocked with 5% non-fat milk, diluted in tris-buffer saline with tween-20 (TBST) for one hour at room temperature and probed with primary antibodies (diluted in TBST with 5% BSA) at 4°C overnight. After washing three times with TBS containing 0.1% Tween-20, horseradish peroxidase (HRP)-conjugated secondary antibodies (diluted in TBST with 5% BSA) were applied for one hour at RT. After washing, the blots were developed in Amersham™ Imager 600 (GE Healthcare, USA) using an enhanced chemiluminescence (ECL) kit. The intensity of the bands was quantified with Amersham™ Imager 600 analysis software.

3.2.6 Polymerase chain reaction (PCR)

3.2.6.1 RNA isolation

The Qiagen RNeasy Mini Kit was used to separate the total RNA of cells and lung tissue. Cells were washed with PBS and 350 µL of RLT Buffer was added. Cells were incubated for 5 mins in the buffer. The lysate was scraped and extracted with the cell scraper. Collected cell lysate was mixed properly with the pipet to ensure no clumps remained. For RNA isolation from lung tissue, 30mg of the tissue was weighed and added to the homogenizing tube with beads. 200µL of RLT was added to the same tube and homogenized twice for 40 seconds in a rotor-stator homogenizer. The tubes were then centrifuged for 5 mins at the maximum speed (14,000 *rpm*) and the supernatant was collected in a tube and stored for further use. Cell lysate or tissue supernatants were applied to the QIAshredder spin column placed in a 2ml collection tube and centrifuged at 13,000 rpm for 2 minutes. 70% ethanol with an equal volume of was added to the supernatant and was mixed well with the pipet. 700µl of the sample along with precipitate was transferred into an RNeasy mini column placed in a 2ml collection tube. The sample was then centrifuged for 15 secs at 10,000 *rpm*. 700 µL of RW1 buffer was added to the RNeasy mini column and centrifuged for 15 sec at 10,000 *rpm*. The flow through was discarded. 500 µL of RPE buffer was added and centrifuged for 15 sec at 10,000 *rpm*. Again the flow through was discarded. The step was repeated twice. For the final elution step, RNeasy mini column was placed in a new 2ml collection tube and and centrifuged for 15 sec at 10,000 *rpm* to remove any excess flow-through. 30-50µL of RNase-free water was added directly to the spin column membrane and centrifuged for 1 min at 10,000 *rpm*. The quality and concentration of total RNA was measured with a NanoDrop spectrophotometer and the RNA was stored at -80°C.

3.2.6.2 Quantitative real-time polymerase chain reaction (qPCR)

QPCR was used to analyze the expression of various genes. NCBI/ Primer-BLAST was used to determine the primers for human, rat and mouse genes. All the primers used were in the range 100 bp - 300 bp. Mx3000P® QPCR system was used to quantify qPCR and iTaq™ SYBR® Green Supermix kit was used with water as negative

control. Manufacturer's protocol was used to measure and quantify the gene expression.

For each gene, the threshold cycle was calculated (Ct values). Hypoxanthine-guanine phosphoribosyl transferase (*HPRT*) was taken as a reference gene and all the Ct values from the specific genes were normalized using the formula ΔCt = Ctreference – Cttarget keeping HPRT as reference gene. ΔΔCt was calculated with control group Ct values being subtracted from treated group. To represent the data in fold change, $2^{-\Delta\Delta CT}$ was calculated to represent the mRNA expression of the genes.

Step	**Temperature**	**Time**	**Cycle**
Activation	**95°C**	**10 min**	**1**
Denaturation	**95°C**	**30 sec**	**40**
Annealing	**58°C**	**30 sec**	**40**
Extension	**72°C**	**30 sec**	**40**
Denaturing	**95°C**	**1 min**	**1**
Dissociation curve	**55-95°C**	**indefinite**	**1**
Hold	**4°C**	**indefinite**	**1**

Table 3: Quantitative PCR program

4.1 Mouse ventricular fibroblasts

Adult murine cardiac fibroblasts (CFs) were isolated with the preparation of the right ventricle and tissue pieces from several animals. All tissues were brought together, washed several times in ice-cold PBS, and the cells digested with the enzyme Liberase DH (cat. No. 05401089001, Roche, Mannheim). Other cell types were separated with several centrifugation steps, and finally, right ventricular fibroblasts were cultivated in DMEM medium (cat.no. E15-806, PAA, Cambridge, UK) with 10% FCS, 100 U/ml penicillin and 10 µg/ml streptomycin. All experiments were carried out with cells of the first or second passage.

4.2 Collagen synthesis in cardiac fibroblasts

CFs were serum starved for 24 hrs. The cells were then treated with 5 µM Juglone and stimulated with TGF-β1 (10 ng/ml) for 72 hours. L-Ascorbic acid, an essential co-factor for collagen synthesis, was added daily to the medium with the end concentration of 0.25 mM. The secreted collagen in the cell culture medium was determined according to the manufacturer's instructions of the Sircol Soluble Collagen Assay (Biocolor Ltd, Carrickfergus, UK). After 72 hours stimulation of the cells, cell culture medium was incubated with the Isolation & Concentration Reagent overnight at 4°C. The following day, the collagen in the sample was specifically stained and the concentration was determined using a spectrophotometer.

5.1 Animals

The animal study protocol (GI20/10 Nr. G82/2018) was approved by the Regierungspraesidium, Giessen, Germany. The in vivo studies were performed on Chronic hypoxia mice and SU5416+Hypoxia induced PAH rat models. The adult male C57Bl6 mice (21–24 g body weight) and adult male Kyoto Wistar rats (200-250g), aged between 10-12 weeks, used in this study were obtained from Charles River Laboratories. All the animals were housed under controlled conditions and were fed standard diet.

5.2 Experimental PH model and treatments

Adult rats were selected in a randomized manner and were divided in control (n=5), placebo (n=5) and Juglone treated (n=10) group. SU5416 was dissolved in DMSO and subcutaneously injected (20 mg/kg body weight) on the neck. After the injection, rats were kept in a hypoxia (10% O_2) chamber for three weeks, followed by re-exposure to normoxia for another two weeks. Saline was given to the control rats, and they were placed in normoxic chambers for the same duration. Hemodynamic measurements were taken at the end of the study and tissue were harvested from the animals. In the Juglone treated group, mice and rats were injected intraperitoneally with Juglone with 3 mg/kg and 1.5 mg/kg per body weight, respectively. Control mice and rats were injected with ethanol.

5.3 Echocardiography

Echocardiographic measurements were performed by Dr. Akylbek Sydykov with the small animal phenotyping platform in the cardio-pulmonary institute (CPI), Gießen. All the measurements were performed noninvasively, and images were acquired with a VEVO 1100 (Visualsonics, Toronto, Canada) high-resolution imaging system equipped with MicroScan linear array transducers. Animals were anesthetized and their chest was shaved. For obtaining echocardiographic measurements, animals were placed in a supine position, and ECG electrodes were taped to the shaved area of the chest. To measure the right ventricle internal diameter (RVID), the distance between the inner linings of the right ventricle free wall to the inner lining of the interventricular septum towards the right ventricle was defined. Measured in millimeters, RVID serves as a parameter of right ventricle hypertrophy and dilatation. Cardiac output (CO) was measured as the volume of blood ejected from the ventricle into the circulation per minute. Cardiac output equals SV multiplied by heart rate. Cardiac index (CI) was measured as the ratio of cardiac output per 100 grams of the body mass; it estimates the performance of cardiac output according to the size of the body.

5.4 Assessment of PH

Animals were anesthetized followed by a subcutaneous injection of heparin (50 IU/kg body mass) to measure the hemodynamic parameters. Animals were tracheotomized and kept ventilated at 60 breaths/minute. A pressure catheter (SPR-671 Mikro-Tip®, Millar Instruments, Houston, Texas, USA) was inserted through the right jugular vein to measure right ventricular systolic pressure (RVSP), and into the left carotid artery to measure arterial pressure. In ideal conditions, RVSP is equivalent to pulmonary artery systolic pressure (PASP). Following the hemodynamic measurements, the heart was harvested with RV and LV with septum separated and weighed for calculation of the RV hypertrophy index (ratio of RV free wall weight over the sum of the septum plus LV free wall weight [RV/LV+S]).

5.5 Lung tissue harvest and preparation

Lungs were flushed through the pulmonary artery with saline and the right lobe was immediately snap frozen in liquid nitrogen and stored at -80ºC for molecular biology assessments. Left lobes were perfused under 22 cm H_2O of pressure with 3.5 to 3.7% formalin, and immersed in formalin for 24 hours. Formalin-fixed lung tissue samples were washed and stored in phosphate-buffered saline for 48 hours. PBS was changed after 24 hours, and lungs were dehydrated overnight in a tissue processor. The lung tissues were then embedded at the embedding station and sectioned to 2µm thick sections on the fully-automated rotation microtome (Leica, Wetzlar, Germany), and mounted on positively charged glass slides. Finally, the slides with lung sections were heated at 40°C and dried overnight in the oven at 37°C.

5.6 Medial wall thickness and occlusion of vessels

The assessment of medial wall thickness (MWT) and the occlusion score was performed with Elastica-van Gieson (EVG) staining. Medial wall thickness is defined as the distance between the internal elastic lamina and external elastic lamina. Muscularized arteries (20-50µm in diameter) percentage was calculated with the formula [(external diameter − internal diameter/external diameter) × 100] in EVG-stained slides. The pulmonary vessels were scored and divided into three categories, open (≥75%), partially closed (75%-25%) and closed (<25%) in respect to the free area within the lamina elastic interna. Around 100 pulmonary vessels were analyzed at 630-fold magnification per lung section from each rat. Light microscope was used for the analysis with Leica Qwin V3 computer-assisted image analysis software.

5.7 Laser-assisted microdissection of pulmonary vessels

Laser-assisted microdissection and pressure-catapulting technology (PALM Microlaser Technologies, Bernried/Germany) was performed. Each individual from non-PAH control (n=6) and IPAH (n=8) provided 150 arteries. Intrapulmonary arteries with a diameter of 250–500 µm were selected and microdissected and RT-PCR analysis was performed from each artery. Detailed method of preparation and collection of artery along with quantitative real-time PCR analyses were as described in [152]. Lung cryosections were stained with Cresyl Violet and Eosin Y before artery

collection. Slow running tap water was used to rinse the sides to remove the excessive dye. Total RNA was isolated using RNeasy Mini kit (74106, Qiagen, Venlo, Netherlands).

5.8 Picrosirius red staining

To determine the total collagen content in the right ventricle, 3 µm thin tissue sections from normoxia, SU5416-hypoxia, and SU5416-hypoxia + juglone treated rats were stained histologically. The tissue was deparaffinized at 58°C for one hour followed by three washes in xylene. The tissue was then rehydrated in an alcohol series (99.6%, 96%, 70% ethanol) for five minutes each. The collagen fibers were stained by incubating the tissue with 0.1% Sirius red in 1.2% picric acid (pH = 2) for 60 minutes. The tissue was then washed three times for two minutes in 1% acetic acid and then decolorized in an increasing ethanol series (70%, 96%, 99.6%). The tissue was finally washed in xylene for one minute and then fixed on slides using Entellan rapid mounting medium (Merck, KGaA, Darmstadt). The sections were analyzed on a light microscope with an integrated camera (Leica Microsystems GmbH, Nussloch) using the Leica Q Win V3 software (Leica Microsystems GmbH, Nussloch). The stained sections were scanned with at least 90 visual fields per heart, so that the mean of all visual fields represents the fibrotic portion of a heart.

RESULTS

6.1 Peptidyl-prolyl isomerase 1 activation in human PAH lungs

Peptidyl-prolyl isomerase 1 (Pin1) expression was assessed in lung specimens of patients with idiopathic pulmonary hypertension (IPAH). In comparison with non-PAH controls, Pin1 immune reactivity was primarily defined in pulmonary vascular compartments of patients with IPAH (Figure 5). Substantial increased expression of Pin1 was found in the medial layer confirmed by co-localization with α-smooth muscle actin (α-SMA) in the pulmonary arterial walls of IPAH lungs.

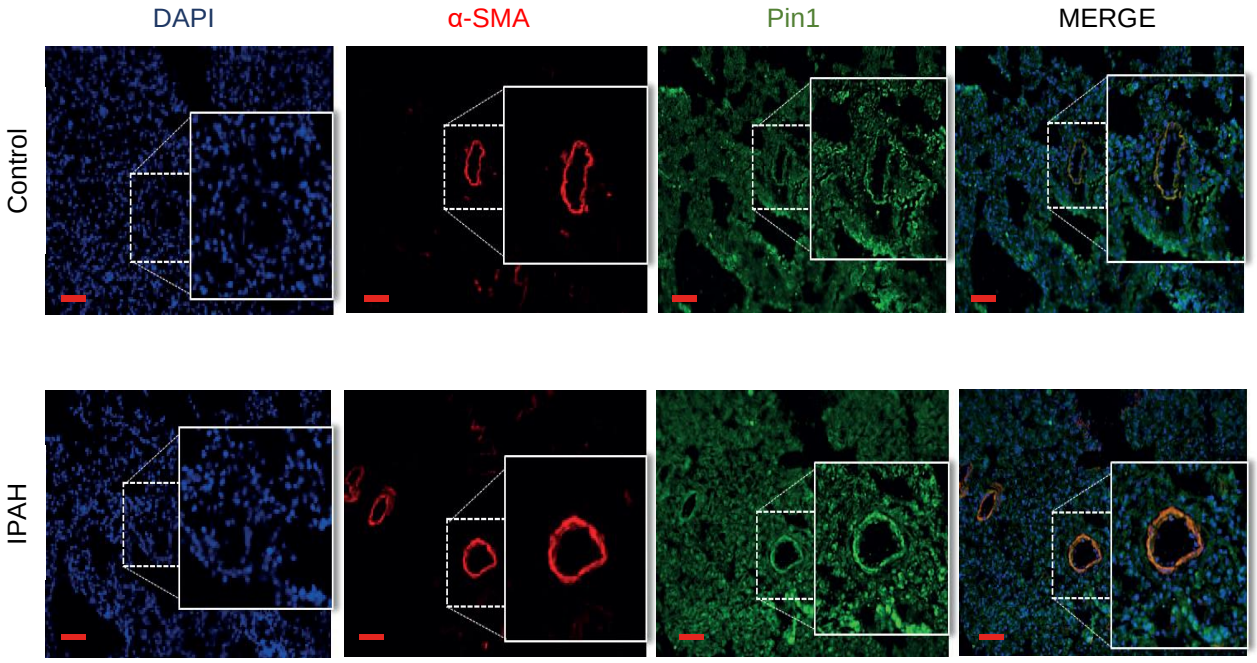

Figure 5. Peptidyl-prolyl isomerase 1 activation in human PAH lungs. Representative immunofluorescence micrograph of cryo-preserved human lung sections from control and IPAH patients. Staining was undertaken for Pin1 (green), and vessel identity was visualized by α-smooth muscle actin (red). DAPI is stained blue. Scale bar: 50 μm.

6.2 Peptidyl-prolyl isomerase 1 activation in human PAH smooth muscle cells and laser-assisted micro-dissected vessels vessels

Pulmonary arterial smooth muscle cell (PASMC) plays a crucial role in the development of PAH; thus we examined the expression of Pin1 in PASMCs isolated from IPAH patients. In contrast with non-PAH control PASMCs, western blot analysis

showed significantly higher Pin1 expression in IPAH-PASMCs (Figure 6a, b). Gene expression analysis from the laser-assisted micro-dissected (LMD) vessels demonstrated no significant difference of *Pin1* transcripts in IPAH and non-PAH controls (Figure 6c).

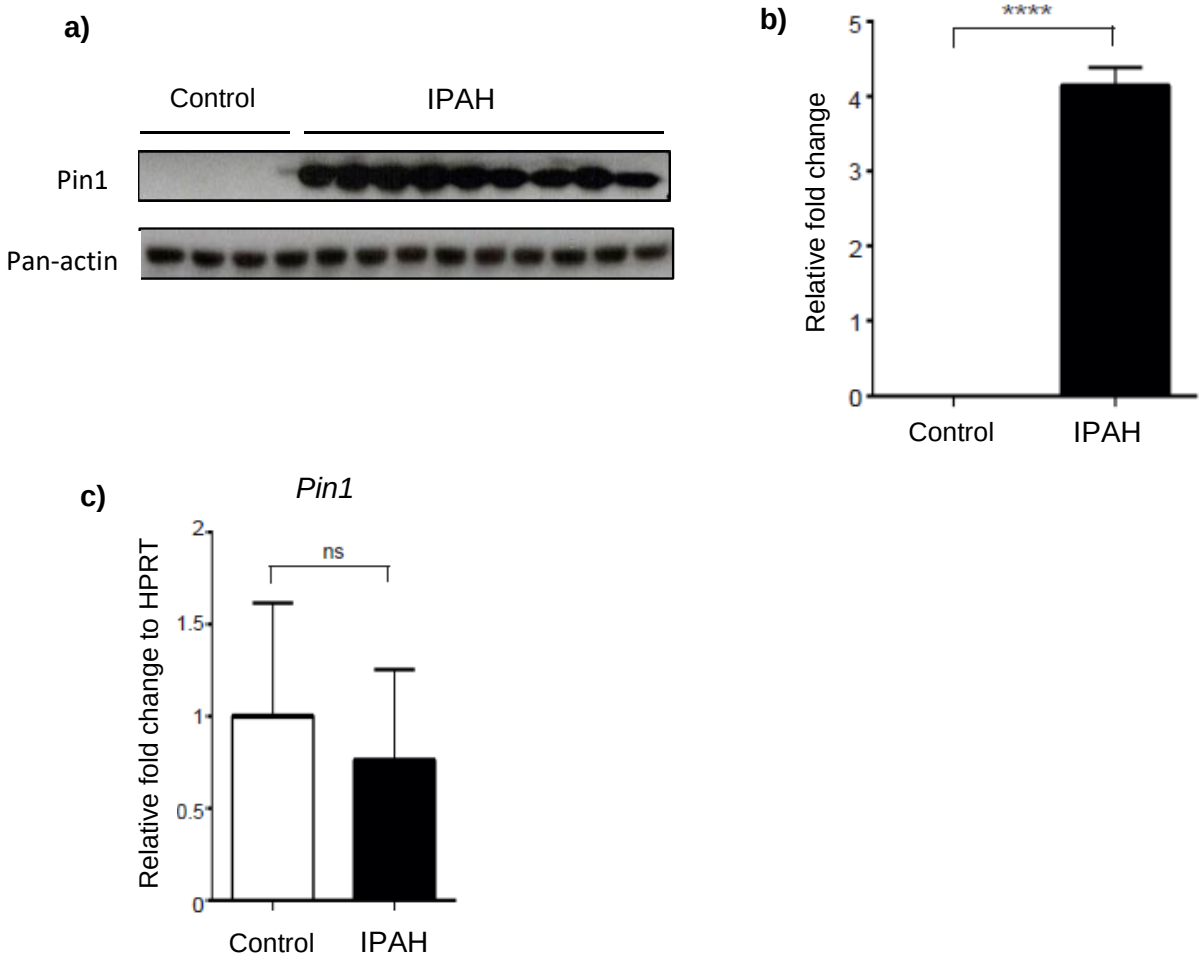

Figure 6. Peptidyl-prolyl isomerase 1 activation in human PAH smooth muscle cells and LMD vessels. a) Protein expression of Pin1 in smooth muscle cells isolated from pulmonary arteries of control and IPAH patients. Regulation at the protein level was analyzed by western blotting, followed by **b)** densitometric analysis. **c)** mRNA expression of *Pin1* in laser-micro-dissected vessels from non-PAH controls and IPAH patients. Pan-actin is used as a loading control. HPRT was used as a reference gene. ****p<0.0001 *versus* controls with Student´s t-test.

6.3 Peptidyl-prolyl isomerase 1 expression is associated with clinical characteristic of IPAH patients

Pin1 protein concentrations were strongly correlated with cardiac index (CI), a marker of cardiovascular risk mortality, measured by right heart catheterization (r = −0.9817; P = 0.0183). There was a tendency towards mild correlation of Pin1 concentration with other clinical parameters such as pulmonary capillary wedge pressure (PCWP; r = −0.9267; P = 0.0733), mean pulmonary artery pressure (mPAP; r = 0.7644; P = 0.0767) and systolic pulmonary artery pressure (sPAP; r = 0.7164, P = 0.0701) measured by echocardiography, albeit without significance (Figure 7b, c, d).

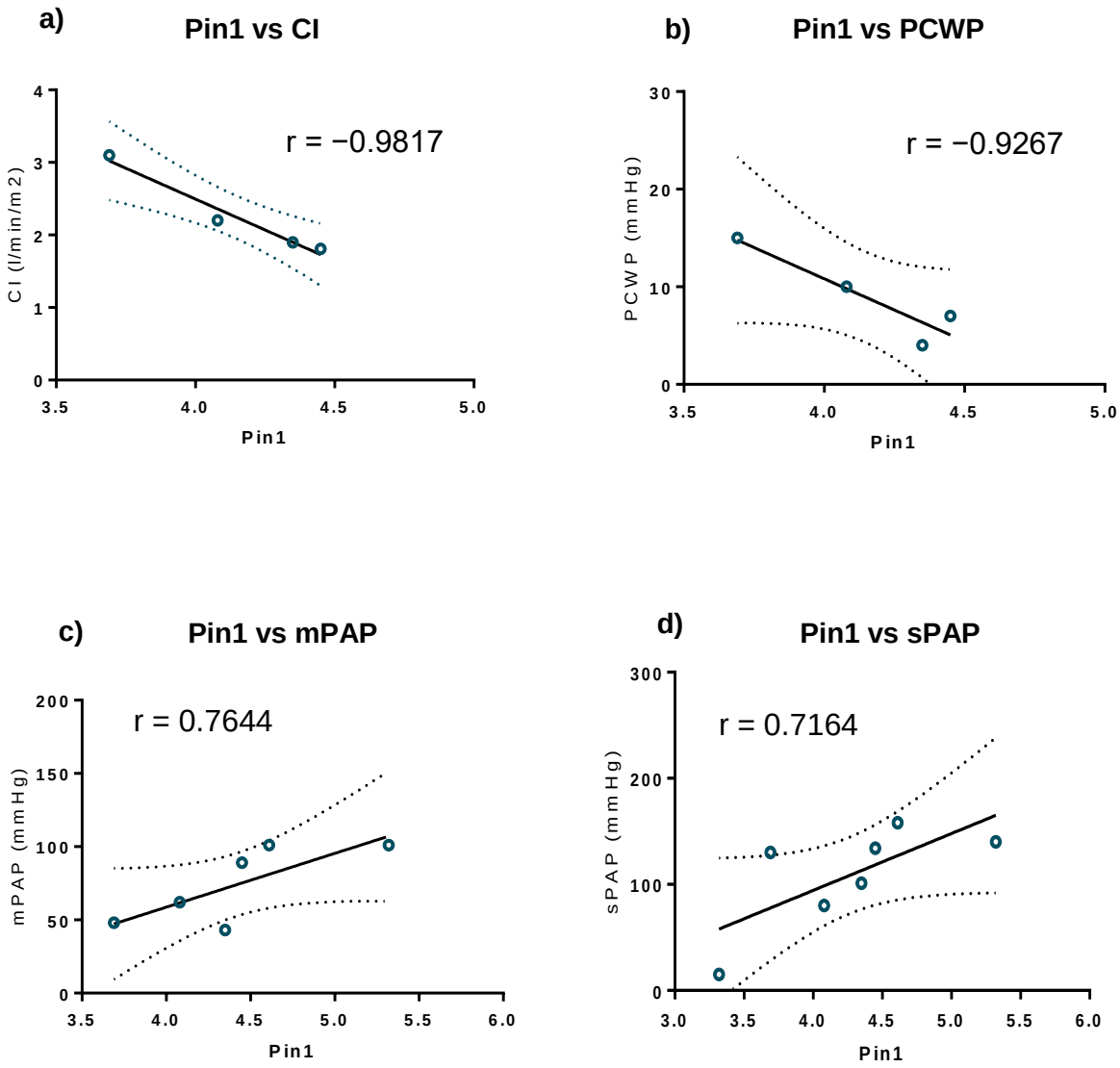

Figure 7. Peptidyl-prolyl isomerase 1 expression is associated with clinical characteristics of IPAH patients. Correlation scatterplot with the best-fit line between Pin1 levels and each of the following: **a)** cardiac index, **b)** pulmonary capillary wedge pressure, **c)** mean pulmonary artery pressure, **d)** systolic pulmonary artery pressure. r, the correlation coefficient

6.4 Peptidyl-prolyl isomerase 1 expression in experimental PAH

We sought to explore expression of Pin1 in experimental PAH. Pin1 was significantly increased in lung homogenates of SU5416/hypoxia (SuHx) rats and a slight, though non-significant increase in lungs of mice exposed to chronic hypoxia, relative to their respective controls (Figure 8a-d) was observed. Similar to IPAH lung tissues, no significant changes in the mRNA expression of *PIN1* were detected in mouse and rat lungs of chronic hypoxia and Sugen5416/Hypoxia-induced PAH, respectively. Hypoxia significantly elevated Pin1 protein accumulation in mouse PASMCs *in vitro* (Figure 8g).

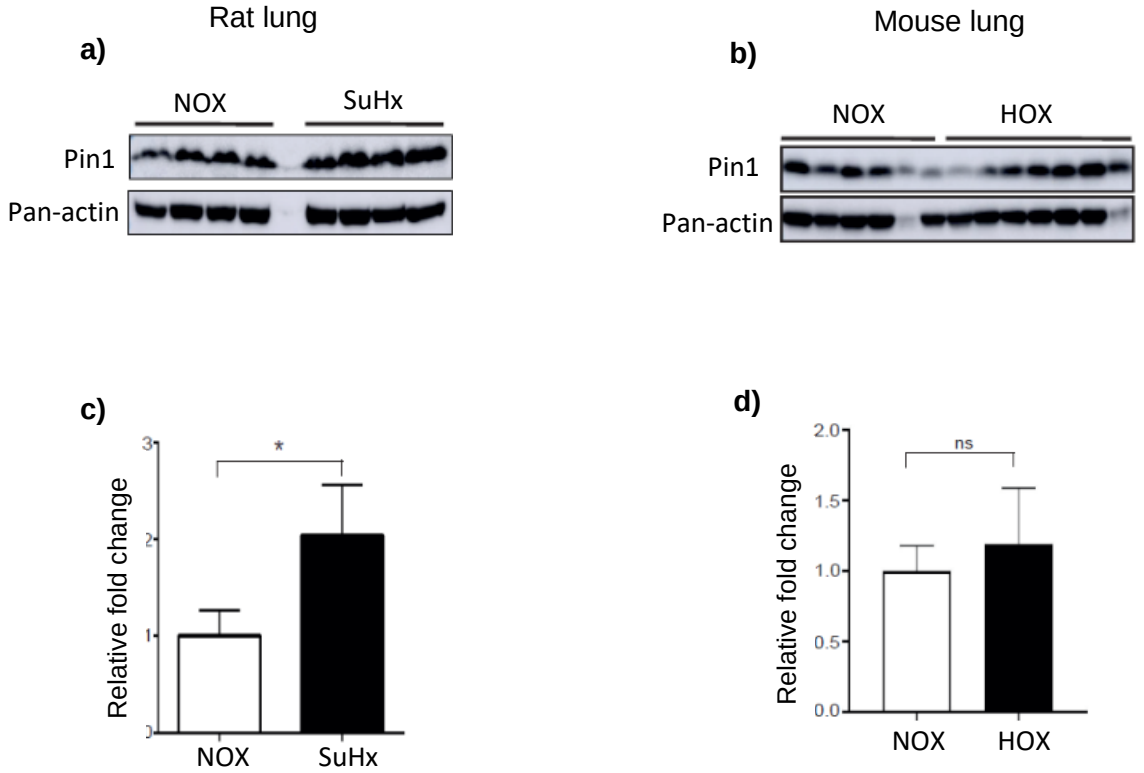

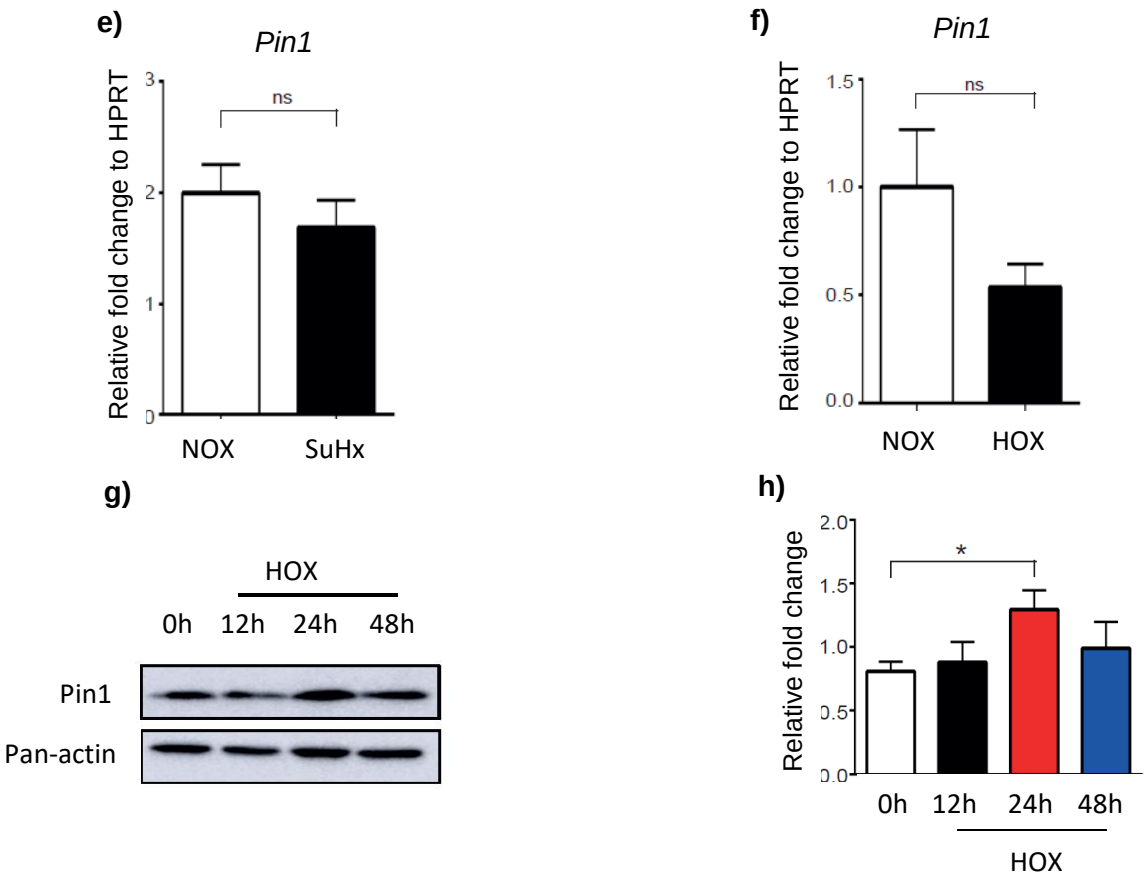

Figure 8. Peptidyl-prolyl isomerase 1 expression in experimental PAH. a), b) Western blot analysis of Pin1 in murine lung homogenates exposed to SuHx and chronic-hypoxia respectively followed by **c), d)** densitometric analysis. **e), f)** mRNA analysis of *Pin1* in lung homogenates from rats and mice respectively, exposed to 10% O_2 for 3 weeks. **g)** Protein expression of Pin1 in mouse PASMCs exposed for 24 hours to 1% O_2 followed by **h)** densitometric analysis. Pan-actin is used as a loading control. HPRT was used as a reference gene. Results are expressed as mean ± SEM; *P<0.05 *versus* controls with Student´s t-test.

6.5 The effect of juglone on the proliferation of human pulmonary arterial smooth muscle cells

Here, we report the effect of pharmacological inhibition of Pin1 by the small molecule inhibitor Juglone on the proliferation of PASMCs. Human PASMCs isolated from control as well as IPAH patients were examined for DNA synthesis to confirm the inhibitory effects of Juglone. Platelet-derived growth factor (PDGF-BB) is a potent mitogen for pulmonary vascular cells and plays a role in the remodeling process of

PAH development by controlling many cellular functions and processes, including cellular proliferation, migration, and extracellular matrix deposition. The incorporation of BrdU reflected the rate of DNA synthesis. PDGF-BB induced the proliferation of PASMCs, and Juglone inhibited PDGF-BB driven proliferation of both non-PAH PASMCs and PASMCs from IPAH patients.

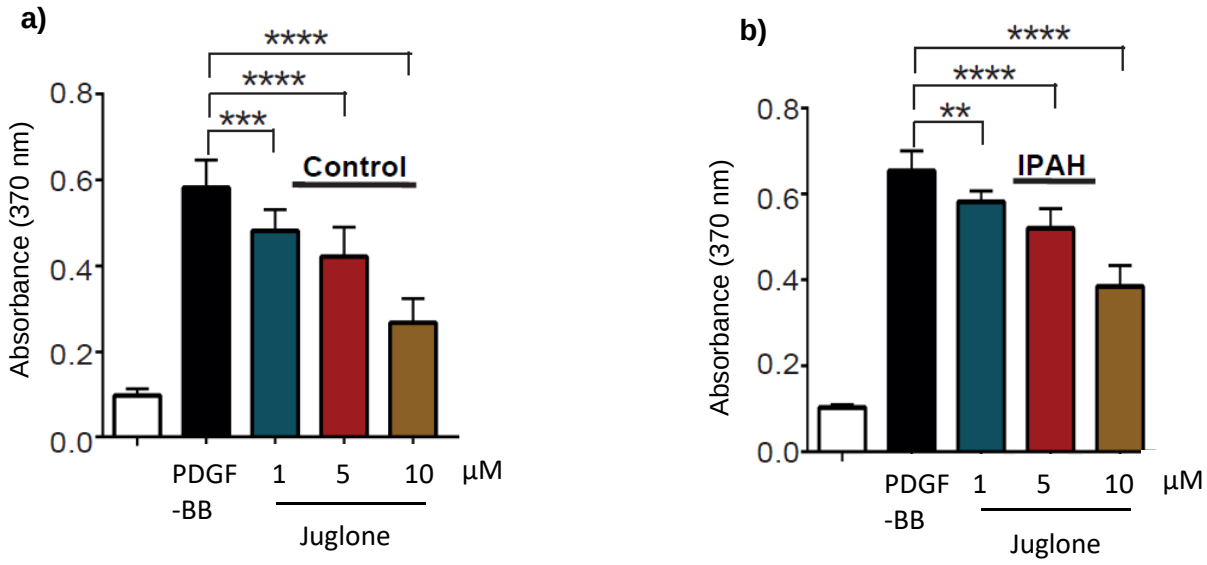

Figure 9. The effect of juglone on the proliferation of human pulmonary arterial smooth muscle cells. Human PASMCs from **a)** non-PAH control and **b)** IPAH patients were stimulated by 30ng/ml of PDGF-BB for 24hours to induce proliferation in the absence or presence of Juglone. The proliferation of human PASMCs was assayed by the incorporation of BrdU into newly synthesized DNA. Results are expressed as mean ± SEM; n=3 independent experiments; **P<0.01, ***P<0.001, ****P<0.0001 *versus* PDGF-BB using one-way ANOVA with Newman-Keuls post-hoc test for multiple comparisons.

6.6 Pin1 gene silencing downregulates cell cycle markers and inhibits proliferation of human pulmonary arterial smooth muscle cells

In the current study, we used small interfering RNA (siRNA) to specifically attenuate Pin1 in PASMCs. We aimed to examine the effects of Pin1 siRNA on the proliferation of PASMCs and to understand the underlying mechanisms. The expression of Pin1 was remarkably downregulated in Pin1-silenced human PASMCs from non-PAH control individuals and IPAH patients, as compared to the scrambled siRNA transfected cells. The attenuation of Pin1 in human PASMCs downregulated the

expression of pro-proliferative markers, Proliferating Cell Nuclear Antigen (PCNA) and Ki-67 under basal conditions. Also, the knockdown of Pin1 suppressed the growth response of human PASMCs stimulated by PDGF-BB as assessed by examining the DNA synthesis.

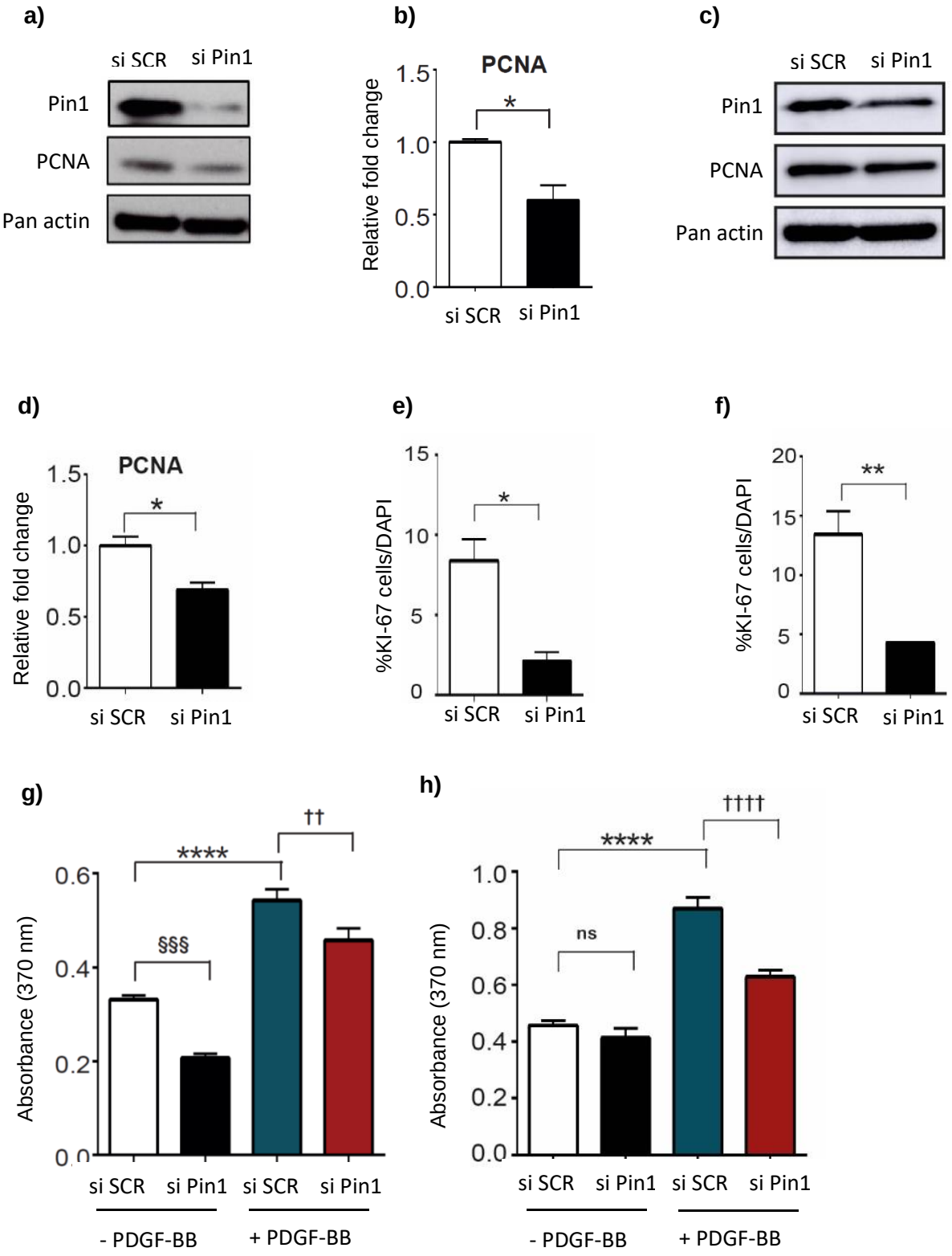

Figure 10. Pin1 gene silencing downregulates cell cycle markers and inhibits proliferation of human pulmonary arterial smooth muscle cells. Representative western blots to determine the function of Pin1, 24 h after mRNA knockdown in **a)** control and in **c)** IPAH human PASMCs followed by **b), and d)** with densitometric analysis. **e)** and **f)** Immunofluorescence analysis of KI-67 in control and IPAH PASMCs after Pin1 silencing **g)** Proliferation of Pin1 silenced control and **h)**, IPAH human PASMCs, in presence or absence of PDGF-BB, is determined by BrdU incorporation. Results are expressed as mean ± SEM. Statistical analysis was performed using one-way ANOVA with Newman-Keuls post-hoc test for multiple comparisons; §§§P<0.001 (si Scr-PDGF-BB *versus* si Pin1-PDGF-BB); *P<0.05, ****P<0.0001 (si Scr-PDGF-BB *versus* si Scr+PDGF-BB); ††P<0.01 (si Scr+PDGF-BB *versus* si Pin1+PDGF-BB).

6.7 Pin1 inhibition results in the initiation of cell apoptosis in human pulmonary arterial smooth muscle cells *in vitro*

We examined the effect of Pin1 inhibition on apoptotic resistance to PASMCs by employing the terminal deoxynucleotidyl transferase dUTP nick end labeling (TUNEL) assay with PASMCs treated with increasing concentrations of Juglone. Pin1 inhibition resulted in the initiation of apoptosis and increased the number of (TUNEL)-positive human PASMCs in Juglone-treated cells, relative to vehicle-treated PASMCs in non-PAH controls and IPAH.

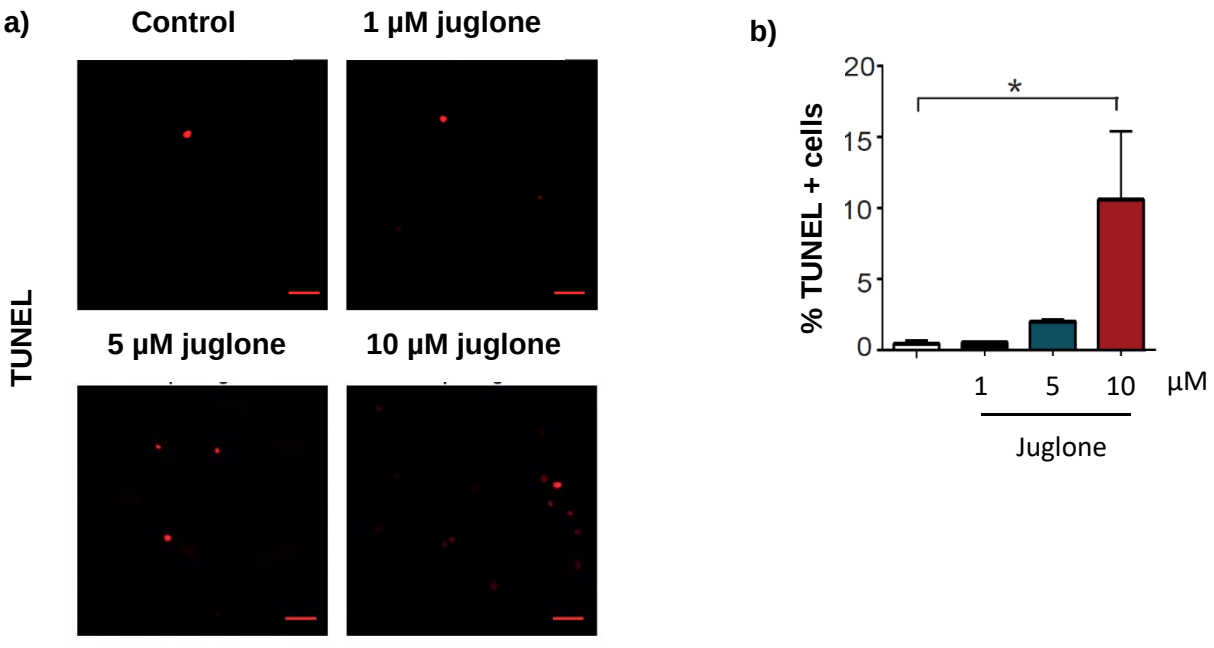

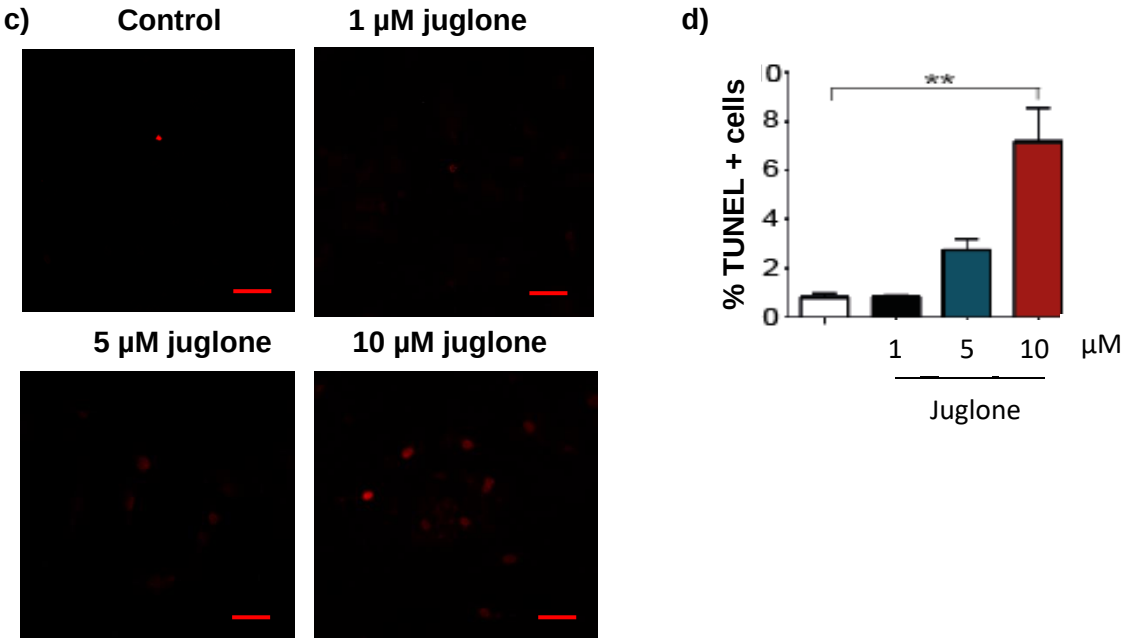

Figure 11. Pin1 inhibition results in the initiation of cell apoptosis in human pulmonary arterial smooth muscle cells *in vitro.* Terminal deoxynucleotidyl transferase dUTP nick end labeling (TUNEL) assay after the treatment of **a), b)** control and **c)**, **d)** of IPAH human PASMCs with increasing concentration of Juglone for 24 h. Results are expressed as mean ± SEM. *P<0.05, **P<0.01. Statistical analysis was performed using one-way ANOVA with Newman-Keuls post-hoc test for multiple comparisons. Scale bar: 50 µm.

6.8 Pin1 inhibition upregulates apoptotic markers in human pulmonary arterial smooth muscle cells *in vitro*

Pin1 inhibition by Juglone increased the expression of the pro-apoptotic active cleaved form of Caspase 3 and inhibited the resistance to apoptosis in human PASMC. Cleaved Poly (ADP-ribose) polymerase (PARP-1), an eminent feature of apoptotic cell death and cleaved by Caspase-3, was also found to be upregulated in comparison to vehicle-treated non-PAH controls (Figure 12a, b, c) and IPAH human PASMCs (Figure 12c, d, f). Furthermore, the inhibition of proliferation precedes the initiation of apoptosis as observed by downregulation of PCNA upon Juglone treatment (Figure 12g, h).

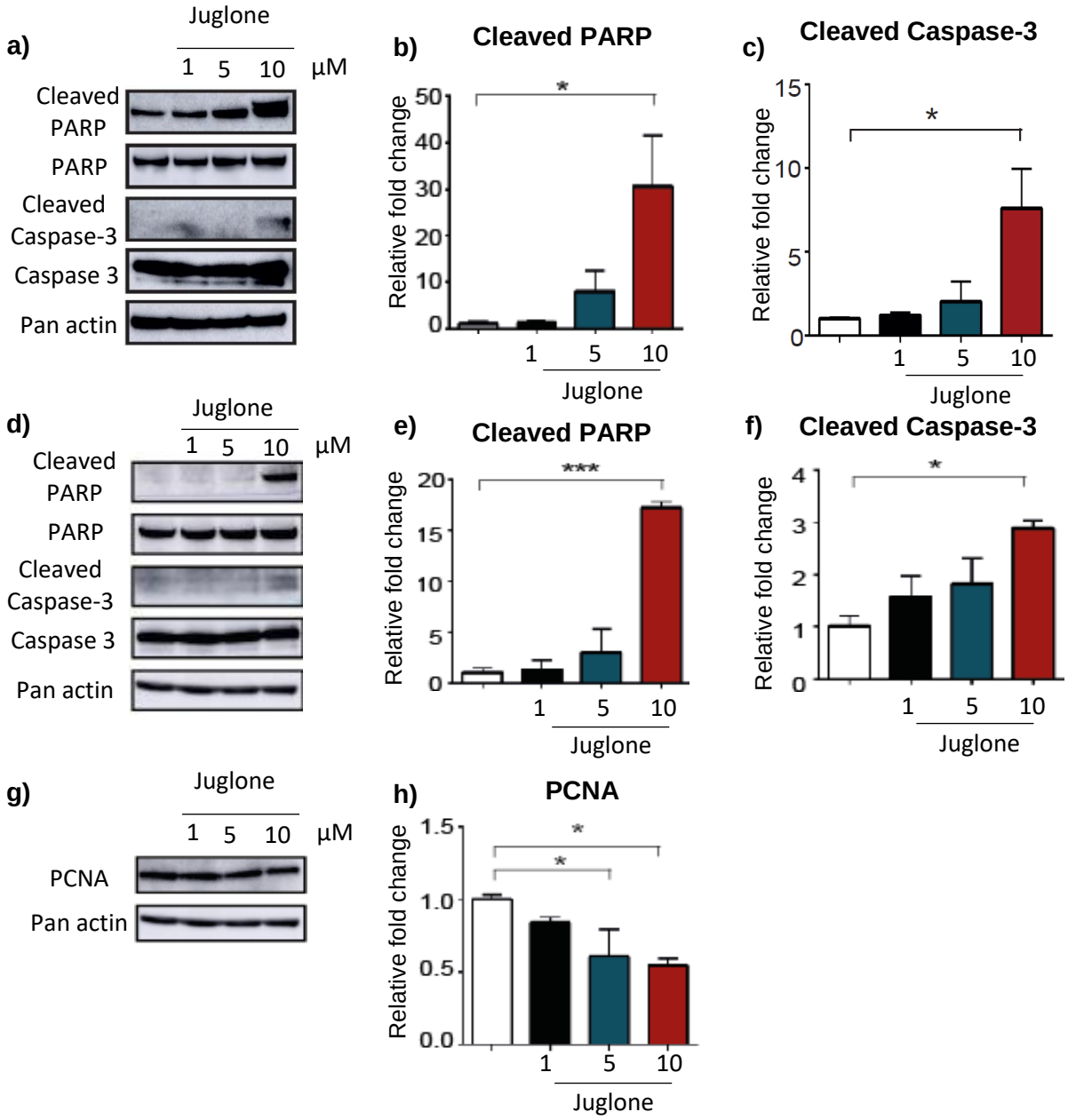

Figure 12. Pin1 inhibition upregulates apoptotic markers in human pulmonary arterial smooth muscle cells *in vitro*. a), d), g) representative western blot and **b-c), e-f), h)** of control PAH human PASMCs treated with juglone for 24h followed by densitometric analysis of cleaved PARP, Cleaved Caspase-3, and PCNA. Results are expressed as mean ± SEM. *P<0.05, ***P<0.001. Statistical analysis was performed using one-way ANOVA with Newman-Keuls post-hoc test for multiple comparisons.

6.9 The effect of Juglone on the proliferation of human pulmonary endothelial cells

The effect of Pin1 inhibition by Juglone on the proliferation of human PAECs isolated from control as well as IPAH patients was also investigated by examining DNA synthesis. Serum, a potent mitogen for pulmonary artery endothelial cells, significantly induced the proliferation of human PAECs which was reduced effectively by treatment with Juglone in both non-PAH PAECs and IPAH PAECs.

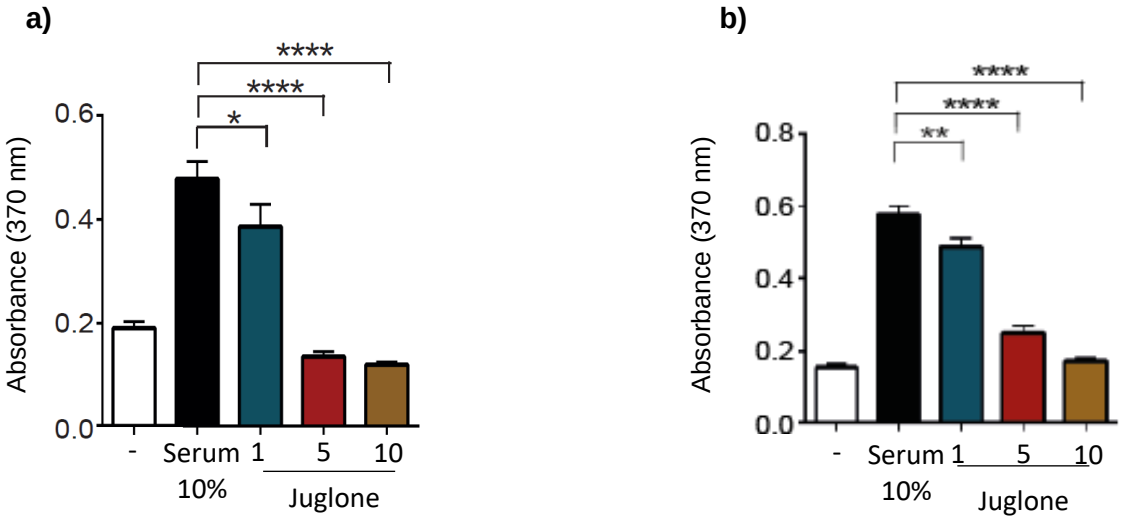

Figure 13. The effect of Juglone on the proliferation of human pulmonary endothelial cells. Human PAECs from **a)** non-PAH control and **b)** IPAH patients were stimulated by 10% of serum for 24hours to induce proliferation in the absence or presence of Juglone. The proliferation of human PAECs was assayed by the incorporation of BrdU into newly synthesized DNA. Results are expressed as mean ± SEM; n=3 independent experiments; *P<0.05, **P<0.01, ****P<0.0001 *versus* PDGF-BB using one-way ANOVA with Newman-Keuls post-hoc test for multiple comparisons.

6.10 Pin1 inhibition results in the initiation of cell apoptosis in human pulmonary endothelial cells *in vitro*

The perpetuation of hyperproliferative apoptotic-resistant endothelial cells in PAH emerges from the altered endothelial cells that have increased pro-survival factors [29]. To investigate if Pin1 inhibition hinders the apoptotic resistance of pulmonary arterial endothelial cells, TUNEL assay was performed in human PAECs treated with increasing concentrations of Juglone. Inhibition of Pin1 led to an increase in apoptotic cells as measured by the number of TUNEL-positive human PAECs in Juglone-treated

cells, in comparison to vehicle-treated human PAECs in **a)** non-PAH controls and **b)** IPAH.

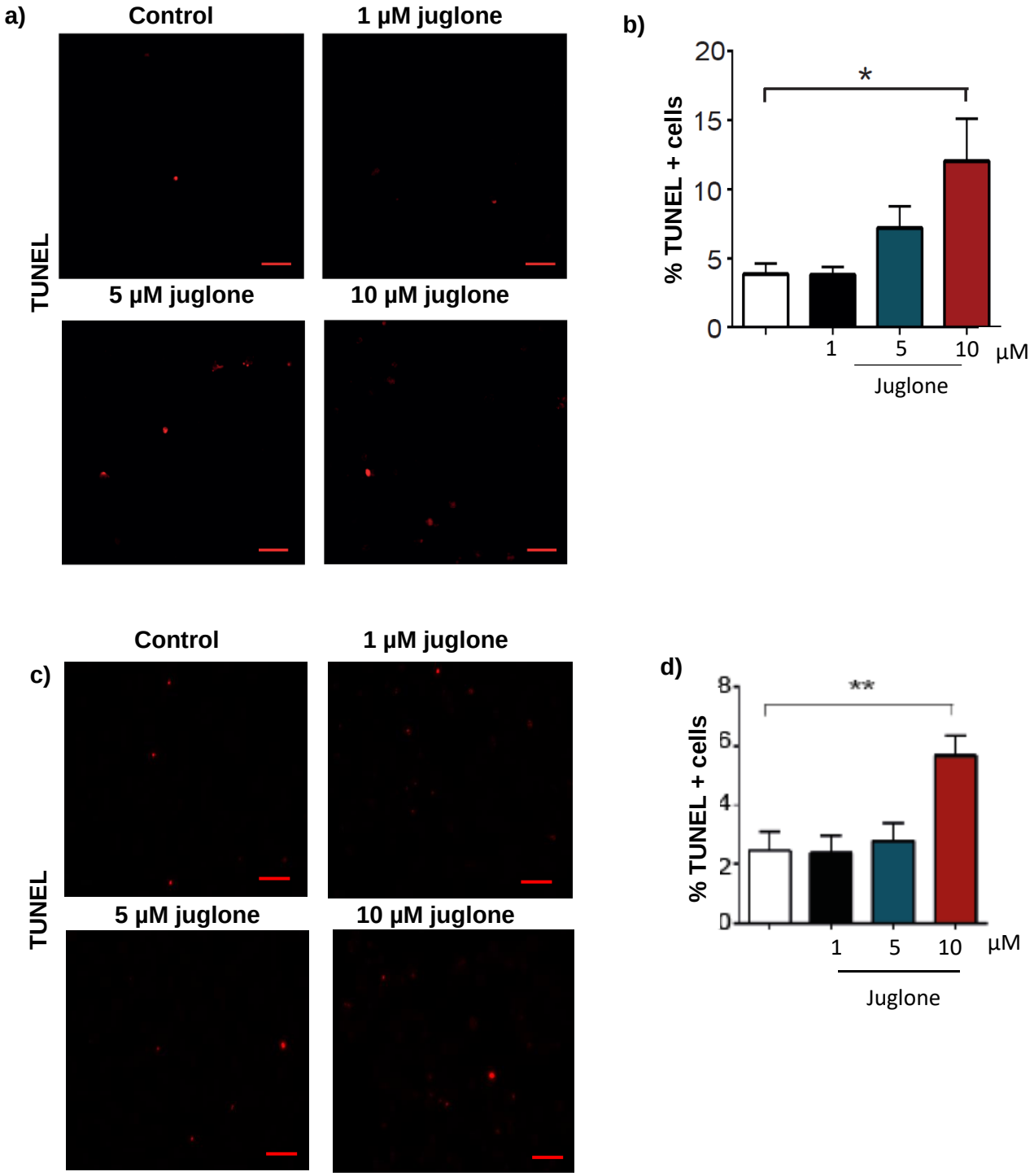

Figure 14. Pin1 inhibition results in the initiation of cell apoptosis in human pulmonary endothelial cells *in vitro.* Terminal deoxynucleotidyl transferase dUTP nick end labeling (TUNEL) assay after the treatment of **a), b)** control and **c)**, **d)** of IPAH human PAECs with

increasing concentration of Juglone for 24 h. Results are expressed as mean ± SEM. *P<0.05, **P<0.01. Statistical analysis was performed using one-way ANOVA with Newman-Keuls post-hoc test for multiple comparisons. Scale bar: 50 µm.

6.11 Pin1 inhibition upregulates apoptotic markers in human pulmonary endothelial cells *in vitro*

Similar to human PASMCs, Juglone upregulated the expression of pro-apoptotic Cleaved Caspase-3 and inhibited the resistance to apoptosis in human PAECs. Cleaved PARP-1 was also upregulated in comparison to vehicle-treated non-PAH control (Figure 15a, b, c) and IPAH human PAECs (Figure 15c, d, f).

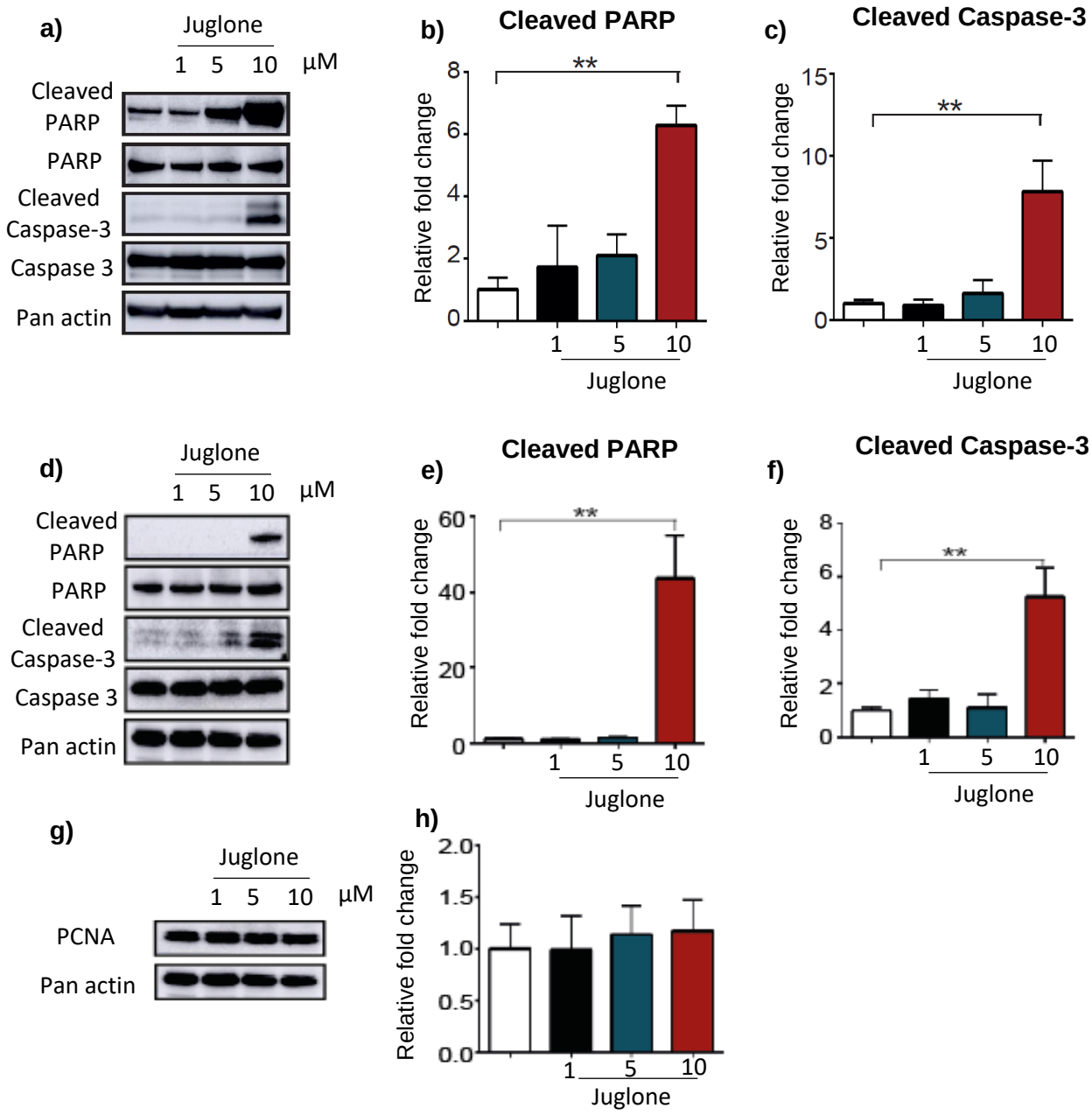

Figure 15. Pin1 inhibition upregulates apoptotic markers in human pulmonary endothelial cells *in vitro*. a), d), g) representative western blot and **b-c), e-f), h)** of control and PAH human PAECs treated with Juglone for 24h followed by densitometric analysis of cleaved PARP, Cleaved Caspase-3, and PCNA. Results are expressed as mean ± SEM. **P<0.01. Statistical analysis was performed using one-way ANOVA with Newman-Keuls post-hoc test for multiple comparisons.

6.12 Pin1 is induced by pro-proliferative growth factors in human pulmonary smooth muscle cells *in vitro*

To determine upstream signal transmission, the effect of various PH-inducing growth factors/pro-inflammatory cytokines on Pin1 expression was observed in human PASMCs. Stimulation with PDGF-BB, Epidermal Growth Factor (EGF), and the Growth Medium (a mixture of growth factors), led to an increase in Pin1 expression in human PASMCs as compared to untreated control cells (Figure 16a). The family of bone morphogenetic proteins (BMPs) and pro-inflammatory cytokines (Tumor Necrosis Factor-a, Interleukin 6) did not modify the expression of Pin1, suggesting a selective mode of regulation of Pin1 in human PASMC.

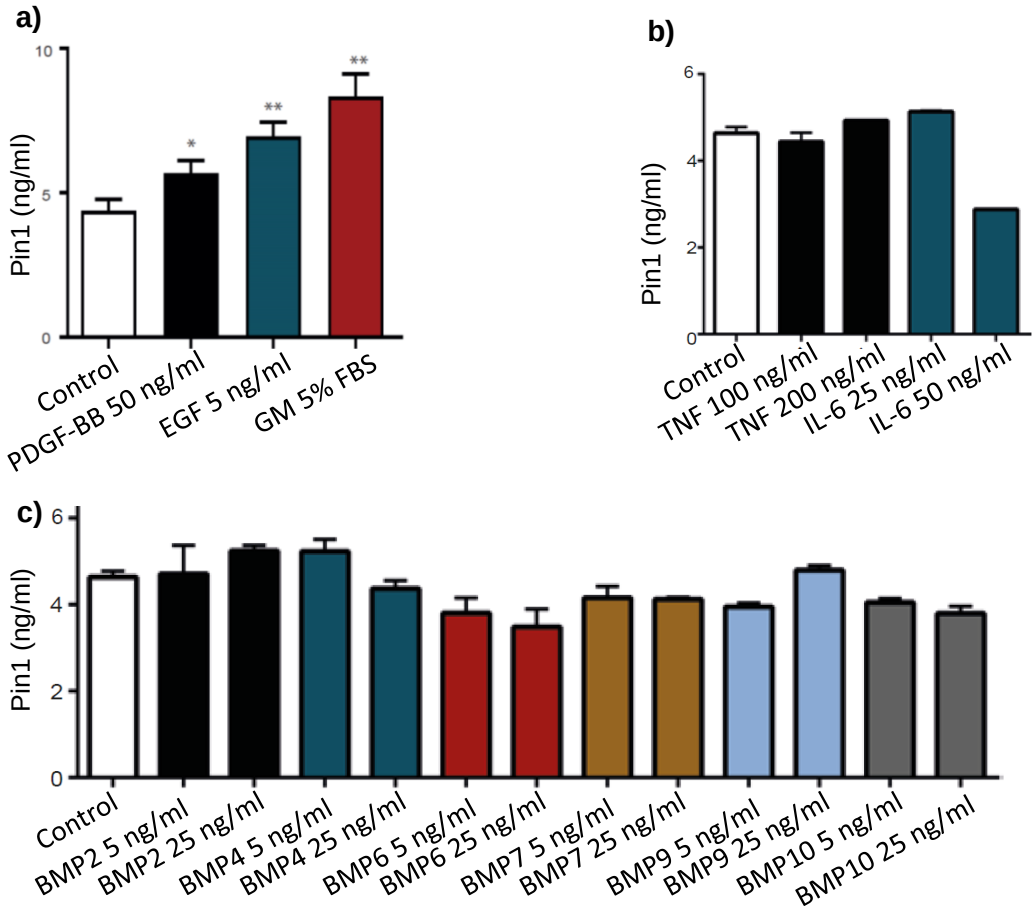

Figure 16. Pin1 is induced by pro-proliferative growth factors in human pulmonary smooth muscle cells *in vitro.* Human PASMCs from controls were serum starved for 24 h and were subjected to **a)** PDGF-BB (50 ng/ml), EGF (5 ng/ml) and Growth Medium (5% fetal bovine serum) stimulation **b)** inflammatory cytokines TNF (100, 200 ng/ml), IL-6 (100, 200 ng/ml) and **c)** BMP2 (5, 25 ng/ml), BMP4 (5, 25 ng/ml), BMP6 (5, 25 ng/ml), BMP7 (5, 25 ng/ml), BMP9 (5, 25 ng/ml), BMP10 (5, 25 ng/ml). Intracellular Pin1 levels were monitored by ELISA. *P<0.05; **P<0.01 *versus* controls with Student´s t-test.

6.13 Pin1 affects various transcription factor's activity

It has been stated that Pin1 induced isomerization plays an important role in the activity of different transcription factors (TFs) that promote numerous pro-proliferation pathways [133, 141]. The activity of a group of 96 TFs from Pin1-silenced control human PASMCs was thus observed by a TF array. Pin1 knock-down reduced the activity of pro-proliferative transcription factors and increased anti-proliferative TFs activity (Figure 17a). Multiple TFs and transcriptional co-activators associated with PH and RV dysfunction such as HIF (Hypoxia-inducible factor), Octamer-binding transcription factor 4 (OCT4), SMAD family (SMADs), Signal transducers and activators of transcription (STATs), Retinoblastoma control element (RB) were dysregulated in Pin1-silenced human PASMCs (Figure 17b).

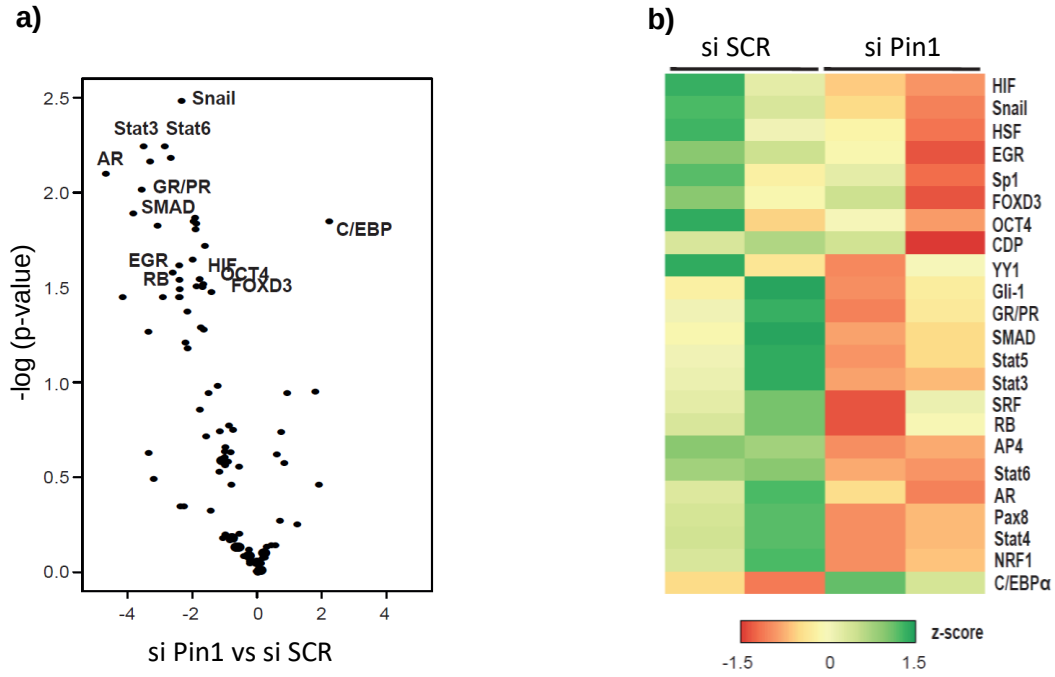

Figure 17. Pin1 affects various transcription factor's activity. a) Pin1-silenced human PASMCs were stimulated with Growth Medium for 24 h and the extracted nuclear protein was used in TF activation profile array, presented as log-transformed signals in a volcano plot. **b)** Heat map of top TF candidates obtained from log-transformed signals used to perform TF activation profile array.

6.14 Pin1 regulates the expression of HIF-1α and CEBPα in human pulmonary smooth muscle cells *in vitro*

Pin1 knockdown in human PASMCs affected the absolute expression of HIF and CCAAT/enhancer-binding protein alpha (C/EPBα) as evidenced by a remarkable decrease in the expression of HIF-1α in control and IPAH PASMCs and upregulation of tumor suppressor C/EBPα levels in Pin1-silenced hypoxia-treated control PASMCs.

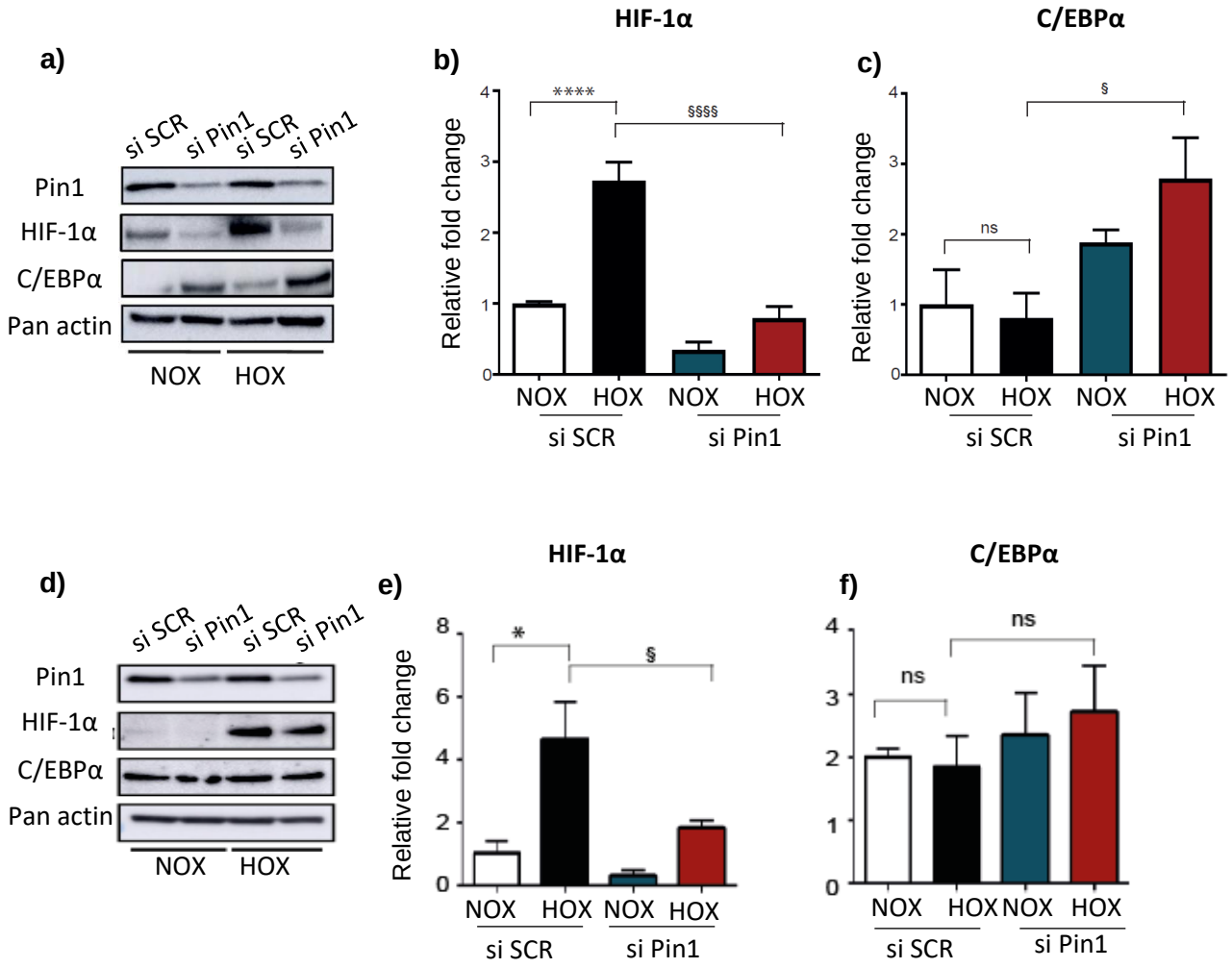

Figure 18. Pin1 regulates the expression of HIF-1α and C/EBPα in human pulmonary smooth muscle cells *in vitro*. Western blot showing expression levels of HIF-1α and C/EBPα

in Pin1-silenced **a-c)** control and **d-f)** IPAH human PASMCs subjected to hypoxia for 24 h. Results are expressed as mean ± SEM. ****P<0.0001 for NOX si Scr *versus* HOX si Scr; §P<0.05; §§§§P<0.0001 for NOX si Pin1 *versus* HOX si Pin1.

6.15 The effect of Juglone on right ventricular systolic pressure and hypertrophy in SuHx rats

Since the *in vitro* effects of Pin1 inhibition by Juglone provided us with promising results, we employed the SuHx rat's model, which highly resembles some forms of PH, to investigate the efficacy of Juglone *in vivo* [153]. SuHx rats exhibited significantly elevated right ventricular systolic pressure (RVSP) compared to normoxic control rats, as shown in **a).** Juglone administration (1.5 mg/kg per body weight) from day 21 to 35 significantly reduced right ventricular systolic pressure (RVSP) in comparison to placebo-treated control rats (56.0 ± 2.4 mm Hg vs. 70.7 ± 3.8 mm Hg for Juglone treated and vehicle respectively; P<0.01). The Fulton index, which is defined as RV/(LV+Septum), and right ventricular internal diameter (RVID) were examined to demonstrate the RV hypertrophy and dilatation. The Fulton index, a marker for right ventricular hypertrophy, was significantly increased in SuHx rats (Figure 19b), and was lower in the Juglone treatment group (0.60 ± 0.01 vs. 0.67 ± 0.03 for Juglone treated and vehicle respectively; P<0.01). Furthermore, the decrease in RVSP and RV hypertrophy in Juglone-treated rats was followed by the diminution in RV dilation (RVID) (3.91 ± 0.01 mm vs. 3.29 ± 0.10 mm, for Juglone treated and vehicle respectively; P<0.01).The administration of Juglone did not affect the systemic blood pressure (Figure 19d).

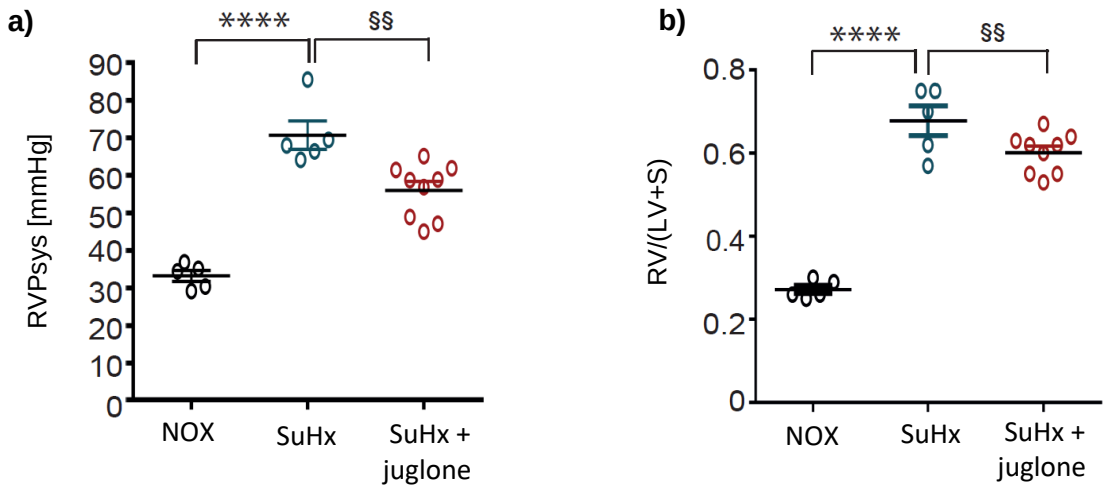

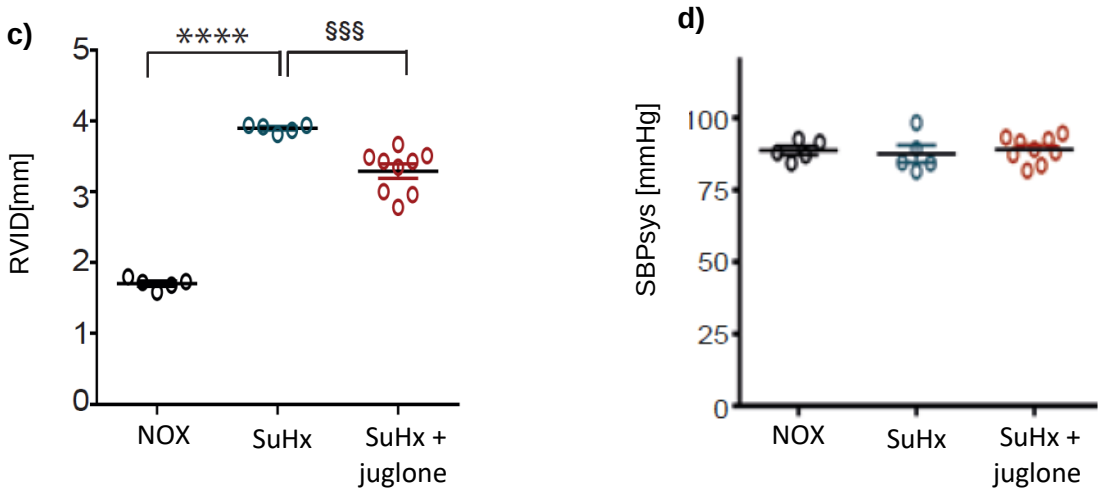

Figure 19. The effect of Juglone on right ventricular systolic pressure and hypertrophy in SuHx rats. a) right ventricle systolic pressure (RVSP); **b)** the ratio of RV to left ventricular, RV/(LV+S); **c)** right ventricle internal diameter (RVID); **d)** systemic blood pressure of the different group. The SuHx rat model was induced by subcutaneously injection with Sugen5416 and exposure to hypoxia for three weeks, followed by re-exposure to normoxia for another two weeks. SuHx rats were administered Juglone intraperitoneally (1.5 mg/kg per body weight) from day 21 to 35. Control animals, which were injected with the same volume of saline, were kept in normoxic conditions for the same duration. The results are expressed as mean ± SEM, , ****P<0.0001 for NOX *versus* SuHx; §P<0.05; §§P<0.01; §§§P<0.001 for SuHx *versus* SuHx+Juglone, NOX, normoxia; SuHx, Sugen-hypoxia; RVSP, right ventricle systolic pressure; RVID, right ventricle internal diameter; RV, right ventricle; LV, left ventricle; S, septum

6.16 The effect of Juglone on right ventricular function in SuHx rats

Right ventricular function is closely correlated with the severity of disease and survival, and right heart failure is the primary cause of death in PAH patients. Echocardiography allows right ventricular function to be non-invasively assessed, and several indices such as TAPSE and CI have been shown to have potential PAH prognostic value. Preservation and recovery of RV function should be essential aspects of pharmacotherapy, considering the role of the right ventricle in PAH [154] In line with RV hypertrophy results, with decreased TAPSE, cardiac output, and cardiac index, SuHx rats showed RV dysfunction. Juglone treated SuHx rats improved TAPSE (1.06

± 0.05 mm vs. 1.40 ± 0.05 mm) as well insignificant improvement in CI (11.17 ± 0.67 vs. 14.23 ± 0.73 [ml min-1] per 100BW) was observed.

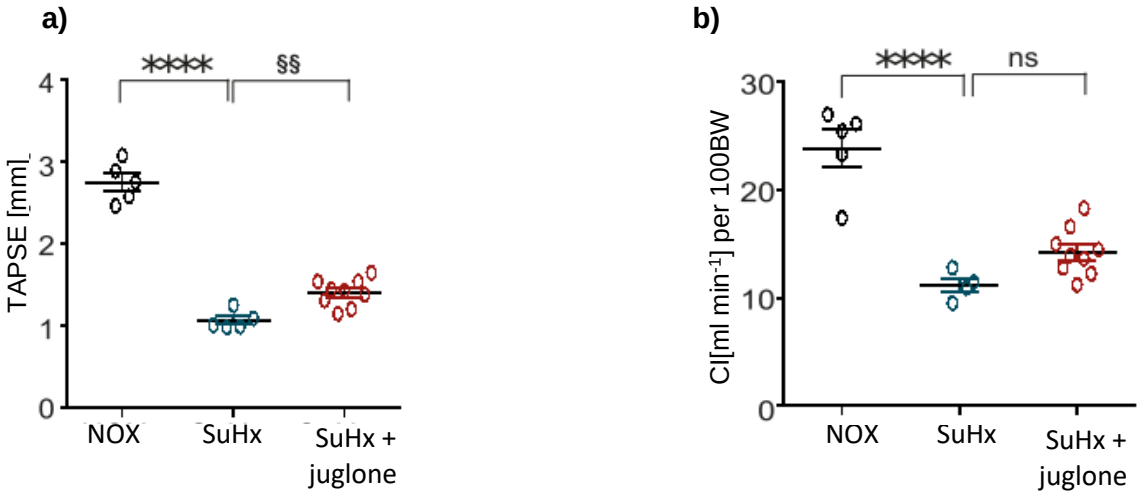

Figure 20. The effect of Juglone on right ventricular function in SuHx rats. Echocardiography was carried out on Juglone-treated [1.5 mg/kg per BW], placebo-treated SuHx rats, and healthy rats 35 days after initiation of SuHx treatment **a)** tricuspid annular plane systolic excursion [TAPSE] and **b)** cardiac index [CI]. The results are expressed as mean ± SEM, ****P<0.0001 for NOX *versus* SuHx; §P<0.05; §§P<0.01; for SuHx *versus* SuHx+Juglone, NOX, normoxia; SuHx, Sugen-hypoxia

6.17 The effect of Juglone on vascular remodeling in SuHx rats

The proliferation of SMCs causing medial layer thickening together with occlusion of vessels increases pulmonary vascular resistance in the arteries leading to severe pathogenesis in PAH. SuHx rats demonstrated severe vascular remodeling with increased media wall thickness, fully closed pulmonary arteries, and occlusion of small vessels (20-50 µm in diameter). Moreover, treatment with Juglone reduced the medial wall thickness, increased the number of non-muscularized arteries, and decreased the number of fully-muscularized as well as occluded vessels causing a significant reduction in pulmonary vascular resistance as compared to placebo-treated rats.

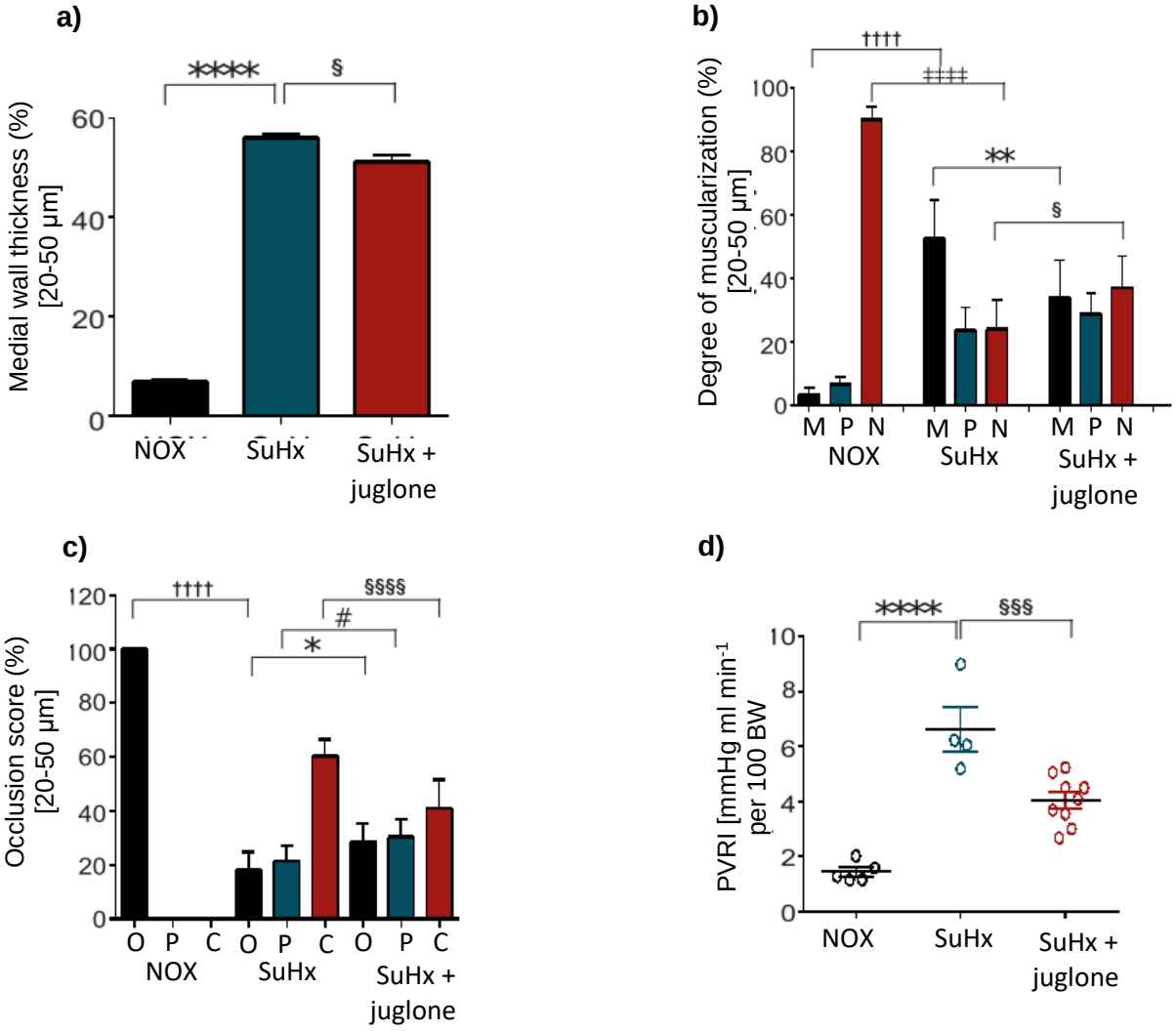

Figure 21. The effect of Juglone on vascular remodeling in SuHx rats. a) Lung sections stained with Elastica-van-Gieson was used to determine the medial wall thickness of vessels [%], **b)** The degree of muscularization of small pulmonary arteries (diameter 20-50 µm) was determined by immunohistological for vWF and α-SMA of lung sections. M: fully muscularized; P: partially muscularized; N: non-muscularized. **c)** occlusion score of vessels [%] with a diameter of 20-50 µm. O: open; P:partial; C: closed and **d)** pulmonary vascular resistance index [PVRI]. The results are expressed as mean ± SEM****P<0.0001 for NOX *versus* SuHx; §P<0.05; §§P<0.01; for SuHx *versus* SuHx+Juglone, NOX, normoxia; SuHx, Sugen-hypoxia

6.18 The effect of Juglone on pulmonary vascular cell proliferation and initiation of apoptosis

DNA replication and cell cycle regulation both are tightly regulated by PCNA. Immunohistochemical staining for PCNA was performed to further assess the inhibitory

effect of Juglone on vascular cell proliferation in the development of vascular remodeling. Results from immunohistochemistry indicate that substantially increased PCNA positive cells in SuHx rat vessels which were significantly reduced upon treatment with Juglone in SuHx rats. Western-blot analysis revealed an elevated expression of Cleaved Caspase 3 in lung homogenates of rats treated with Juglone.

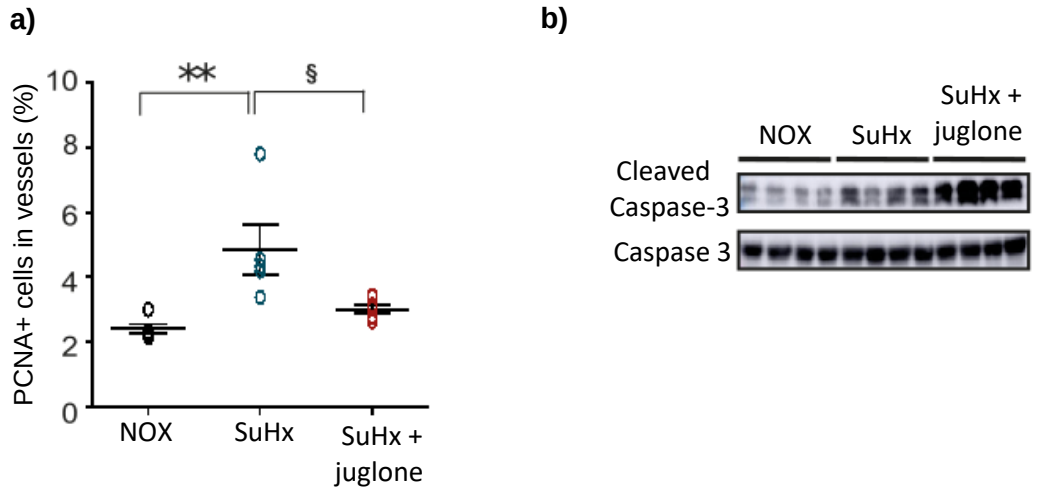

Figure 22. The effect of Juglone on pulmonary vascular cell proliferation and initiation of apoptosis. a) PCNA positive cells per vessels (20-50 µm in diameter) **b)** Cleaved Caspase-3 and Caspase 3 expression were checked by western blot in lung homogenates. The results are expressed as mean ± SEM, **P<0.01 for NOX *versus* SuHx; §P<0.05; for SuHx *versus* SuHx+Juglone, NOX, normoxia; SuHx, Sugen-hypoxia

6.19 The effect of Juglone on RV fibrosis and secreted collagen content in isolated cardiac-fibroblasts

The antifibrotic effects of Juglone on RV was assessed via Sircol assay staining of RV sections. The analysis revealed that Pin1 inhibition provided beneficial, although non-significant, effects on RV fibrosis, in comparison to Placebo-treated control rats. Cardiac fibroblasts (CFs) treated with transforming growth factor beta-1 resulted in the secretion of collagens. Treatment of CFs with Juglone led to the reduction in secreted collagen.

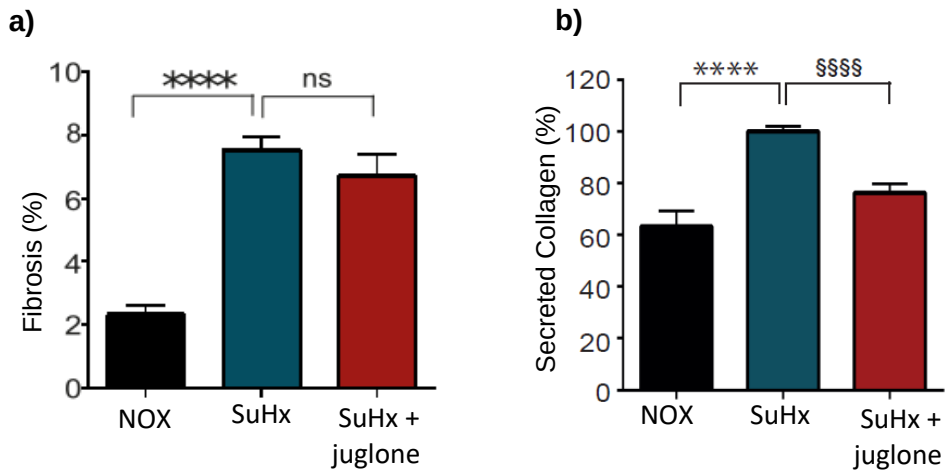

Figure 23. The effect of Juglone on RV fibrosis and secreted collagen content in isolated cardiac-fibroblasts. a) Ex-vivo analysis of Juglone on right ventricle sections for fibrosis by Sircol assay. **b)** Measurement of secreted collagen content in isolated cardiac-fibroblasts. The results are expressed as mean ± SEM, ****P<0.0001 for NOX *versus* SuHx; §§§§P<0.05; for SuHx *versus* SuHx+Juglone, NOX, normoxia; SuHx, Sugen-hypoxia

6.20 The effect of Juglone on right ventricular systolic pressure and hypertrophy in chronic hypoxia mice

The effect of Pin1 inhibition was examined in another specie specific animal model, chronic-hypoxic mice. PH established in mice subjected to 35 days of chronic hypoxia demonstrated by a rise in RVSP and RV hypertrophy (Figure 24a, b). Juglone therapy (3 mg/kg) from day 21 to 35 resulted in a small, but not significant, decrease in the RVSP and Fulton index compared to placebo-treated control mice. RVID was significantly decreased upon treatment with Juglone in chronic-hypoxic mice as compared to placebo mice (1.34 ± 0.01 mm vs. 1.22 ± 0.01 mm). After the administration of Juglone, no differences in systemic blood pressure were reported.

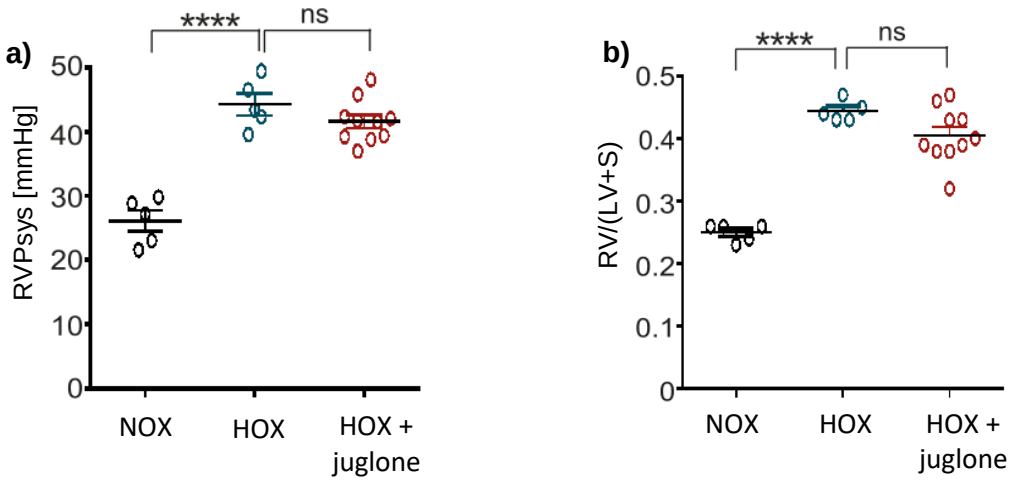

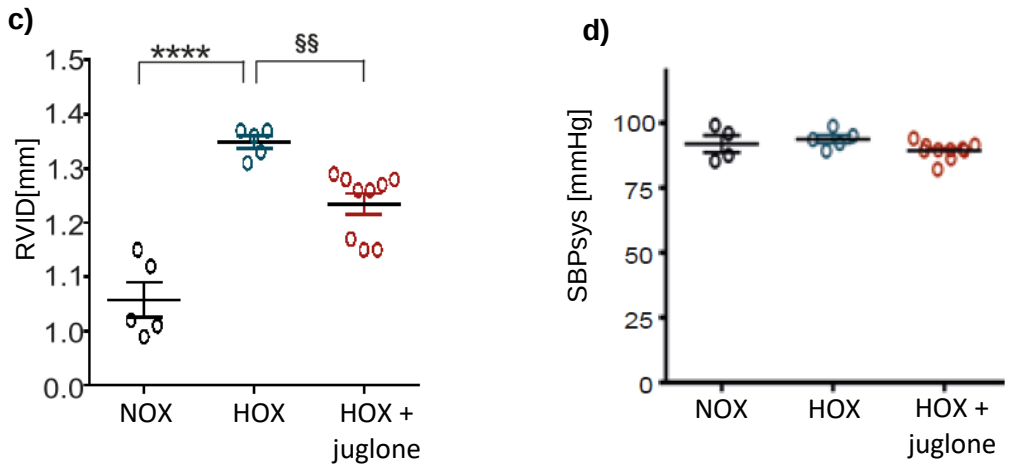

Figure 24. The effect of Juglone on right ventricular systolic pressure and right ventricular hypertrophy in chronic hypoxia mice. a) Right ventricular systolic pressure [RVSP] as measured by right heart catheterization, **b)** ratio of RV mass to the mass of left ventricle plus septum [RV/(LV+S)], and **c)** right ventricle internal diameter [RVID] **d)** systemic blood pressure of three different group. Physiological measurements were carried out on Juglone-treated [3 mg/kg per BW], placebo-treated HOX mice, and healthy mice 35 days after initiation of hypoxia treatment. The results are expressed as mean ± SEM, ****p<0.0001 for NOX *versus* HOX; §§p<0.01; for HOX *versus* HOX+Juglone.

6.21 The effect of Juglone on right ventricular function in chronic hypoxia mice

The significant decrease in RVID upon Juglone treatment was followed by a substantial and significant improvement in CI (0.67 ± 0.02 vs. 0.80 ± 0.02 [ml min-1] per 100BW) and a slight though non-significant increase in TAPSE (0.88 ± 0.00 mm vs. 0.95 ± 0.03 mm) as compared to placebo-treated chronic hypoxia mice showing cardiac dysfunction.

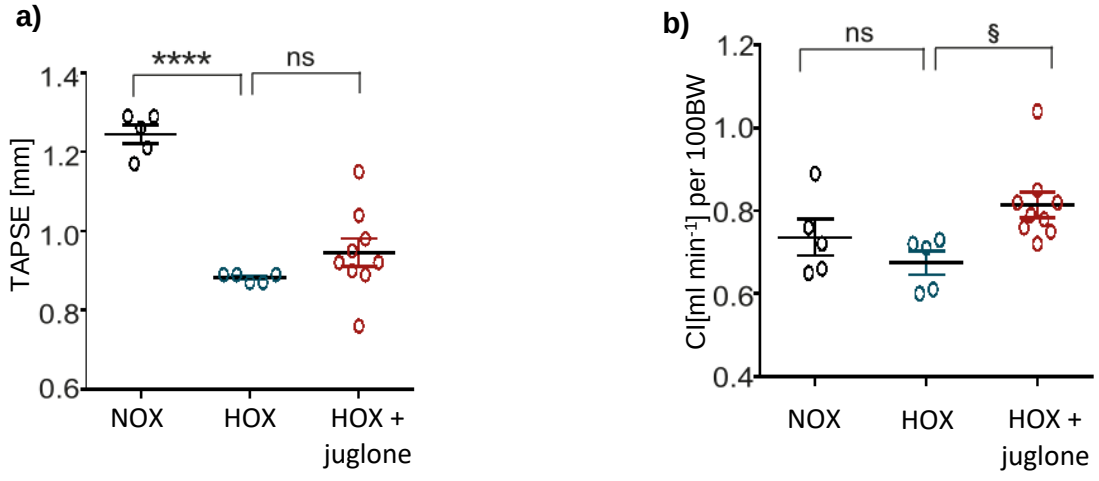

Figure 25. The effect of Juglone on right ventricular function in chronic hypoxia mice. **a)** tricuspid annular plane systolic excursion [TAPSE] and **b)** cardiac index [CI]. Echocardiography was carried out on Juglone-treated [3 mg/kg per BW], placebo-treated chronic hypoxia, and healthy mice. The results are expressed as mean ± SEM, ****p<0.0001 for NOX *versus* HOX; §p<0.05; for HOX *versus* HOX+Juglone

6.22 The effect of Juglone on vascular remodeling in chronic hypoxia mice

The immunological staining revealed the proportion of fully muscularized arteries was remarkably increased, and non-muscularized arteries were significantly decreased in chronic hypoxia mice. Juglone attenuated the development of the fully-muscularized arteries and reduced the pulmonary vascular resistance in the vessels significantly.

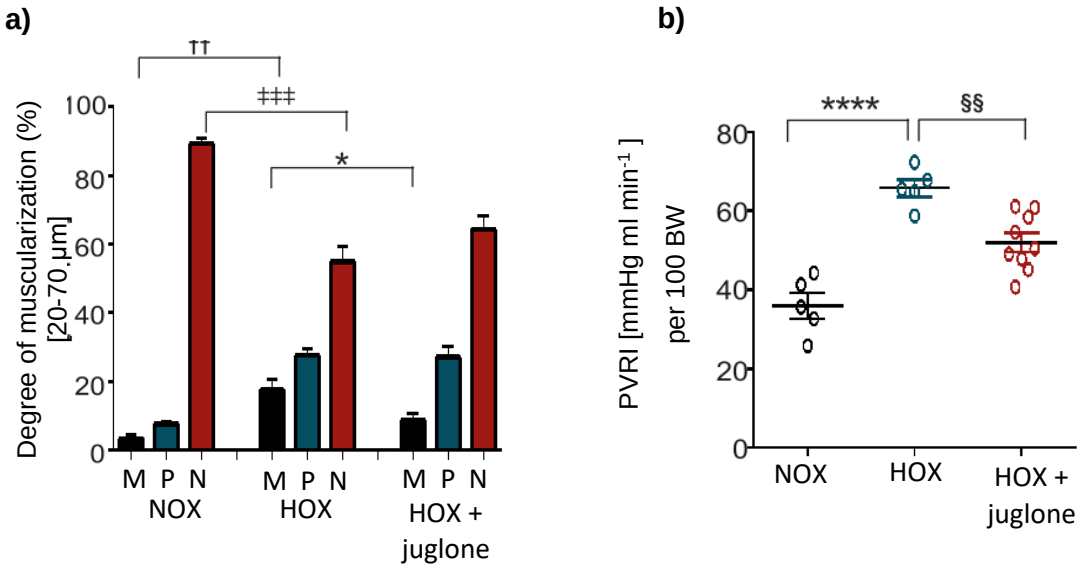

Figure 26. The effect of Juglone on vascular remodeling in chronic hypoxia mice. a) The degree of muscularization of small pulmonary arteries (diameter 20-70 µm) was determined by immunohistological for vWF and α-sma of lung sections. M: fully muscularized; P: partially muscularized; N: non-muscularized. and **b)** pulmonary vascular resistance index [PVRI]. The results are expressed as mean ± SEM; ****p<0.0001 for NOX *versus* HOX; §§p<0.01; §§§p<0.001 for HOX *versus* HOX+Juglone.

6.23 The effect of Juglone on apoptosis in lungs of chronic hypoxia mice

We examined the effects of Juglone on the initiation of apoptosis in mouse lungs *in vivo* and *ex vivo*. In comparison to placebo-treated control mice, apoptosis was

significantly increased in the lungs of Juglone-treated mice. Apoptosis in the lungs was determined by Fluorescence Molecular Tomography (FMT) employing Annexin-Vivo™ 750 probe (marks the early stages of apoptosis) (Figure 27a, b). A significant increase in TUNEL-positive vascular cells of mice treated with Juglone was also observed in ex-vivo studies (Figure 27c, d)

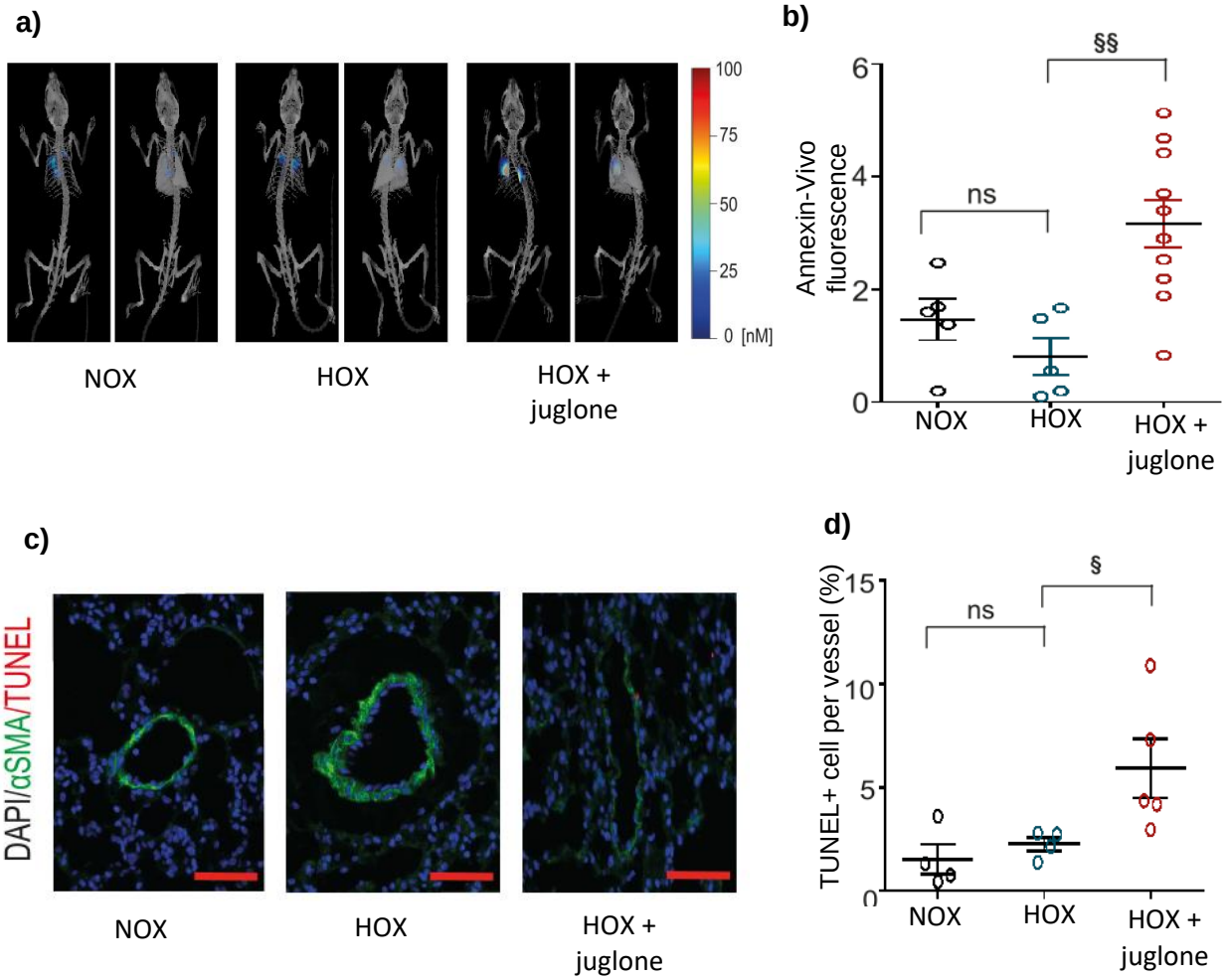

Figure 27. The effect of Juglone on the initiation of apoptosis in lungs of chronic hypoxia mice. a) Fluorescence *in vivo* imaging of mice detected by Fluorescence Molecular Tomography (FMT) using Annexin-Vivo 750 with representative images for all three groups and **b)** quantification. **c)** and **d)** ex-vivo analysis of apoptosis in lung sections of mice by TUNEL staining and its quantification. The results are expressed as mean ± SEM; $^{\S}p<0.05$; $^{\S\S}p<0.01$; for HOX *versus* HOX+Juglone.

DISCUSSION

Pulmonary arterial hypertension (PAH) is a progressive pulmonary disease characterized by vasoconstriction, thrombosis *in situ*, and vascular remodeling [155]. Elevated pulmonary arterial pressure (PAP) due to increased vascular resistance ultimately leads to right heart failure and death. Pulmonary arterial remodeling is a complex pathological mechanism that involves endothelial dysfunction, augmented migration, and hyperproliferation of pulmonary artery smooth muscle cells and resistance to apoptosis of cells of pulmonary vessels [16]. Multiple gene mutations and/or dysregulated gene expression contribute to pro-proliferative PAH pathogenesis and promote the resistance to apoptosis of pulmonary vascular cells. None of the current FDA approved drugs provides a cure against PH; hence it is essential to explore the mechanisms contributing to PAH pathogenesis and develop therapies targeting pro-proliferative and apoptotic resistant features of vascular cells.

Our study provides evidence that peptidyl-prolyl cis/trans isomerase (Pin1) is upregulated in clinical PAH and experimental models of PH: a mouse model of chronic-induced hypoxia and a rat model SU5416/hypoxia-induced (SuHx) PAH. Pin1 expression is associated with clinical characteristics of patients with PAH and might indicate disease severity. Pin1 inhibition (pharmacological and siRNA) *in vitro* resulted in suppression of vascular cell proliferation and initiation of cell apoptosis in PASMCs and PAECs from controls and IPAH patients. Pin1 is induced by PDGF-BB and growth factors in PASMCs. Using a Transcription Factor Array, we demonstrated that PIN1 regulates the activity of several transcription factors implicated in PH emergence and development. Finally, pharmacological inhibition of Pin1 *in vivo* using Juglone ameliorates hemodynamics, reduces pulmonary vascular remodeling and improves RV function in SuHx rats. In addition, we showed that Juglone, by improving RV function, impairs the progression of pulmonary hypertension induced by chronic-hypoxia in mice. Our data suggest that Pin1 is a critical player in the disease pathogenesis of PAH, and Pin1 inhibition by Juglone reverses the proliferative and anti-apoptotic capacity of vascular cells, leading to reversal of pulmonary vascular remodeling; thus, Pin1 might be an attractive therapeutic target for the treatment of PAH and disease secondary to PAH.

7.1 Peptidyl-prolyl isomerase 1 activation in experimental and human PAH

Several studies described the role of PIN1 in the cardiovascular context. Pin1 was found to be upregulated in the neointimal region in a wire-guided injury model of intimal hyperplasia, while Juglone significantly suppressed the neointima formation caused by the injury [146]. Costantino et al. reported that Pin1 prevented nitric oxide (NO) bioavailability by inhibiting endothelial nitric oxide synthase (eNOS) activity [156]. Similarly, Ruan et al. reported Pin1 overexpression in bovine aortic endothelial cells (BAECs) reduced cellular release of NO; on the other hand, Juglone increased NO production, indicating negative regulation of eNOS by Pin1 [157]. In diabetes-induced vascular dysfunction, Pin1 gene-silencing in aortic endothelial cells or Pin1 knockout mice exhibit restored NO release and reduced vascular dysfunction. In addition, the blood Pin1 levels were increased in diabetic patients compared to healthy controls [151]. In 2017, Hu et al. demonstrated that Pin1 regulates the stability, transcriptional activity, and oncogenic potential of Bromodomain-containing protein 4 (Brd4), known to play a critical role in PAH [158]. Pin1 plays a major role in alcohol-induced left-ventricular dysfunction. Furthermore, Toko et al. found that genetic deletion of Pin1 blunts hypertrophic responses induced by transaortic constriction and consequent cardiac failure *in vivo* [145, 159].

The role of Pin1 has not been elucidated in the context of PAH till now. In our study we demonstrate that the expression of Pin1 protein is upregulated in the lungs of both experimental models of PH and in pulmonary arterial smooth muscle cells (PASMCs) from patients with PAH. Mouse smooth muscle cells exposed to hypoxia revealed significant increase in the expression of Pin1. Laser-assisted micro-dissected vessels exhibited no significant difference of *PIN1* transcripts between IPAH and non-PAH controls individuals. Similarly, in our experimental PAH animal models, *PIN1* mRNA expression is not altered between healthy and disease animals. Pin1 is known to be subjected to proteasomal-mediated degradation facilitating dephosophorylation of Bcl-2, inhibiting its anti-apoptotic function, and Polo-like kinase 1 (PLK1) inhibits ubiquitination of Pin1, thus stabilizing Pin1 in human cells [105, 160]. The anti-apoptotic function of Bcl-2 and pro-proliferative effects of Polo-like kinase 1 are well studied in the field of PH [161-163] and could explain the discrepancy between the mRNA and Pin1 protein levels PAH. Pin1 expression is known to predict poor

prognosis in many cancer diseases [164-166]. In our patient derived PASMCs cohort, the protein concentration of Pin1 was negatively correlated with cardiac-index of IPAH patients. Pin1 concentration in PASMCs also showed a tendency towards correlation with other clinical parameters such as pulmonary capillary wedge pressure, mean pulmonary artery pressure and systolic pulmonary artery pressure measured by echocardiography, albeit without significance. Cardiac-index is a well-known marker for cardiovascular risk mortality, and thus strong correlation might relate Pin1 expression with the disease severity in our patient cohort.

7.2 Pin1 inhibition impairs vascular cell proliferation

Pin1 is involved in the cell cycle process of various diseases [167-169]. The entry and progression of the cell cycle, characterized by phosphorylation-dependent events, underlines the various levels of PIN1 intervention. In order to elicit cell cycle progression and cell division in response to pro-proliferative stimuli, Pin1 plays a crucial role in fine-tuning and regulating multiple phospho-proteins and thus the duration and intensity of different signals during the different stages of the cell cycle. Pin1 regulates cell cycle checkpoints dynamically and is needed during all phases of the cell cycle [133]. By directly repressing pRB, Pin1 regulates the G1-S transition and as a result, pRB no longer inhibits E2 transcription factor (E2F), and Cyclin D1 expression is induced [124]. Pin1 further stimulates cyclin-dependent kinase (CDK) of the G1 phase to facilitate the transition from G1 phase to S phase [170]. Pin1 promotes Cyclin E degradation and modulates p27Kip1 activity at a later stage [171].

In pulmonary vascular remodeling, a critical event is the proliferation of vascular smooth muscle cells, which is a prominent hallmark of PAH. It has been generally accepted and acknowledged that growth factors play a pivotal role in PAH pathogenesis. A number of studies emphasize that PDGF-BB induces PASMC proliferation and vascular remodeling, which eventually causes PAH [36, 172, 173]. Our study confirms the inhibitory effect of Juglone on PAMSC proliferation induced by PDGF-BB. We further examined the expression of Ki-67 and PCNA. PCNA, a mediator of cell cycle progression and apoptotic inhibition, is an important component of small pulmonary arterial remodeling leading to PAH. We showed that Pin1 inhibition either by siRNA or by Juglone remarkably declined the expression of Ki-67 and PCNA, two

molecules serving as biomarkers of cell proliferation, suggesting an anti-proliferative capacity of Pin1 inhibition on PASMCs. In PAH, a multifactorial disease, uncontrolled and disorganized endothelial cell proliferation is essential to the pathogenesis that leads to plexiform lesions in PAH [16, 29]. The perpetuation of more proliferative cells reinforces the idea that IPAH also arises from autonomous development of phenotypically altered endothelial cell [174]. We show that Pin1 inhibition either by siRNA or by Juglone led to the reduction in serum-induced proliferation of PAECs. *In vivo*, the proliferation of pulmonary artery vascular cells was assessed by PCNA staining. In the Juglone-treated rats, fewer PCNA-positive pulmonary vascular cells were detected than in the vehicle-treated rats, indicating inhibition of proliferation by Juglone. We observed a decrease in the medial but not intimal layer, signifying a specific anti-proliferative effect of Juglone in SuHx treated rats.

Multiple studies have described the anti-proliferative effects of Juglone on various cell types, including vascular smooth muscle cells and cardiac fibroblasts [144, 175, 176], human endothelial cells [177], breast cancer cells [178] and lung cancer cell lines [179-181]. Here we demonstrate, that Pin1 deletion either by Juglone treatment or by siRNA-knockdown resulted in a marked decrease in the proliferative responses of vascular cells, indicating that endogenous Pin1 contributes to the pseudo-malignant phenotype of PAH.

7.3 Pin1 inhibition initiates cell apoptosis in vascular cells

The equilibrium between proliferation and programmed cell death is strictly regulated under physiological conditions to maintain the integrity of organs and tissues. Anti-apoptotic resistance of vascular cells is another hallmark of PAH [182]. In several vascular proliferative diseases including PH, the activation of proliferative signals as well as the inhibition of death processes leading to survival have been documented [117, 183]. Pulmonary vascular cells such as endothelial and SMCs originating from PAH patients apart from having higher proliferative capacity, are more likely to resist apoptosis induction as compared to control cells [184, 185]. Studies indicate that changes in the relationship between Mouse double minute 2 homolog (MDM2) and tumor protein p53 (p53), and several autoantibodies can occur in human PAH and may partially lead to defects of senescence and apoptosis [182]. DNA damage or any other

apoptotic stimuli cause the activation of certain particular proteases, called Caspases. Activation of death receptors leads to cleavage of procaspase-3 to generate the active effector Caspase 3, inducing cell death [186]. Induction of apoptosis and augmentation of Caspase 3 in hypertrophied PASMCs in pulmonary vessels has been shown to prevent the development of medial hypertrophy and reverse pulmonary vascular remodeling in experimental animal models [187-189]. Apoptotic cell death caused by caspase is achieved by cleavage of several main proteins necessary for cellular functioning and survival, as poly (ADP-ribose) polymerase-1 (PARP-1) [190]. Initiation of apoptosis via PARP-1 cleavage by caspase-3 has been indicated to impair the progression of PAH [191].

We could confirm in our study that PASMCs and PAECs rendered no apoptotic resistance upon Pin1 inhibition by Juglone. Pin1 inhibition upregulated the expression of active, cleaved form of Caspase 3, cleaved PARP-1 and increased the number of TUNEL-positive cells. While apoptosis was observed at a higher concentration with Juglone, a decrease in vascular cell hyperproliferation begins at a lower concentration, suggesting that the antiproliferative effects of Pin1 inhibition might precede the initiation of apoptosis in vascular cells. An increase in Cleaved caspase 3 lung protein homogenates was also detected *in vivo* in SuHx rats treated with Juglone. We also sought to determine the amount of apoptosis by Fluorescence Molecular Tomography (FMT) and could observe increased apoptosis in the lungs of Juglone-treated mice in comparison to Placebo-treated control mice and did not detect any apoptotic signal in the heart. Apoptosis primarily occurred in the vascular cells of pulmonary vessels as observed with increased TUNEL+ cells in the lungs of chronic-hypoxia mice treated with Juglone.

Pin1 has already been shown to be involved in cell death in various pathological conditions [192, 193], and Juglone has been used in cancer studies for its growth inhibitory effect and apoptosis induction [194-196]. In the human breast cancer cell line MCF-7, Juglone induced apoptosis via activation of Caspase 3, cytochrome 3 release and increased Bax/Bcl-2 ratio [197]. *In vivo*, Juglone induced apoptosis via oxidative stress and prevented tumor progression in mice by slowing the cell cycle [198]. In line with the above evidence, here we show that Pin1 inhibition initiates apoptosis of apoptotic-resistant cells of pulmonary vasculature.

7.4 Pin1 is induced by growth factors in PASMCs

Growth factors control variety of cellular processes, such as survival, proliferation, migration and differentiation, and thus not only play an essential part in repair mechanisms but are also involved in the pathogenesis of PAH [36, 199, 200]. Platelet-derived growth factor PDGF-BB/PDGFR controls pulmonary vascular tone through prostaglandin production, calcium enhancement, MAPK-or PI3K/AKT/mTOR signaling activation, and actin remodeling [201]. Genetic ablation of PDGF-dependent phophatidyl-inositol-3-kinase and PLCγ activity is adequate to eradicate the pathogenic responses *in vivo* [202]. Targeting PDGF with the inhibitor imatinib has been shown to reverse pulmonary hypertension in preclinical and clinical trials [36]. It is well established that epidermal growth factor receptors (EGFRs) contribute to the proliferative response of smooth muscle cells, and reversal of pulmonary hypertension was evident with the application of EGFR blocker, available for clinical use [199]. A potent activator of the AKT signaling pathway, insulin-like growth factor-1 (IGF-1) is activated in pulmonary endothelial cells and SMCs [203], and SMC-specific deletion of IGF-1 attenuated hypoxia induced PH [200]. Similarly, in our study it was shown that PDGF-BB, EGF and the Growth Medium (a mixture of growth factors including IGF-1) could induce Pin1 in PASMCs. The Bone-morphogenetic proteins or cytokines could not trigger the expression of Pin1 in PASMCs, suggesting an exclusive GF- induced initiation of Pin1 signaling in PASMCs.

Kim et al. observed that PDGF enhanced Pin1 expression in a concentration-dependent way in vascular SMCs and is associated with neointimal formation [146]. IGF-1 via phosphatidylinositol 3-kinase and the MAP kinase pathways mediates the induction of Pin1 in human breast cancer cells [204]. While BMPs [205] and cytokines [206, 207] are involved in the modification of Pin1 expression and activity, the inability of either of them to induce Pin1 expression suggests a mechanism selective to the PASMCs.

7.5 Pin1 affects various transcription factor's activity

In response to intra and/or extracellular stimuli, several transcription factors (TFs) and transcription-related proteins undergo phosphorylation and activate gene expression. The activity of certain sequence-specific DNA-binding transcription factors and co-regulators is essential for the transcriptional regulation of gene expression that promotes vascular cell phenotypes associated with pulmonary hypertension [40]. Hypoxia inducible factors (HIF-s) are the main regulators of hypoxia related molecular responses, and studies show that SMC-specific conditional knockout of HIF-1α enhances PH in chronically hypoxic mice [208, 209]. The signal transducers and activators of transcription (STAT) protein 3 has been implicated early in the etiology of PH [184]. STAT3 is a crucial intermediary in PAH pathology as it activates a wide variety of TFs and proteins including efficient hypoxic expression of HIF-1α [210]. Many STAT3 intermediaries are involved in proliferation control and apoptosis resistance, contributing to the production of PAH [211].

Our findings show that the inhibition of Pin1 decreased growth-promoting TF activity and increased activity of proliferation restraining factors. Numerous TFs and transcriptional co-activators associated with PH and RV dysfunction, such as HIF-1/2, Octamer binding transcription factor 4 (OCT4), SMAD family (SMADs), Signal transducers and transcription activators (STATs), and Retinoblastoma control element (RB) were dysregulated in Pin1-deficient PASMCs. We also observed a remarkable decrease in HIF-1α protein accumulation in Pin1-silenced hypoxia-treated non-PAH and PAH-SMCs and upregulation of tumor suppressor CCAAT enhancer binding protein α (C/EBPα) TF in non-PAH SMCs.

The reversible serine or threonine residue phosphorylation prior to proline (pSer/Thr-Pro) has emerged as a pivotal switch for regulating the gene expression activities of participating transcription components. The ability of Pin1 to influence many cellular processes could depend on its ability to regulate the expression of different genes by binding to the phosphorylated transcription regulators [127]. Pin1-mediated isomerization has been shown to play an important role in the activity of various TFs that facilitate multiple proliferation-supporting pathways [127, 212, 213]. Pin1 is known to increase the stability and transactivation of HIF-1α by interacting and promoting conformational changes leading to angiogenesis [128, 214]. It was also demonstrated

that the transcriptional activity of STAT3 was compromised in Pin1-deficient cells, affecting cell-cycle regulation and apoptosis in vascular SMC and epithelial-mesenchymal transition in breast cancer cells and gall bladder cancer cells [144, 215, 216]. On one hand, Pin1 could increase the stability of Oct4, affecting stem cell pluripotency [129]; on the other hand, it decreased the stability of Smad3, leading to its proteasomal degradation [217]. New therapeutic approaches for a variety of Pin1 associated disorders could be developed by understanding the Pin1-related transcriptional modulations affecting the cell-cycle and could provide a better understanding of the pathophysiological function of Pin1. In our study, we have established that Pin1 silencing in SMCs resulted in a substantial decrease in the activity of key TFs, which are involved in proliferation, cell cycle control and apoptosis contributing to chronic inflammation, tissue remodeling, and PH.

7.6 Juglone decreased right ventricular systolic pressure in SuHx rats

In the present investigation, established animal models of PH were employed to further study the role of Pin1 in pathogenesis of PH. To observe the pathological changes found in human PAH and to be able to recapitulate all the changes occurring in the human disease, namely intimal proliferation and plexiform lesions, which are absent in monocrotaline (MCT) rat model, a well-established SU5416/hypoxia rat model was employed [218]. The biggest determinant of pulmonary vascular resistance is the abnormal vascular remodeling of the small pulmonary arterioles [219]. In severe PAH, major histological findings include medial wall thickening due to SMC proliferation, occlusion of small vessels and formation of plexiform lesions which reduce the luminal area of the small pulmonary arteries and result in vascular pulmonary resistance, ultimately contributing to the abnormal vascular remodeling. Various studies have shown beneficial effects in PAH by targeting thickened medial wall and could even reverse the vascular remodeling observed in PAH patients and experimental PH models [6].

Juglone significantly reduced right ventricular systolic pressure (RVSP), coupled with structural changes in the pulmonary vascular wall leading to the reduction in pulmonary vascular resistance and decreased vascular remodeling in SuHx rats. Juglone specifically reduced the thickening of the medial wall without changing the intimal wall thickness, which could be explained by the anti-proliferative effect of Juglone on

PASMCs of medial layer, also observed with the reduction of PCNA+ cells in the vessels. Furthermore, the reduction in RVSP in the present investigation may not only be due to anti-proliferative effects of Juglone but to the initiation of apoptosis as well. In the lungs of SuHx rats, we observed the initiation of apoptosis in the Juglone treated group as compared to placebo-control rats. Juglone along with the other naphthaquinones currently are intensively studied in cancer *in vivo* [220-222]. Previously, Plumbagin, a very similar napthaquinone, was reported to decrease medial wall thickness and mean (PAP) in experimental PAH rat models by inhibiting PAH-PASMC proliferation and initiation of apoptosis [189].

PAH pathobiology is centered on the mechanism of vascular remodeling. This process includes structural and functional changes of pulmonary vessels, resulting in severe muscularization, medial hypertrophy and plexiform lesions. This study revealed that Juglone improved hemodynamics, reduced pulmonary vascular resistance, and decreased the medial wall thickening in the SuHx model. Juglone also inhibited progression of occlusive lesions. The effect of Juglone on the reversal of the pulmonary vascular remodeling could be attributed to the inhibition in proliferation and resistance to apoptosis.

7.7 Juglone improved right ventricular function and hypertrophy in SuHx rats

The changes in the pulmonary vasculature directly impact on the right ventricle (RV) where any compromise in vascular reserve leads to the compromise in RV ejection, increased right atrial pressure and decreased cardiac output. The increased afterload of the RV provides an excessive burden and over time, results in right ventricle hypertrophy, right ventricle dysfunction, and right-sided heart failure consecutively [223]. Vascular remodeling, even though being the main pathology in the vasculature, is not the main determining index in the prognosis of PAH, but right ventricular function is. Right ventricle failure is one of the primary causes of dysfunction or death in patients with PAH [224].

In line with the reduction in RVSP and improvement in pulmonary vascular remodeling, treatment with Juglone in SuHx rats also improved right ventricle function. Tricuspid annular plane systolic excursion (TAPSE) increased with an insignificant increase in cardiac index (CI), whereas right ventricular internal diameter (RVID) decreased after treatment with Juglone compared to the vehicle. Juglone reduced right ventricle

hypertrophy in this study, reflected by decreased internal right ventricle diameter and the Fulton index, which are also the right ventricle hypertrophy markers.

An ongoing debate remains about the role of RV fibrosis in PH. Changes in the extracellular matrix collagen network can help prevent ventricular dilatation in the pressure-overloaded RV [225]. In contrast, fibrosis impairs the function of the heart, and an increasing body of experimental evidence indicates that fibrosis plays a crucial role in the development of RV failure [226].

We sought to determine the effect of Pin1 inhibition on right heart remodeling and noted a non-significant reduction in RV fibrosis upon Pin1 inhibition in comparison to placebo-treated control rats. CFs treated with TGF-β1 resulted in increased secreted collagen, which was significantly reduced with Juglone treatment. Mild reduction in fibrosis along with the reduced secreted collagen in CFs indicate that Pin1 is key mediator in regulation of fibrosis in the right heart.

Pin1 plays a central role in the regulation of cardiac hypertrophy and remodeling. Although Pin1 deletion diminishes hypertrophic response *in-vivo* and *in-vitro*, the effect of signaling mechanisms related with overexpression of Pin1 is debatable [142]. Toko et al. showed that Pin-1 loss results in lower Akt and MEK signals leading to lower hypertrophy and preserved cardiac function, while Pin1 over-expression increases RAF-1 phosphorylation in the Ser259 autoinhibitor site and decreases MEK activation, blunting the hypertrophic response [145]. Additionally, Wu et al. showed that Pin1 facilitated cardiac extracellular matrix deposition and oxidative stress damage by controlling the phosphorylation of the MEK1/2-ERK1/2 signaling pathway and the expression of α-SMA. Pin1 inactivation by Juglone reduced the cardiac damage and fibrosis, indicating the role of Pin1 in cardiac remodeling [227].

In line with the above evidence, here we demonstrate that right ventricle hypertrophy was decreased along with improved right ventricle function following the reduction of systolic right ventricle pressure by treatment with Juglone. Thus, inactivation of Pin1 may be a novel therapeutic candidate for the treatment of heart failure due to pulmonary vascular disease.

7.8 Juglone impairs the progression of pulmonary hypertension in chronic hypoxia mice

In order to analyze the contribution of Pin1 signaling in PH due to different etiology, we further investigated the role of Pin1 and inhibitor Juglone in chronic-hypoxia induced PH mice model. The chronic hypoxia model represents group 3 (PH due to lung diseases and/or hypoxia) [228] and furthermore, addresses the aspects of interspecies differences. Mice exposed to chronic hypoxia is associated with only limited vascular remodeling, compared to rats, though increased pulmonary artery pressure exists. Muscularization of previously non-muscularized vessels and a minimal thickening of vessels are the most common findings in hypoxic mice [229]. There is no indication of a loss of pulmonary microvessels, of plexiform lesions or of intimal fibrosis [230]. Lower disease severity in this model could be observed in chronic hypoxia mice with mild increase in RVSP and could explain the reason for Juglone being less effective in improving the RVSP and RV hypertrophy. Upon treatment with Juglone, we observed a slight improvement in TAPSE with significant increase in CI. The changes in the cardiac function were associated with reduced PVRI in Juglone-treated mice. Interestingly, Juglone treated mice demonstrated a marked reversal in vessel remodeling, evidenced by significant reduction in fully muscularized pulmonary arteries. We postulate that improved cardiac function with diminution in the muscularized arteries and pulmonary vascular resistance serve as a background for maintained RVSP in Juglone-treated mice. Taken together our data demonstrate that Pin1 inhibition improves RV function and reverses pulmonary vascular remodeling in hypoxia-exposed mice.

7.9 Limitations

Cellular heterogeneity exists in PAH and further complicates the process of pulmonary vascular remodeling in arterial walls. Indeed, each cell type such as PASMCs, ECs, fibroblasts, pericytes and inflammatory cells, plays a significant role in the progression of PAH. Shen et al. demonstrated the involvement of Pin1 in interstitial pulmonary fibrosis after bleomycin injury. Specifically, Pin1 knock-out (-/-) mice exhibited attenuated expression of collagens and tissue inhibitors of metalloproteinases in response to injury [231]. Immunological disturbances exist in PAH patients, and macrophages and lymphocytes are present in plexiform lesion of severe patients. Also,

the circulating levels of pro-inflammatory cytokines such as IL-1, IL-6. IL-17, IL-21, TNF-α, MCP-1 are upregulated in PH along with the autoantibodies [46, 232]. Pin1 regulates the cytokine production and contributes to allergic lung fibrosis in pulmonary eosinophils, while Juglone reduces inflammation, collagen deposition and airway remodeling in allergen-challenged animals [233]. Since this study focused on SMCs and ECs and with the beneficial effects of Juglone on interstitial fibrosis and inflammation, it would be of great interest to explore Pin1 inhibitory effects on the other cell types as well.

Pin1 is known to regulate the cardiac hypertrophy [227, 234], and the inability to differentiate the mechanisms underlying RV dysfunction from the accompanying changes in the pulmonary circulation is a shortcoming of the employed animal models in this study. The PAB model overcomes this drawback in which the immediate, physical constriction of the pulmonary artery leading to an increase in RV afterload enables us to understand the processes of right heart remodeling and function, regardless of the impact on the pulmonary vasculature [235] and could be employed in future studies. Although we did not observe either cardiac dysfunction or apoptosis signal (FMT) in the heart, studies carrying out the effect of induction of apoptosis in the heart could be performed.

The specificity of Juglone on Pin1 activity should be studied in a more extensive manner since some reports provide evidence of Juglone being a specific inhibitor of Pin1, while other studies show Pin1 independent effects of Juglone [236-238]. In our study, based on the extensive literature search, the doses of Juglone were chosen to have no off-target effects due to cytotoxicity [220, 227, 233]. Still, additional studies are warranted to examine possible Pin1-indepedent effects of Juglone.

SUMMARY

Pulmonary arterial hypertension (PAH) is a condition that is characterized by an increased pulmonary vascular resistance due to prolonged pulmonary vascular remodeling. It encompasses complex pathological mechanisms including dysregulated proliferation and resistance to apoptosis of all three vascular cell types, leading to the emergence and development of PAH. Clinical trials of various therapeutic products targeting vascular remodeling are underway, although effective and successful therapeutical treatment of the disease currently remains a major challenge. Existing evidence strongly supports the involvement of Pin1 signaling in vascular homoeostasis. However, the role of Pin1 in PAH has not been studied, and this led us to investigate the expression and potential contribution of Pin1 signaling in PAH and Juglone as an attractive future therapy for PAH.

Pin1 is a unique enzyme, which induces *cis*/*trans* conformational changes by interacting with specific Ser/thr-Pro motifs present in its phosphorylated substrates. Pin1 guided isomerization of various substrates results in different biological outcomes, offering an alternative signaling pathway under different cellular conditions. Pin1 is involved in the cell cycle regulation in various diseases. This study provides evidence for the first time that Pin1 is upregulated in clinical and experimental models of PAH, specifically in a mouse model of chronic-hypoxia and rat model SU5416/hypoxia-induced PAH. Pin1 expression is correlated with clinical characteristics of patients with PAH such as CI and might correlate with disease severity. In vasculature, Pin1 expression is observed in both pulmonary artery smooth muscle cells (PASMCs) as well as pulmonary artery endothelial cells (PAECs). Here we show, that genetic and pharmacological inhibition of Pin1 resulted in downregulation of proliferating cell nuclear antigen (PCNA) and Ki-67, leading to a marked decrease in proliferative responses of human PASMCs and PAECs. Thus, endogenous Pin1 is a significant contributor in cancer-like proliferation of vascular cells. Apoptotic resistant vascular cell growth exhibits an alternative paradigm of the PAH phenotype. Pin1 modulates various signaling pathways including the regulation of cell death signaling and contributes to the pathogenesis of various diseases. In our study, Pin1 deletion led to an initiation of apoptosis in human vascular cells as evidenced by an increase in Cleaved Caspase-3 and cleaved PARP in both PASMCs and PAECs.

Pin1 was induced by growth factors in PASMCs, and siRNA-mediated deletion of Pin1 resulted in a strong decrease of the activity of key TFs, which have been previously implicated in chronic inflammation, tissue remodeling, and PH, such as STAT3, HIF, EGR, OCT4 and SMADs. *In-vivo*, Juglone administration lowered pulmonary vascular resistance, enhanced RV function, improved pulmonary vascular and cardiac remodeling in the SU5416/hypoxia rat model of PAH and the chronic hypoxia-induced PH model in mice. Pin1 inhibition in vascular cells of the lung resulted in inhibition of proliferative (PCNA) and activation of pro-apoptotic responses (Cleaved Caspase-3), implicating Pin1 for PH emergence. The unique ability of Pin1 to bind with phosphorylated trans forms of Ser/Thr-containing proteins either enhances degradation and/or stabilizes the protein and makes it an effective molecular switch of multiple downstream cellular functions. To establish personalized therapeutic approaches based on Pin1 inhibition, a thorough understanding of the upstream and downstream molecular mechanisms driving Pin1 regulation and the molecular and cellular effects driven by Pin1 in diseased vascular cells is important. A proposed overview of Pin1 signaling has been illustrated in figure 28.

Taken together, this study puts forward a role of Pin1 signaling in the regulation of proliferation and apoptosis of smooth muscle and endothelial cells contributing to PAH pathogenesis. Thus, Pin1 represents a novel target, and Juglone a potential new strategy for the prevention of cardiovascular diseases, including pulmonary arterial hypertension.

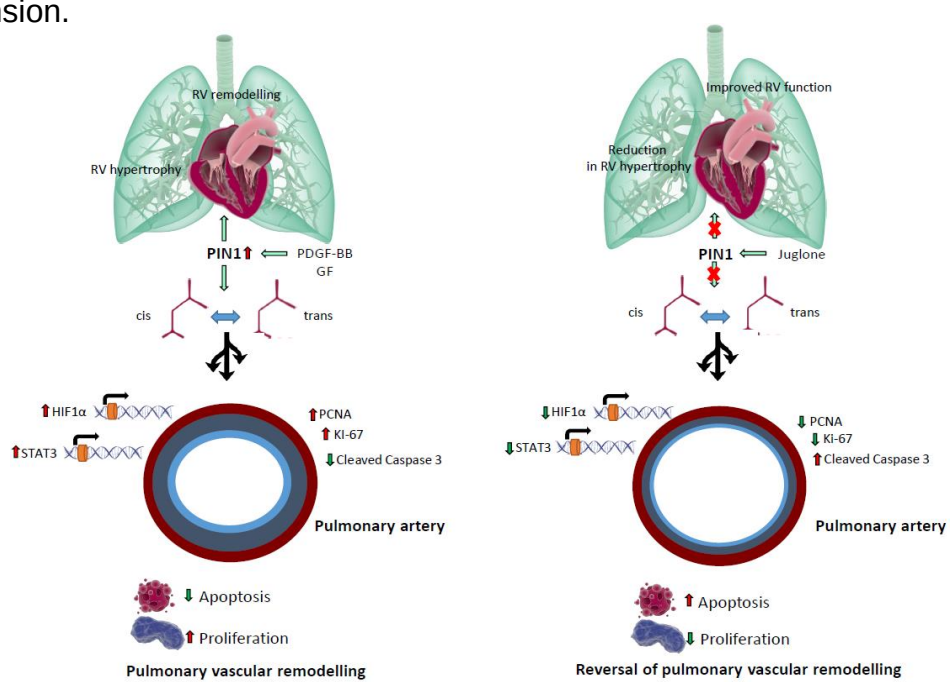

Figure 28. A proposed mechanism depicting Pin1 signaling in pulmonary hypertension.

ZUSAMMENFASSUNG

Die pulmonal arterielle Hypertonie (PAH) ist eine Erkrankung, die durch erhöhten pulmonalen Gefäßwiderstand aufgrund von strukturellem Umbau der pulmonalen Gefäße („Remodeling“) entsteht. Dabei spielen komplexe pathologische Mechanismen wie dysregulierte Proliferation und Resistenz gegen Apoptose von Gefäßzellen eine entscheidende Rolle. Zurzeit sind zahlreiche Medikamente zur Behandlung der PAH zugelassen, allerdings gibt es keine Heilung dieser Erkrankung, da diese Medikamente lediglich den Gefäßtonus beeinflussen, aber keine kausale Therapie darstellen. Die Rolle der Isomerase Pin1 wurde in der PAH noch nicht erforscht, was uns dazu führte, die Expression und potentielle Beteiligung von Pin1 in der PAH zu untersuchen. Mit dem Pin1 Hemmstoff Juglone stand zudem eine attraktive zukünftige Therapiemöglichkeit der PAH zur Verfügung.

Pin1 ist ein einzigartiges Enzym, das *cis/trans* konformative Veränderungen durch Interaktion mit spezifischen Ser/Thr-Pro Mustern in seiner phosphorylierten Form verursacht. Die durch Pin1 verursachte Isomerisierung verschiedener Substrate führt zu verschiedenen biologischen Wirkungen, die alternative Signalwege unter verschiedenen zellulären Konditionen bieten. Pin1 ist in die Regulierung des Zellzyklus verschiedener Krankheiten involviert. Diese Arbeit zeigt, dass Pin1 in humanem Gewebe und dem experimentellen Maus-Modell mit chronischer Hypoxie sowie einem Ratten-Modell mit SU5416/Hypoxie-verursachter PAH hochreguliert ist. Die Expression von Pin1 korreliert mit klinischen Charakteristika von Patienten mit PAH (wie dem Herzzeitvolumen) und könnte möglicherweise auf den Schweregrad der Krankheit hinweisen. In Blutgefäßen kommt Pin1 sowohl in pulmonalen arteriellen glatten Muskelzellen (PASMCs) als auch in pulmonalen arteriellen Endothelzellen (PAECs) vor. Hier zeigt sich, dass die genetische (siRNA) und pharmakologische (Juglone) Hemmung von Pin1 zu einer Herabregulation des Proliferating-Cell-Nuclear-Antigen (PCNA) sowie Ki-67 führt, was eine Reduktion der Proliferation humaner PASMCs und PAECs zur Folge hat. Das zeigt die Rolle von endogenem Pin1 bei der tumorartigen Proliferation von vaskulären Zellen. Pin1 moduliert verschiedene Signalwege wie die Regulierung des Zelltods und wirkt bei verschiedenen Krankheitsentstehungen mit. In dieser Studie führte die Hemmung von Pin1 zu einer Einleitung der Apoptose in humanen Gefäßzellen, was sich durch einen Anstieg von Cleaved Caspase-3 und Cleaved-PARP in PASMCs und PAECs zeigte.

Pin1 wurde durch Wachstumsfaktoren in PASMCs induziert und die siRNA-vermittelte Herabregulation von Pin1 führte zu einem starken Rückgang der Aktivität von entscheidenden Transkriptionsfaktoren (TFs) wie STAT3, HIF, EGR, OCT4 und SMADs, die bei chronischer Entzündung, Gewebe-Remodeling und PH aktiv sind. Die Gabe von Juglon verminderte *in-vivo* den pulmonalen vaskulären Widerstand und steigerte die Funktion des rechten Herzens. Außerdem verbesserte sich das kardiale und pulmonale Gefäß-Remodeling im SU5416/Hypoxie Rattenmodell für PAH und im chronischen Hypoxie-induzierten Mausmodell der PH. Die Hemmung von Pin1 in vaskulären Zellen der Lunge führt zu Hemmung proliferativer (PCNA) und Aktivierung pro-apoptotischer Signalwege (Cleaved Caspase-3), was die Entstehung von PH durch Pin1 impliziert.

Zusammenfassend stellt diese Studie die Rolle des Pin1-Signalweges in der Regulierung der Proliferation und Apoptose von Glattmuskelzellen und Endothelzellen in der Krankheitsentstehung der PAH vor. Pin1 stellt ein neuartiges Ziel dar und Juglon eine potentielle neue Strategie für die Prävention kardiovaskulärer Krankheiten, wie die pulmonale arterielle Hypertonie.

REFERENCES

1. Schermuly, R.T., et al., *Mechanisms of disease: pulmonary arterial hypertension.* Nat Rev Cardiol, 2011. **8**(8): p. 443-55.
2. Simonneau, G., et al., *Haemodynamic definitions and updated clinical classification of pulmonary hypertension.* Eur Respir J, 2019. **53**(1).
3. Galie, N., et al., *2015 ESC/ERS Guidelines for the diagnosis and treatment of pulmonary hypertension: The Joint Task Force for the Diagnosis and Treatment of Pulmonary Hypertension of the European Society of Cardiology (ESC) and the European Respiratory Society (ERS): Endorsed by: Association for European Paediatric and Congenital Cardiology (AEPC), International Society for Heart and Lung Transplantation (ISHLT).* Eur Heart J, 2016. **37**(1): p. 67-119.
4. Yaghi, S., A. Novikov, and T. Trandafirescu, *Clinical update on pulmonary hypertension.* J Investig Med, 2020. **68**(4): p. 821-827.
5. Tuder, R.M., et al., *Development and pathology of pulmonary hypertension.* J Am Coll Cardiol, 2009. **54**(1 Suppl): p. S3-9.
6. Shimoda, L.A. and S.S. Laurie, *Vascular remodeling in pulmonary hypertension.* J Mol Med (Berl), 2013. **91**(3): p. 297-309.
7. Arrigo, M., et al., *Right Ventricular Failure: Pathophysiology, Diagnosis and Treatment.* Card Fail Rev, 2019. **5**(3): p. 140-146.
8. Abe, K., et al., *Formation of plexiform lesions in experimental severe pulmonary arterial hypertension.* Circulation, 2010. **121**(25): p. 2747-54.
9. Chemla, D., et al., *Pulmonary vascular resistance and compliance relationship in pulmonary hypertension.* Eur Respir J, 2015. **46**(4): p. 1178-89.
10. Sobin, S.S., W.G. Frasher, Jr., and H.M. Tremer, *Vasa vasorum of the pulmonary artery of the rabbit.* Circ Res, 1962. **11**: p. 257-63.
11. Townsley, M.I., *Structure and composition of pulmonary arteries, capillaries, and veins.* Compr Physiol, 2012. **2**(1): p. 675-709.
12. Brown, I.A.M., et al., *Vascular Smooth Muscle Remodeling in Conductive and Resistance Arteries in Hypertension.* Arterioscler Thromb Vasc Biol, 2018. **38**(9): p. 1969-1985.

13. Perros, F., et al., *Smooth Muscle Phenotype in Idiopathic Pulmonary Hypertension: Hyper-Proliferative but not Cancerous.* Int J Mol Sci, 2019. **20**(14).
14. Tuder, R.M., et al., *Pathology of pulmonary hypertension.* Clin Chest Med, 2007. **28**(1): p. 23-42, vii.
15. Lan, N.S.H., et al., *Pulmonary Arterial Hypertension: Pathophysiology and Treatment.* Diseases, 2018. **6**(2).
16. Humbert, M., et al., *Cellular and molecular pathobiology of pulmonary arterial hypertension.* J Am Coll Cardiol, 2004. **43**(12 Suppl S): p. 13S-24S.
17. Morrell, N.W., et al., *Cellular and molecular basis of pulmonary arterial hypertension.* J Am Coll Cardiol, 2009. **54**(1 Suppl): p. S20-31.
18. Awad, K.S., et al., *Novel signaling pathways in pulmonary arterial hypertension (2015 Grover Conference Series).* Pulm Circ, 2016. **6**(3): p. 285-94.
19. Sakao, S., et al., *Initial apoptosis is followed by increased proliferation of apoptosis-resistant endothelial cells.* FASEB J, 2005. **19**(9): p. 1178-80.
20. Tajsic, T. and N.W. Morrell, *Smooth muscle cell hypertrophy, proliferation, migration and apoptosis in pulmonary hypertension.* Compr Physiol, 2011. **1**(1): p. 295-317.
21. Pu, X., et al., *Stem/Progenitor Cells and Pulmonary Arterial Hypertension.* Arterioscler Thromb Vasc Biol, 2021. **41**(1): p. 167-178.
22. Stenmark, K.R., M.G. Frid, and M.E. Yeager, *Fibrocytes: potential new therapeutic targets for pulmonary hypertension?* Eur Respir J, 2010. **36**(6): p. 1232-5.
23. Ranchoux, B., et al., *Endothelial dysfunction in pulmonary arterial hypertension: an evolving landscape (2017 Grover Conference Series).* Pulm Circ, 2018. **8**(1): p. 2045893217752912.
24. Sakao, S., K. Tatsumi, and N.F. Voelkel, *Endothelial cells and pulmonary arterial hypertension: apoptosis, proliferation, interaction and transdifferentiation.* Respir Res, 2009. **10**: p. 95.
25. Patan, S., *Vasculogenesis and angiogenesis as mechanisms of vascular network formation, growth and remodeling.* J Neurooncol, 2000. **50**(1-2): p. 1-15.

26. Pan, P., et al., *Angiotensin II upregulates the expression of placental growth factor in human vascular endothelial cells and smooth muscle cells.* BMC Cell Biol, 2010. **11**: p. 36.
27. Dardik, A., et al., *Shear stress-stimulated endothelial cells induce smooth muscle cell chemotaxis via platelet-derived growth factor-BB and interleukin-1alpha.* J Vasc Surg, 2005. **41**(2): p. 321-31.
28. Tuder, R.M., et al., *Expression of angiogenesis-related molecules in plexiform lesions in severe pulmonary hypertension: evidence for a process of disordered angiogenesis.* J Pathol, 2001. **195**(3): p. 367-74.
29. Xu, W. and S.C. Erzurum, *Endothelial cell energy metabolism, proliferation, and apoptosis in pulmonary hypertension.* Compr Physiol, 2011. **1**(1): p. 357-72.
30. Sakao, S., et al., *VEGF-R blockade causes endothelial cell apoptosis, expansion of surviving CD34+ precursor cells and transdifferentiation to smooth muscle-like and neuronal-like cells.* FASEB J, 2007. **21**(13): p. 3640-52.
31. Le Hiress, M., et al., *Proinflammatory Signature of the Dysfunctional Endothelium in Pulmonary Hypertension. Role of the Macrophage Migration Inhibitory Factor/CD74 Complex.* Am J Respir Crit Care Med, 2015. **192**(8): p. 983-97.
32. Lyle, M.A., J.P. Davis, and F.V. Brozovich, *Regulation of Pulmonary Vascular Smooth Muscle Contractility in Pulmonary Arterial Hypertension: Implications for Therapy.* Front Physiol, 2017. **8**: p. 614.
33. Morrell, N.W., et al., *Altered growth responses of pulmonary artery smooth muscle cells from patients with primary pulmonary hypertension to transforming growth factor-beta(1) and bone morphogenetic proteins.* Circulation, 2001. **104**(7): p. 790-5.
34. Frump, A., A. Prewitt, and M.P. de Caestecker, *BMPR2 mutations and endothelial dysfunction in pulmonary arterial hypertension (2017 Grover Conference Series).* Pulm Circ, 2018. **8**(2): p. 2045894018765840.
35. Launay, J.M., et al., *Function of the serotonin 5-hydroxytryptamine 2B receptor in pulmonary hypertension.* Nat Med, 2002. **8**(10): p. 1129-35.
36. Schermuly, R.T., et al., *Reversal of experimental pulmonary hypertension by PDGF inhibition.* J Clin Invest, 2005. **115**(10): p. 2811-21.

37. Jones, P.L., K.N. Cowan, and M. Rabinovitch, *Tenascin-C, proliferation and subendothelial fibronectin in progressive pulmonary vascular disease.* Am J Pathol, 1997. **150**(4): p. 1349-60.
38. Chelladurai, P., W. Seeger, and S.S. Pullamsetti, *Matrix metalloproteinases and their inhibitors in pulmonary hypertension.* Eur Respir J, 2012. **40**(3): p. 766-82.
39. Wang, C., et al., *Peroxisome Proliferator-Activated Receptor-gamma Knockdown Impairs Bone Morphogenetic Protein-2-Induced Critical-Size Bone Defect Repair.* Am J Pathol, 2019. **189**(3): p. 648-664.
40. Pullamsetti, S.S., et al., *Transcription factors, transcriptional coregulators, and epigenetic modulation in the control of pulmonary vascular cell phenotype: therapeutic implications for pulmonary hypertension (2015 Grover Conference series).* Pulm Circ, 2016. **6**(4): p. 448-464.
41. Pugliese, S.C., et al., *The role of inflammation in hypoxic pulmonary hypertension: from cellular mechanisms to clinical phenotypes.* Am J Physiol Lung Cell Mol Physiol, 2015. **308**(3): p. L229-52.
42. Stenmark, K.R., et al., *The adventitia: Essential role in pulmonary vascular remodeling.* Compr Physiol, 2011. **1**(1): p. 141-61.
43. Steinbrech, D.S., et al., *Fibroblast response to hypoxia: the relationship between angiogenesis and matrix regulation.* J Surg Res, 1999. **84**(2): p. 127-33.
44. Itoh, T., et al., *Increased plasma monocyte chemoattractant protein-1 level in idiopathic pulmonary arterial hypertension.* Respirology, 2006. **11**(2): p. 158-63.
45. Stenmark, K.R., et al., *Hypoxia, leukocytes, and the pulmonary circulation.* J Appl Physiol (1985), 2005. **98**(2): p. 715-21.
46. Groth, A., et al., *Inflammatory cytokines in pulmonary hypertension.* Respir Res, 2014. **15**: p. 47.
47. Savale, L., et al., *Impact of interleukin-6 on hypoxia-induced pulmonary hypertension and lung inflammation in mice.* Respir Res, 2009. **10**: p. 6.
48. El Chami, H. and P.M. Hassoun, *Immune and inflammatory mechanisms in pulmonary arterial hypertension.* Prog Cardiovasc Dis, 2012. **55**(2): p. 218-28.
49. Stenmark, K.R., et al., *Role of the adventitia in pulmonary vascular remodeling.* Physiology (Bethesda), 2006. **21**: p. 134-45.

50. Huertas, A., et al., *Chronic inflammation within the vascular wall in pulmonary arterial hypertension: more than a spectator.* Cardiovasc Res, 2020. **116**(5): p. 885-893.
51. Taraseviciene-Stewart, L., et al., *Inhibition of the VEGF receptor 2 combined with chronic hypoxia causes cell death-dependent pulmonary endothelial cell proliferation and severe pulmonary hypertension.* FASEB J, 2001. **15**(2): p. 427-38.
52. Golpon, H.A., et al., *Life after corpse engulfment: phagocytosis of apoptotic cells leads to VEGF secretion and cell growth.* FASEB J, 2004. **18**(14): p. 1716-8.
53. Sakao, S., et al., *Apoptosis of pulmonary microvascular endothelial cells stimulates vascular smooth muscle cell growth.* Am J Physiol Lung Cell Mol Physiol, 2006. **291**(3): p. L362-8.
54. Orcholski, M.E., et al., *Drug-induced pulmonary arterial hypertension: a primer for clinicians and scientists.* Am J Physiol Lung Cell Mol Physiol, 2018. **314**(6): p. L967-L983.
55. Yu, Q. and S.Y. Chan, *Mitochondrial and Metabolic Drivers of Pulmonary Vascular Endothelial Dysfunction in Pulmonary Hypertension.* Adv Exp Med Biol, 2017. **967**: p. 373-383.
56. Poon, I.K., et al., *Apoptotic cell clearance: basic biology and therapeutic potential.* Nat Rev Immunol, 2014. **14**(3): p. 166-80.
57. Fogarty, C.E. and A. Bergmann, *The Sound of Silence: Signaling by Apoptotic Cells.* Curr Top Dev Biol, 2015. **114**: p. 241-65.
58. Schubert, S.Y., et al., *Primary monocytes regulate endothelial cell survival through secretion of angiopoietin-1 and activation of endothelial Tie2.* Arterioscler Thromb Vasc Biol, 2011. **31**(4): p. 870-5.
59. Furuya, Y., T. Satoh, and M. Kuwana, *Interleukin-6 as a potential therapeutic target for pulmonary arterial hypertension.* Int J Rheumatol, 2010. **2010**: p. 720305.
60. Weigert, A., et al., *Apoptotic cells promote macrophage survival by releasing the antiapoptotic mediator sphingosine-1-phosphate.* Blood, 2006. **108**(5): p. 1635-42.
61. Portt, L., et al., *Anti-apoptosis and cell survival: a review.* Biochim Biophys Acta, 2011. **1813**(1): p. 238-59.

62. Majesky, M.W., et al., *Production of transforming growth factor beta 1 during repair of arterial injury.* J Clin Invest, 1991. **88**(3): p. 904-10.
63. Hinz, B., *The extracellular matrix and transforming growth factor-beta1: Tale of a strained relationship.* Matrix Biol, 2015. **47**: p. 54-65.
64. Matsushita, H., et al., *Hypoxia-induced endothelial apoptosis through nuclear factor-kappaB (NF-kappaB)-mediated bcl-2 suppression: in vivo evidence of the importance of NF-kappaB in endothelial cell regulation.* Circ Res, 2000. **86**(9): p. 974-81.
65. Michiels, C., et al., *Hypoxia stimulates human endothelial cells to release smooth muscle cell mitogens: role of prostaglandins and bFGF.* Exp Cell Res, 1994. **213**(1): p. 43-54.
66. Laplante, P., et al., *Caspase-3-mediated secretion of connective tissue growth factor by apoptotic endothelial cells promotes fibrosis.* Cell Death Differ, 2010. **17**(2): p. 291-303.
67. Kanmogne, G.D., C. Primeaux, and P. Grammas, *Induction of apoptosis and endothelin-1 secretion in primary human lung endothelial cells by HIV-1 gp120 proteins.* Biochem Biophys Res Commun, 2005. **333**(4): p. 1107-15.
68. Diwanji, N. and A. Bergmann, *An unexpected friend - ROS in apoptosis-induced compensatory proliferation: Implications for regeneration and cancer.* Semin Cell Dev Biol, 2018. **80**: p. 74-82.
69. Rabinovitch, M., et al., *Inflammation and immunity in the pathogenesis of pulmonary arterial hypertension.* Circ Res, 2014. **115**(1): p. 165-75.
70. Rafikova, O., I. Al Ghouleh, and R. Rafikov, *Focus on Early Events: Pathogenesis of Pulmonary Arterial Hypertension Development.* Antioxid Redox Signal, 2019. **31**(13): p. 933-953.
71. Goldenberg, N.M., et al., *Therapeutic Targeting of High-Mobility Group Box-1 in Pulmonary Arterial Hypertension.* Am J Respir Crit Care Med, 2019. **199**(12): p. 1566-1569.
72. Scaffidi, P., T. Misteli, and M.E. Bianchi, *Release of chromatin protein HMGB1 by necrotic cells triggers inflammation.* Nature, 2002. **418**(6894): p. 191-5.
73. Carley, A.N., H. Taegtmeyer, and E.D. Lewandowski, *Matrix revisited: mechanisms linking energy substrate metabolism to the function of the heart.* Circ Res, 2014. **114**(4): p. 717-29.

74. Shi, J., et al., *Metabolism of vascular smooth muscle cells in vascular diseases.* Am J Physiol Heart Circ Physiol, 2020. **319**(3): p. H613-H631.
75. Rafikov, R., et al., *Complex I dysfunction underlies the glycolytic switch in pulmonary hypertensive smooth muscle cells.* Redox Biol, 2015. **6**: p. 278-286.
76. Rafikova, O., et al., *Recurrent inhibition of mitochondrial complex III induces chronic pulmonary vasoconstriction and glycolytic switch in the rat lung.* Respir Res, 2018. **19**(1): p. 69.
77. Lei, W., et al., *Expression and analyses of the HIF-1 pathway in the lungs of humans with pulmonary arterial hypertension.* Mol Med Rep, 2016. **14**(5): p. 4383-4390.
78. Zhu, W., et al., *Dihydroartemisinin suppresses glycolysis of LNCaP cells by inhibiting PI3K/AKT pathway and downregulating HIF-1alpha expression.* Life Sci, 2019. **233**: p. 116730.
79. Goncharova, E.A., *mTOR and vascular remodeling in lung diseases: current challenges and therapeutic prospects.* FASEB J, 2013. **27**(5): p. 1796-807.
80. Kim, J.W., et al., *HIF-1-mediated expression of pyruvate dehydrogenase kinase: a metabolic switch required for cellular adaptation to hypoxia.* Cell Metab, 2006. **3**(3): p. 177-85.
81. Park, S., et al., *Role of the Pyruvate Dehydrogenase Complex in Metabolic Remodeling: Differential Pyruvate Dehydrogenase Complex Functions in Metabolism.* Diabetes Metab J, 2018. **42**(4): p. 270-281.
82. Sun, X.Q., et al., *Reversal of right ventricular remodeling by dichloroacetate is related to inhibition of mitochondria-dependent apoptosis.* Hypertens Res, 2016. **39**(5): p. 302-11.
83. Michelakis, E.D., et al., *Inhibition of pyruvate dehydrogenase kinase improves pulmonary arterial hypertension in genetically susceptible patients.* Sci Transl Med, 2017. **9**(413).
84. He, Z., L. Li, and S. Luan, *Immunophilins and parvulins. Superfamily of peptidyl prolyl isomerases in Arabidopsis.* Plant Physiol, 2004. **134**(4): p. 1248-67.
85. Davis, T.L., et al., *Structural and biochemical characterization of the human cyclophilin family of peptidyl-prolyl isomerases.* PLoS Biol, 2010. **8**(7): p. e1000439.

86. Wang, T., P.K. Donahoe, and A.S. Zervos, *Specific interaction of type I receptors of the TGF-beta family with the immunophilin FKBP-12.* Science, 1994. **265**(5172): p. 674-6.
87. Spiekerkoetter, E., et al., *FK506 activates BMPR2, rescues endothelial dysfunction, and reverses pulmonary hypertension.* J Clin Invest, 2013. **123**(8): p. 3600-13.
88. Uittenbogaard, A., Y. Ying, and E.J. Smart, *Characterization of a cytosolic heat-shock protein-caveolin chaperone complex. Involvement in cholesterol trafficking.* J Biol Chem, 1998. **273**(11): p. 6525-32.
89. Jin, Z.G., et al., *Cyclophilin A is a proinflammatory cytokine that activates endothelial cells.* Arterioscler Thromb Vasc Biol, 2004. **24**(7): p. 1186-91.
90. Jin, Z.G., et al., *Cyclophilin A is a secreted growth factor induced by oxidative stress.* Circ Res, 2000. **87**(9): p. 789-96.
91. Nigro, P., et al., *Cyclophilin A is an inflammatory mediator that promotes atherosclerosis in apolipoprotein E-deficient mice.* J Exp Med, 2011. **208**(1): p. 53-66.
92. *Correction to: Extracellular Cyclophilin A, Especially Acetylated, Causes Pulmonary Hypertension by Stimulating Endothelial Apoptosis, Redox Stress, and Inflammation.* Arterioscler Thromb Vasc Biol, 2017. **37**(6): p. e68.
93. Zhou, X.Z., et al., *Pin1-dependent prolyl isomerization regulates dephosphorylation of Cdc25C and tau proteins.* Mol Cell, 2000. **6**(4): p. 873-83.
94. Greenwood, A.I., et al., *Complete determination of the Pin1 catalytic domain thermodynamic cycle by NMR lineshape analysis.* J Biomol NMR, 2011. **51**(1-2): p. 21-34.
95. Hanes, S.D., P.R. Shank, and K.A. Bostian, *Sequence and mutational analysis of ESS1, a gene essential for growth in Saccharomyces cerevisiae.* Yeast, 1989. **5**(1): p. 55-72.
96. Stukenberg, P.T. and M.W. Kirschner, *Pin1 acts catalytically to promote a conformational change in Cdc25.* Mol Cell, 2001. **7**(5): p. 1071-83.
97. Napoli, M., et al., *Wiring the oncogenic circuitry: Pin1 unleashes mutant p53.* Oncotarget, 2011. **2**(9): p. 654-6.

98. Lu, K.P. and X.Z. Zhou, *The prolyl isomerase PIN1: a pivotal new twist in phosphorylation signalling and disease.* Nat Rev Mol Cell Biol, 2007. **8**(11): p. 904-16.
99. Lufei, C. and X. Cao, *Nuclear import of Pin1 is mediated by a novel sequence in the PPIase domain.* FEBS Lett, 2009. **583**(2): p. 271-6.
100. Matena, A., et al., *Structure and function of the human parvulins Pin1 and Par14/17.* Biol Chem, 2018. **399**(2): p. 101-125.
101. Lee, Y.M. and Y.C. Liou, *Gears-In-Motion: The Interplay of WW and PPIase Domains in Pin1.* Front Oncol, 2018. **8**: p. 469.
102. Labeikovsky, W., et al., *Structure and dynamics of pin1 during catalysis by NMR.* J Mol Biol, 2007. **367**(5): p. 1370-81.
103. Driver, J.A., X.Z. Zhou, and K.P. Lu, *Pin1 dysregulation helps to explain the inverse association between cancer and Alzheimer's disease.* Biochim Biophys Acta, 2015. **1850**(10): p. 2069-76.
104. Butterfield, D.A., et al., *Pin1 in Alzheimer's disease.* J Neurochem, 2006. **98**(6): p. 1697-706.
105. Eckerdt, F., et al., *Polo-like kinase 1-mediated phosphorylation stabilizes Pin1 by inhibiting its ubiquitination in human cells.* J Biol Chem, 2005. **280**(44): p. 36575-83.
106. Zannini, A., et al., *Oncogenic Hijacking of the PIN1 Signaling Network.* Front Oncol, 2019. **9**: p. 94.
107. Zhou, X.Z., et al., *Phosphorylation-dependent prolyl isomerization: a novel signaling regulatory mechanism.* Cell Mol Life Sci, 1999. **56**(9-10): p. 788-806.
108. Jacobs, D.M., et al., *Peptide binding induces large scale changes in inter-domain mobility in human Pin1.* J Biol Chem, 2003. **278**(28): p. 26174-82.
109. Joseph, J.D., et al., *The peptidyl-prolyl isomerase Pin1.* Prog Cell Cycle Res, 2003. **5**: p. 477-87.
110. Alao, J.P., *The regulation of cyclin D1 degradation: roles in cancer development and the potential for therapeutic invention.* Mol Cancer, 2007. **6**: p. 24.
111. Wulf, G.M., et al., *Pin1 is overexpressed in breast cancer and cooperates with Ras signaling in increasing the transcriptional activity of c-Jun towards cyclin D1.* EMBO J, 2001. **20**(13): p. 3459-72.

112. Rustighi, A., et al., *PIN1 in breast development and cancer: a clinical perspective.* Cell Death Differ, 2017. **24**(2): p. 200-211.
113. Strzalka, W. and A. Ziemienowicz, *Proliferating cell nuclear antigen (PCNA): a key factor in DNA replication and cell cycle regulation.* Ann Bot, 2011. **107**(7): p. 1127-40.
114. Luo, Y., et al., *[Different expression and significance of VEGF and PCNA in aorta and pulmonary artery smooth muscle cells of rats with hypoxia pulmonary hypertension].* Xi Bao Yu Fen Zi Mian Yi Xue Za Zhi, 2006. **22**(1): p. 103-5.
115. Khanal, P., et al., *Prolyl isomerase Pin1 negatively regulates the stability of SUV39H1 to promote tumorigenesis in breast cancer.* FASEB J, 2013. **27**(11): p. 4606-18.
116. Lv, L., et al., *Prevention of Neointimal Hyperplasia by Local Application of Lentiviral Vectors Encoding Pin1 shRNA in Pluronic F127.* Curr Gene Ther, 2015. **15**(6): p. 572-80.
117. Tu, L., et al., *Autocrine fibroblast growth factor-2 signaling contributes to altered endothelial phenotype in pulmonary hypertension.* Am J Respir Cell Mol Biol, 2011. **45**(2): p. 311-22.
118. Braun, C., et al., *Inhibition of peptidyl-prolyl isomerase (PIN1) and BRAF signaling to target melanoma.* Am J Transl Res, 2019. **11**(7): p. 4425-4437.
119. El Boustani, M., et al., *A Guide to PIN1 Function and Mutations Across Cancers.* Front Pharmacol, 2018. **9**: p. 1477.
120. Liao, Y., et al., *Peptidyl-prolyl cis/trans isomerase Pin1 is critical for the regulation of PKB/Akt stability and activation phosphorylation.* Oncogene, 2009. **28**(26): p. 2436-45.
121. Kang, C., et al., *The natively disordered loop of Bcl-2 undergoes phosphorylation-dependent conformational change and interacts with Pin1.* PLoS One, 2012. **7**(12): p. e52047.
122. Li, L., et al., *Ser46 phosphorylation of p53 is an essential event in prolyl-isomerase Pin1-mediated p53-independent apoptosis in response to heat stress.* Cell Death Dis, 2019. **10**(2): p. 96.
123. Baquero, J., et al., *Nuclear Tau, p53 and Pin1 Regulate PARN-Mediated Deadenylation and Gene Expression.* Front Mol Neurosci, 2019. **12**: p. 242.

124. Rizzolio, F., et al., *Retinoblastoma tumor-suppressor protein phosphorylation and inactivation depend on direct interaction with Pin1.* Cell Death Differ, 2012. **19**(7): p. 1152-61.
125. Rustighi, A., et al., *The prolyl-isomerase Pin1 is a Notch1 target that enhances Notch1 activation in cancer.* Nat Cell Biol, 2009. **11**(2): p. 133-42.
126. Ciarapica, R., et al., *Prolyl isomerase Pin1 and protein kinase HIPK2 cooperate to promote cortical neurogenesis by suppressing Groucho/TLE:Hes1-mediated inhibition of neuronal differentiation.* Cell Death Differ, 2014. **21**(2): p. 321-32.
127. Hu, X. and L.F. Chen, *Pinning Down the Transcription: A Role for Peptidyl-Prolyl cis-trans Isomerase Pin1 in Gene Expression.* Front Cell Dev Biol, 2020. **8**: p. 179.
128. Han, H.J., et al., *Peptidyl Prolyl Isomerase PIN1 Directly Binds to and Stabilizes Hypoxia-Inducible Factor-1alpha.* PLoS One, 2016. **11**(1): p. e0147038.
129. Nishi, M., et al., *A distinct role for Pin1 in the induction and maintenance of pluripotency.* J Biol Chem, 2011. **286**(13): p. 11593-603.
130. Yang, H.C., et al., *Pin1-mediated Sp1 phosphorylation by CDK1 increases Sp1 stability and decreases its DNA-binding activity during mitosis.* Nucleic Acids Res, 2014. **42**(22): p. 13573-87.
131. La Montagna, R., et al., *Androgen receptor serine 81 mediates Pin1 interaction and activity.* Cell Cycle, 2012. **11**(18): p. 3415-20.
132. Pulikkan, J.A., et al., *PIN1 Blocks Granulocytic Differentiation Via C-Jun in Acute Myeloid Leukemia with CEBPA Mutations.* Blood, 2008. **112**(11): p. 1205-1205.
133. Zhou, X.Z. and K.P. Lu, *The isomerase PIN1 controls numerous cancer-driving pathways and is a unique drug target.* Nat Rev Cancer, 2016. **16**(7): p. 463-78.
134. Driver, J.A. and K.P. Lu, *Pin1: a new genetic link between Alzheimer's disease, cancer and aging.* Curr Aging Sci, 2010. **3**(3): p. 158-65.
135. Kimura, T., et al., *Isomerase Pin1 stimulates dephosphorylation of tau protein at cyclin-dependent kinase (Cdk5)-dependent Alzheimer phosphorylation sites.* J Biol Chem, 2013. **288**(11): p. 7968-77.
136. Pastorino, L., et al., *The prolyl isomerase Pin1 regulates amyloid precursor protein processing and amyloid-beta production.* Nature, 2006. **440**(7083): p. 528-34.

137. Chen, Y., et al., *Prolyl isomerase Pin1: a promoter of cancer and a target for therapy.* Cell Death Dis, 2018. **9**(9): p. 883.
138. Kim, C.J., et al., *Pin1 overexpression in colorectal cancer and its correlation with aberrant beta-catenin expression.* World J Gastroenterol, 2005. **11**(32): p. 5006-9.
139. Tan, X., et al., *Pin1 expression contributes to lung cancer: Prognosis and carcinogenesis.* Cancer Biol Ther, 2010. **9**(2): p. 111-9.
140. Zhu, Z., et al., *Pin1 promotes prostate cancer cell proliferation and migration through activation of Wnt/beta-catenin signaling.* Clin Transl Oncol, 2016. **18**(8): p. 792-7.
141. Lu, Z. and T. Hunter, *Prolyl isomerase Pin1 in cancer.* Cell Res, 2014. **24**(9): p. 1033-49.
142. Hariharan, N. and M.A. Sussman, *Pin1: a molecular orchestrator in the heart.* Trends Cardiovasc Med, 2014. **24**(6): p. 256-62.
143. Lv, L., et al., *Inhibition of peptidyl-prolyl cis/trans isomerase Pin1 induces cell cycle arrest and apoptosis in vascular smooth muscle cells.* Apoptosis, 2010. **15**(1): p. 41-54.
144. Lv, L., et al., *Essential role of Pin1 via STAT3 signalling and mitochondria-dependent pathways in restenosis in type 2 diabetes.* J Cell Mol Med, 2013. **17**(8): p. 989-1005.
145. Toko, H., et al., *Regulation of cardiac hypertrophic signaling by prolyl isomerase Pin1.* Circ Res, 2013. **112**(9): p. 1244-52.
146. Kim, S.E., et al., *Role of Pin1 in neointima formation: down-regulation of Nrf2-dependent heme oxygenase-1 expression by Pin1.* Free Radic Biol Med, 2010. **48**(12): p. 1644-53.
147. Tousoulis, D., et al., *The role of nitric oxide on endothelial function.* Curr Vasc Pharmacol, 2012. **10**(1): p. 4-18.
148. Tonelli, A.R., et al., *Nitric oxide deficiency in pulmonary hypertension: Pathobiology and implications for therapy.* Pulm Circ, 2013. **3**(1): p. 20-30.
149. Qian, J. and D. Fulton, *Post-translational regulation of endothelial nitric oxide synthase in vascular endothelium.* Front Physiol, 2013. **4**: p. 347.
150. Chiasson, V.L., et al., *Pin1 deficiency causes endothelial dysfunction and hypertension.* Hypertension, 2011. **58**(3): p. 431-8.

151. Paneni, F., et al., *Targeting prolyl-isomerase Pin1 prevents mitochondrial oxidative stress and vascular dysfunction: insights in patients with diabetes.* Eur Heart J, 2015. **36**(13): p. 817-28.
152. Schermuly, R.T., et al., *Phosphodiesterase 1 upregulation in pulmonary arterial hypertension: target for reverse-remodeling therapy.* Circulation, 2007. **115**(17): p. 2331-9.
153. Colvin, K.L. and M.E. Yeager, *Animal Models of Pulmonary Hypertension: Matching Disease Mechanisms to Etiology of the Human Disease.* J Pulm Respir Med, 2014. **4**(4).
154. Vonk Noordegraaf, A. and N. Galie, *The role of the right ventricle in pulmonary arterial hypertension.* Eur Respir Rev, 2011. **20**(122): p. 243-53.
155. Schermuly, R.T., et al., *Riociguat for the treatment of pulmonary hypertension.* Expert Opin Investig Drugs, 2011. **20**(4): p. 567-76.
156. Costantino, S., et al., *Pin1 inhibitor Juglone prevents diabetic vascular dysfunction.* Int J Cardiol, 2016. **203**: p. 702-7.
157. Ruan, L., et al., *Pin1 prolyl isomerase regulates endothelial nitric oxide synthase.* Arterioscler Thromb Vasc Biol, 2011. **31**(2): p. 392-8.
158. Hu, X., et al., *Prolyl isomerase PIN1 regulates the stability, transcriptional activity and oncogenic potential of BRD4.* Oncogene, 2017. **36**(36): p. 5177-5188.
159. Wang, Y., et al., *Targeting Pin1 Protects Mouse Cardiomyocytes from High-Dose Alcohol-Induced Apoptosis.* Oxid Med Cell Longev, 2016. **2016**: p. 4528906.
160. Basu, A., et al., *Proteasomal degradation of human peptidyl prolyl isomerase pin1-pointing phospho Bcl2 toward dephosphorylation.* Neoplasia, 2002. **4**(3): p. 218-27.
161. Yang, C., et al., *The roles of bcl-2 gene family in the pulmonary artery remodeling of hypoxia pulmonary hypertension in rats.* Chin Med Sci J, 2001. **16**(3): p. 182-4.
162. Zhao, T.F., et al., *MiR-593-5p promotes the development of hypoxic-induced pulmonary hypertension via targeting PLK1.* Eur Rev Med Pharmacol Sci, 2019. **23**(8): p. 3495-3502.

163. Wilson, J.L., et al., *Participation of PLK1 and FOXM1 in the hyperplastic proliferation of pulmonary artery smooth muscle cells in pulmonary arterial hypertension.* PLoS One, 2019. **14**(8): p. e0221728.
164. Chen, X., et al., *Cytoplasmic Pin1 expression is increased in human cutaneous melanoma and predicts poor prognosis.* Sci Rep, 2018. **8**(1): p. 16867.
165. Ayala, G., et al., *The prolyl isomerase Pin1 is a novel prognostic marker in human prostate cancer.* Cancer Res, 2003. **63**(19): p. 6244-51.
166. Lu, K.P., *Prolyl isomerase Pin1 as a molecular target for cancer diagnostics and therapeutics.* Cancer Cell, 2003. **4**(3): p. 175-80.
167. Lin, C.H., et al., *Landscape of Pin1 in the cell cycle.* Exp Biol Med (Maywood), 2015. **240**(3): p. 403-8.
168. Cheng, C.W. and E. Tse, *PIN1 in Cell Cycle Control and Cancer.* Front Pharmacol, 2018. **9**: p. 1367.
169. Liou, Y.C., X.Z. Zhou, and K.P. Lu, *Prolyl isomerase Pin1 as a molecular switch to determine the fate of phosphoproteins.* Trends Biochem Sci, 2011. **36**(10): p. 501-14.
170. Ryo, A., et al., *PIN1 is an E2F target gene essential for Neu/Ras-induced transformation of mammary epithelial cells.* Mol Cell Biol, 2002. **22**(15): p. 5281-95.
171. Zhou, W., et al., *Pin1 catalyzes conformational changes of Thr-187 in p27Kip1 and mediates its stability through a polyubiquitination process.* J Biol Chem, 2009. **284**(36): p. 23980-8.
172. Antoniu, S.A., *Targeting PDGF pathway in pulmonary arterial hypertension.* Expert Opin Ther Targets, 2012. **16**(11): p. 1055-63.
173. Barst, R.J., *PDGF signaling in pulmonary arterial hypertension.* J Clin Invest, 2005. **115**(10): p. 2691-4.
174. Tuder, R.M., et al., *Exuberant endothelial cell growth and elements of inflammation are present in plexiform lesions of pulmonary hypertension.* Am J Pathol, 1994. **144**(2): p. 275-85.
175. Wu, Y., et al., *Anti-Diabetic Atherosclerosis by Inhibiting High Glucose-Induced Vascular Smooth Muscle Cell Proliferation via Pin1/BRD4 Pathway.* Oxid Med Cell Longev, 2020. **2020**: p. 4196482.

176. Liu, X., et al., *Inhibition of Pin1 alleviates myocardial fibrosis and dysfunction in STZ-induced diabetic mice.* Biochem Biophys Res Commun, 2016. **479**(1): p. 109-15.
177. Liu, M., et al., *The Essential Role of Pin1 via NF-kappaB Signaling in Vascular Inflammation and Atherosclerosis in ApoE(-/-) Mice.* Int J Mol Sci, 2017. **18**(3).
178. Hu, Y.G., Y.F. Shen, and Y. Li, *Effect of Pin1 inhibitor juglone on proliferation, migration and angiogenic ability of breast cancer cell line MCF7Adr.* J Huazhong Univ Sci Technolog Med Sci, 2015. **35**(4): p. 531-534.
179. Aithal, B.K., et al., *Juglone, a naphthoquinone from walnut, exerts cytotoxic and genotoxic effects against cultured melanoma tumor cells.* Cell Biol Int, 2009. **33**(10): p. 1039-49.
180. Xu, H.L., et al., *Juglone, from Juglans mandshruica Maxim, inhibits growth and induces apoptosis in human leukemia cell HL-60 through a reactive oxygen species-dependent mechanism.* Food Chem Toxicol, 2012. **50**(3-4): p. 590-6.
181. Zhang, X.B., et al., *Activity guided isolation and modification of juglone from Juglans regia as potent cytotoxic agent against lung cancer cell lines.* BMC Complement Altern Med, 2015. **15**: p. 396.
182. Guignabert, C., et al., *Pathogenesis of pulmonary arterial hypertension: lessons from cancer.* Eur Respir Rev, 2013. **22**(130): p. 543-51.
183. Mannarino, E. and M. Pirro, *Molecular biology of atherosclerosis.* Clin Cases Miner Bone Metab, 2008. **5**(1): p. 57-62.
184. Masri, F.A., et al., *Hyperproliferative apoptosis-resistant endothelial cells in idiopathic pulmonary arterial hypertension.* Am J Physiol Lung Cell Mol Physiol, 2007. **293**(3): p. L548-54.
185. Tu, L., et al., *A critical role for p130Cas in the progression of pulmonary hypertension in humans and rodents.* Am J Respir Crit Care Med, 2012. **186**(7): p. 666-76.
186. Gurbanov, E. and X. Shiliang, *The key role of apoptosis in the pathogenesis and treatment of pulmonary hypertension.* Eur J Cardiothorac Surg, 2006. **30**(3): p. 499-507.
187. Price, L.C., et al., *Dexamethasone induces apoptosis in pulmonary arterial smooth muscle cells.* Respir Res, 2015. **16**: p. 114.

188. McMurtry, M.S., et al., *Dichloroacetate prevents and reverses pulmonary hypertension by inducing pulmonary artery smooth muscle cell apoptosis.* Circ Res, 2004. **95**(8): p. 830-40.
189. Courboulin, A., et al., *Plumbagin reverses proliferation and resistance to apoptosis in experimental PAH.* Eur Respir J, 2012. **40**(3): p. 618-29.
190. Tewari, M., et al., *Yama/CPP32 beta, a mammalian homolog of CED-3, is a CrmA-inhibitable protease that cleaves the death substrate poly(ADP-ribose) polymerase.* Cell, 1995. **81**(5): p. 801-9.
191. Dai, J., et al., *Alpha-enolase regulates the malignant phenotype of pulmonary artery smooth muscle cells via the AMPK-Akt pathway.* Nat Commun, 2018. **9**(1): p. 3850.
192. Sorrentino, G., et al., *The prolyl-isomerase Pin1 activates the mitochondrial death program of p53.* Cell Death Differ, 2013. **20**(2): p. 198-208.
193. Zheng, M., et al., *Inhibition of the prolyl isomerase Pin1 enhances the ability of sorafenib to induce cell death and inhibit tumor growth in hepatocellular carcinoma.* Oncotarget, 2017. **8**(18): p. 29771-29784.
194. Xu, H.L., et al., *Anti-proliferative effect of Juglone from Juglans mandshurica Maxim on human leukemia cell HL-60 by inducing apoptosis through the mitochondria-dependent pathway.* Eur J Pharmacol, 2010. **645**(1-3): p. 14-22.
195. Ji, Y.B., Z.Y. Qu, and X. Zou, *Juglone-induced apoptosis in human gastric cancer SGC-7901 cells via the mitochondrial pathway.* Exp Toxicol Pathol, 2011. **63**(1-2): p. 69-78.
196. Fang, F., et al., *Juglone exerts antitumor effect in ovarian cancer cells.* Iran J Basic Med Sci, 2015. **18**(6): p. 544-8.
197. Ji, Y.B., et al., *Mechanism of juglone-induced apoptosis of MCF-7 cells by the mitochondrial pathway.* Genet Mol Res, 2016. **15**(3).
198. Ourique, F., et al., *In vivo inhibition of tumor progression by 5 hydroxy-1,4-naphthoquinone (juglone) and 2-(4-hydroxyanilino)-1,4-naphthoquinone (Q7) in combination with ascorbate.* Biochem Biophys Res Commun, 2016. **477**(4): p. 640-646.
199. Merklinger, S.L., et al., *Epidermal growth factor receptor blockade mediates smooth muscle cell apoptosis and improves survival in rats with pulmonary hypertension.* Circulation, 2005. **112**(3): p. 423-31.

200. Sun, M., et al., *Smooth Muscle Insulin-Like Growth Factor-1 Mediates Hypoxia-Induced Pulmonary Hypertension in Neonatal Mice.* Am J Respir Cell Mol Biol, 2016. **55**(6): p. 779-791.
201. Rieg, A.D., et al., *PDGF-BB regulates the pulmonary vascular tone: impact of prostaglandins, calcium, MAPK- and PI3K/AKT/mTOR signalling and actin polymerisation in pulmonary veins of guinea pigs.* Respir Res, 2018. **19**(1): p. 120.
202. Ten Freyhaus, H., et al., *Genetic Ablation of PDGF-Dependent Signaling Pathways Abolishes Vascular Remodeling and Experimental Pulmonary Hypertension.* Arterioscler Thromb Vasc Biol, 2015. **35**(5): p. 1236-45.
203. Yang, Q., et al., *IGF-1 signaling in neonatal hypoxia-induced pulmonary hypertension: Role of epigenetic regulation.* Vascul Pharmacol, 2015. **73**: p. 20-31.
204. You, H., et al., *IGF-1 induces Pin1 expression in promoting cell cycle S-phase entry.* J Cell Biochem, 2002. **84**(2): p. 211-6.
205. Shen, Z.J., et al., *Pin1 null mice exhibit low bone mass and attenuation of BMP signaling.* PLoS One, 2013. **8**(5): p. e63565.
206. Boussetta, T., et al., *The prolyl isomerase Pin1 acts as a novel molecular switch for TNF-alpha-induced priming of the NADPH oxidase in human neutrophils.* Blood, 2010. **116**(26): p. 5795-802.
207. Nechama, M., et al., *The IL-33-PIN1-IRAK-M axis is critical for type 2 immunity in IL-33-induced allergic airway inflammation.* Nat Commun, 2018. **9**(1): p. 1603.
208. Ball, M.K., et al., *Regulation of hypoxia-induced pulmonary hypertension by vascular smooth muscle hypoxia-inducible factor-1alpha.* Am J Respir Crit Care Med, 2014. **189**(3): p. 314-24.
209. Hickey, M.M., et al., *von Hippel-Lindau mutation in mice recapitulates Chuvash polycythemia via hypoxia-inducible factor-2alpha signaling and splenic erythropoiesis.* J Clin Invest, 2007. **117**(12): p. 3879-89.
210. Pawlus, M.R., L. Wang, and C.J. Hu, *STAT3 and HIF1alpha cooperatively activate HIF1 target genes in MDA-MB-231 and RCC4 cells.* Oncogene, 2014. **33**(13): p. 1670-9.

211. Courboulin, A., et al., *Kruppel-like factor 5 contributes to pulmonary artery smooth muscle proliferation and resistance to apoptosis in human pulmonary arterial hypertension.* Respir Res, 2011. **12**: p. 128.
212. Shaw, P.E., *Peptidyl-prolyl cis/trans isomerases and transcription: is there a twist in the tail?* EMBO Rep, 2007. **8**(1): p. 40-5.
213. Hanes, S.D., *Prolyl isomerases in gene transcription.* Biochim Biophys Acta, 2015. **1850**(10): p. 2017-34.
214. Jalouli, M., et al., *The prolyl isomerase Pin1 regulates hypoxia-inducible transcription factor (HIF) activity.* Cell Signal, 2014. **26**(8): p. 1649-56.
215. Lufei, C., et al., *Pin1 is required for the Ser727 phosphorylation-dependent Stat3 activity.* Oncogene, 2007. **26**(55): p. 7656-64.
216. Nakada, S., et al., *Roles of Pin1 as a Key Molecule for EMT Induction by Activation of STAT3 and NF-kappaB in Human Gallbladder Cancer.* Ann Surg Oncol, 2019. **26**(3): p. 907-917.
217. Nakano, A., et al., *Pin1 down-regulates transforming growth factor-beta (TGF-beta) signaling by inducing degradation of Smad proteins.* J Biol Chem, 2009. **284**(10): p. 6109-15.
218. Vitali, S.H., et al., *The Sugen 5416/hypoxia mouse model of pulmonary hypertension revisited: long-term follow-up.* Pulm Circ, 2014. **4**(4): p. 619-29.
219. Chamarthy, M.R., A. Kandathil, and S.P. Kalva, *Pulmonary vascular pathophysiology.* Cardiovasc Diagn Ther, 2018. **8**(3): p. 208-213.
220. Aithal, K.B., et al., *Tumor growth inhibitory effect of juglone and its radiation sensitizing potential: in vivo and in vitro studies.* Integr Cancer Ther, 2012. **11**(1): p. 68-80.
221. Wang, P., et al., *ROS -mediated p53 activation by juglone enhances apoptosis and autophagy in vivo and in vitro.* Toxicol Appl Pharmacol, 2019. **379**: p. 114647.
222. Wu, J., et al., *Juglone induces apoptosis of tumor stem-like cells through ROS-p38 pathway in glioblastoma.* BMC Neurol, 2017. **17**(1): p. 70.
223. Pinsky, M.R., *The right ventricle: interaction with the pulmonary circulation.* Crit Care, 2016. **20**: p. 266.

224. Schrier, R.W. and S. Bansal, *Pulmonary hypertension, right ventricular failure, and kidney: different from left ventricular failure?* Clin J Am Soc Nephrol, 2008. **3**(5): p. 1232-7.
225. Frangogiannis, N.G., *Fibroblasts and the extracellular matrix in right ventricular disease.* Cardiovasc Res, 2017. **113**(12): p. 1453-1464.
226. Andersen, S., et al., *Right Ventricular Fibrosis.* Circulation, 2019. **139**(2): p. 269-285.
227. Wu, X., et al., *Pin1 facilitates isoproterenolinduced cardiac fibrosis and collagen deposition by promoting oxidative stress and activating the MEK1/2ERK1/2 signal transduction pathway in rats.* Int J Mol Med, 2018. **41**(3): p. 1573-1583.
228. Nathan, S.D., et al., *Pulmonary hypertension in chronic lung disease and hypoxia.* Eur Respir J, 2019. **53**(1).
229. Paddenberg, R., et al., *Rapamycin attenuates hypoxia-induced pulmonary vascular remodeling and right ventricular hypertrophy in mice.* Respir Res, 2007. **8**: p. 15.
230. Stenmark, K.R., et al., *Animal models of pulmonary arterial hypertension: the hope for etiological discovery and pharmacological cure.* Am J Physiol Lung Cell Mol Physiol, 2009. **297**(6): p. L1013-32.
231. Shen, Z.J., et al., *Pin1 protein regulates Smad protein signaling and pulmonary fibrosis.* J Biol Chem, 2012. **287**(28): p. 23294-305.
232. Soon, E., et al., *Elevated levels of inflammatory cytokines predict survival in idiopathic and familial pulmonary arterial hypertension.* Circulation, 2010. **122**(9): p. 920-7.
233. Shen, Z.J., et al., *Pin1 regulates TGF-beta1 production by activated human and murine eosinophils and contributes to allergic lung fibrosis.* J Clin Invest, 2008. **118**(2): p. 479-90.
234. Snyderman, C.H., et al., *Anterior cranial base reconstruction: role of galeal and pericranial flaps.* Laryngoscope, 1990. **100**(6): p. 607-14.
235. Rai, N., et al., *Effect of Riociguat and Sildenafil on Right Heart Remodeling and Function in Pressure Overload Induced Model of Pulmonary Arterial Banding.* Biomed Res Int, 2018. **2018**: p. 3293584.

236. Teplukhin Iu, V., B.V. Karal'nik, and L.A. Gorbunova, *[Erythrocyte immunoreagents for demonstrating Opisthorchis antigens and their diagnostic use].* Med Parazitol (Mosk), 1986(5): p. 37-40.
237. Muellenbach, J.M., et al., *Integrating Information Literacy and Evidence-Based Medicine Content within a New School of Medicine Curriculum: Process and Outcome.* Med Ref Serv Q, 2018. **37**(2): p. 198-206.
238. Campaner, E., et al., *A covalent PIN1 inhibitor selectively targets cancer cells by a dual mechanism of action.* Nat Commun, 2017. **8**: p. 15772.
239. Becker, E.B. and A. Bonni, *Pin1 in neuronal apoptosis.* Cell Cycle, 2007. **6**(11): p. 1332-5.
240. Ryo, A., et al., *A suppressive role of the prolyl isomerase Pin1 in cellular apoptosis mediated by the death-associated protein Daxx.* J Biol Chem, 2007. **282**(50): p. 36671-81.

DECLARATION

I hereby declare that the present thesis is my original work and that it has not been previously presented in this or any other university for any degree. I have appropriately acknowledged and referenced all text passages that are derived literally from, or are based on, the content of the published or unpublished work of others and all information that relates to verbal communications. I have also abided by the principles of good scientific conduct outlined in the charter of the Justus Liebig University of Giessen while conducting the investigations described in this dissertation.

……..

Nabham Rai, Gießen

ACKNOWLEDGEMENT

First and foremost, I would like to express my sincere gratitude to Prof. Dr. rer. nat. Ralph Schermuly for allowing me to conduct my doctoral work under his guidance. I would like to thank him for his constructive ideas, discussion, and support throughout the doctoral program. I am grateful to him for providing me with the opportunities to present my research works at various international conferences, thus enhancing my confidence and presentation skills.

I would like to express sincere gratitude to my mentor Dr. Tatyana Novoyatleva for initiation of this project, her knowledge, guidance and support during this project, and her helpful comments as well as experimental advice. The completion of the doctoral work would not be possible without her immense contribution.

I would like to thank Dr. Akylbek Sydykov for helping with echocardiography and Dr. Baktybek Kojonazarov for FMT analysis of the animals.

Many thanks to Christina Vroom for her help with the animal experiment, Ewa Bieniek for the help with histology work as well as Carina Lepper, and Sophia Hattesohl.

I would also like to express gratitude to Dr. Rory Morty and Dr. Elie El Agha for their tutoring in the Molecular Biology and Medicine of the Lung graduate program.

I would also like to give a special thank you to Prof. Dr. Werner Seeger, who always has extended his support for research.

Many thanks also to Prof. Dr. Norbert Weissmann, Prof. Dr. Ardeschir Ghofrani, and Prof. Dr. Friedrich Grimminger for the cooperative support.

I would like to thank Elizabeta Krstic, Daniela Weber and Lisa Marie Junker for all the organizational help.

I would like to thank Megan Grether for critical proofreading of my thesis.

I express my heartily thanks to Swathi Veeroju for being a good friend, a fine lab companion to work with and helping me during my initial days. I would also like to thank all other wonderful colleagues for offering experimental tips, and for the nice working atmosphere they created and all those enjoyable moments outside of work.

I would like to thank Tahira Zar for all the support as well as Vishnu, Chanil and Arun for their friendship and their kind help and moral support during my study and life in Giessen.

Finally I am forever grateful to my parents Rajesh Rai and Kiran Rai for having faith in me and allowing me to pursue my dream in Germany. My sincere and heartily thanks

to my sister Shubham Rai for her endless love, patience, moral support and assistance in every possible way and for being my pillar and confidant throughout the years. A special mention to my niece Amaira Chowdhary, who during this time filled my life with love and happiness. I would not have achieved anything in my life without the support of my family.